Midwest State's Regional Pooled Fund Research Program
Fiscal Year 1995-1996 (Year 6)
Research Project Number SPR-3(017)

DESIGN AND EVALUATION OF THE TL-4 MINNESOTA COMBINATION TRAFFIC/BICYCLE BRIDGE RAIL

Submitted by

Karla A. Polivka, B.S.M.E., E.I.T.
Graduate Research Assistant

Eric A. Keller, B.S.M.E., E.I.T.
Computer Design Technician II

John R. Rohde, Ph.D., P.E.
Associate Professor

Ronald K. Faller, Ph.D.,P.E.
Research Assistant Professor

Dean L. Sicking, Ph.D., P.E.
Associate Professor and MwRSF Director

James C. Holloway, M.S.C.E., E.I.T.
Research Associate Engineer

MIDWEST ROADSIDE SAFETY FACILITY
University of Nebraska-Lincoln
1901 "Y" Street, Building "C"
Lincoln, Nebraska 68588-0601
(402) 472-6864

Submitted to

MIDWEST STATE'S REGIONAL POOLED FUND PROGRAM
Nebraska Department of Roads
1500 Nebraska Highway 2
Lincoln, Nebraska 68502

MwRSF Research Report No. TRP-03-74-98

November 30, 1998

Technical Report Documentation Page

1. Report No.	2.	3. I
SPR-3(017)		PB99-140998

4. Title and Subtitle	5. Report Date
Design and Evaluation of the TL-4 Minnesota Combination Traffic/Bicycle Bridge Rail	November 30, 1998
	6.

7. Author(s)	8. Performing Organization Report No.
Polivka, K.A., Faller, R.K., Keller, E.A., Sicking, D.L., Rohde, J.R., and Holloway, J.C.	TRP-03-74-98

9. Performing Organization Name and Address	10. Project/Task/Work Unit No.
Midwest Roadside Safety Facility (MwRSF) University of Nebraska - Lincoln 1901 Y Street, Building C Lincoln, NE 68588-0601	11. Contract © or Grant (G) No. SPR-3(017)

12. Sponsoring Organization Name and Address	13. Type of Report and Period Covered
Midwest State's Regional Pooled Fund Program Nebraska Department of Roads 1500 Nebraska Highway 2 Lincoln, Nebraska 68502	Final Report 1995 - 1998
	14. Sponsoring Agency Code

15. Supplementary Notes

Prepared in cooperation with U.S. Department of Transportation, Federal Highway Administration

16. Abstract (Limit: 200 words)

A combination traffic and bicycle bridge rail was developed and crash tested. The combination bridge rail was constructed with a standard New Jersey safety shaped barrier and special steel panels formed from tubular steel posts and rails, and square vertical spindle bars. Two cables were installed inside the tubular rails to prevent detachment of large pieces of debris from causing hazardous conditions for vehicles and pedestrians below. Although the crash tested bridge rail was constructed using the New Jersey safety shape, it is believed that this combination traffic/bicycle bridge rail could be easily adapted to other safety shape barriers or rectangular parapets with no need for further crash testing. Due to the modular nature of the steel panel sections, the combination traffic/bicycle bridge rail can be repaired very easily following a vehicular impact.

Two full-scale vehicle crash tests were performed on Minnesota's combination traffic/bicycle bridge railing. The tests were conducted and reported in accordance with the requirements specified in NCHRP Report No. 350, *Recommended Procedures for the Safety Performance Evaluation of Highway Features*. The safety performance of the combination traffic/bicycle bridge rail was determined to be acceptable according to Test Level 4 of the NCHRP 350 criteria.

17. Document Analysis/Descriptors		18. Availability Statement
Highway Safety, Longitudinal Barrier, Bridge Rail, Roadside Features	Crash Test, Compliance Test, Design, Bicycle Rail	No restrictions. Document available from: National Technical Information Services, Springfield, Virginia 22161

19. Security Class (this report)	20. Security Class (this page)	21. No. of Pages	22. Price
Unclassified	Unclassified	109	

DISCLAIMER STATEMENT

The contents of this report reflect the views of the authors who are responsible for the facts and the accuracy of the data presented herein. The contents do not necessarily reflect the official views or policies of the State Highway Departments participating in the Midwest State's Pooled Fund Research Program nor the Federal Highway Administration. This report does not constitute a standard, specification, or regulation.

ACKNOWLEDGMENTS

The authors wish to acknowledge several sources that made a contribution to this project: (1) the Midwest State's Regional Pooled Fund Program funded by the Iowa Department of Transportation, Kansas Department of Transportation, Minnesota Department of Transportation, Missouri Department of Transportation, Nebraska Department of Roads, South Dakota Department of Transportation, and Wisconsin Department of Transportation for sponsoring this project; (2) MwRSF personnel for constructing the barriers and conducting the crash tests; and (3) the Center for Infrastructure Research and the University of Nebraska-Lincoln for matching support.

A special thanks is given to the following individuals who made a contribution to the completion of this research project.

Midwest Roadside Safety Facility

B.T. Rosson, Ph.D., P.E., Associate Professor
J.D. Reid, Ph.D., Assistant Professor
B.G. Pfeifer, Ph.D., P.E., Research Associate Engineer
K.L. Krenk, B.S.M.A., Field Operations Manager
M.L. Hanau, Laboratory Mechanic I
Undergraduate and Graduate Assistants

Iowa Department of Transportation

David Little, P.E., Design Methods Engineer

Kansas Department of Transportation

Ron Seitz, P.E., Road Design Squad Leader

Minnesota Department of Transportation

Ray Cekalla, P.E., Preliminary Bridge Plans Engineer
Dan Dorgan, P.E., Bridge Planning and Program Engineer
Ron Cassellius, Research Program Coordinator

Missouri Department of Transportation

Vince Imhoff, P.E., Senior Research and Development Engineer

Nebraska Department of Roads

Leona Kolbet, Research Coordinator
Ken Sieckmeyer, Transportation Planning Manager

Ohio Department of Transportation

Monique Evans, P.E., Standards Engineer

South Dakota Department of Transportation

David Huft, P.E., Research Engineer

Wisconsin Department of Transportation

Rory Rhinesmith, P.E., Chief Roadway Development Engineer
Fred Wisner, Standards Development Engineer

Dunlap Photography

James Dunlap, President and Owner

TABLE OF CONTENTS

List of Figures

Page

List of Tables

Page

1 INTRODUCTION

1.1 Problem Statement

The Minnesota Department of Transportation as well as other highway departments have been considering the accommodation of pedestrians and bicyclists along their roadways and bridges. One area of particular concern are bridges with standard height rails. A standard height bridge rail, typically measuring 813 mm in height, is not capable of restraining a bicyclist during even a minor impact with the bridge railing. To protect bicyclists, it is necessary to substantially increase the height of most TL-4 bridge rails. Since many existing railings have been proven adequate for containing vehicular impacts, this rail height extension could be utilized on a number of different TL-4 barriers once testing has showed the extension to be crashworthy. The traffic/bicycle bridge rail should provide an economical alternative to the more costly option of constructing a separate bicycle bridge or replacing existing bridge rails.

1.2 Objective

The objective of the research project was to develop a combination traffic/bicycle bridge rail for use with concrete parapet bridge rails and to determine if the new rail could be feasiblely retrofitted to other existing bridge rails without additional crash testing. This design was to address all structural concerns, aesthetic considerations, as well as to minimize the potential for spearing, snagging, and problems associated with hazardous debris. The bridge railing was developed to meet the Test Level 4 (TL-4) safety performance criteria set forth in the National Cooperative Highway Research Program (NCHRP) Report No. 350, *Recommended Procedures for the Safety Performance Evaluation of Highway Features* (1).

1.3 Scope

The research objective was accomplished with a series of tasks. First, a literature search was performed to review similar bridge rails, including the identification of key features of each design that would provide insight into how the combination bridge rail would perform during a vehicular impact. Second, an analysis phase was undertaken to determine which concrete parapet configuration should be used as the basis of the combination railing system. Third, a design phase was conducted in order to determine the best method for attaching the bicycle railing to the traffic railing. Fourth, static component testing was performed on posts to optimize the post-weakening breakaway feature. After final design and subsequent fabrication, two full-scale vehicle crash tests were performed according to the TL-4 impact conditions of NCHRP Report 350. The first test, MNPD-1, used a Ford F-250 ¾-ton pickup, weighing approximately 2,000 kg, with a target impact speed and angle of 100 km/hr and 25 degrees, respectively. The second test, MNPD-2, used a Ford F-800 single unit truck, weighing approximately 8,000 kg, with a target impact speed and angle of 80 km/hr and 15 degrees, respectively. Finally, the test results were analyzed, evaluated, and documented. Conclusions and recommendations were then made that pertain to the safety performance of the new combination traffic/bicycle bridge rail.

2 LITERATURE REVIEW

2.1 Pedestrian/Bicycle Railings and Other Protection Fences

Historically, very little research has been performed on the development and crash testing of pedestrian/bicycle railings. Specifically, three pedestrian/bicycle railings and one vandal protection fence have been evaluated by full-scale crash testing (2-4).

The first pedestrian/bicycle railing or BR27D consisted of two horizontal, tubular steel rails supported by vertical, tubular steel posts and was attached to a rectangular concrete parapet (2-3). In addition, the BR27D railing system was constructed in two configurations - with and without a raised concrete sidewalk. For both configurations, the pedestrian/bicycle railing was evaluated using two full-scale vehicle crash tests and was determined to be acceptable according to the Performance Level 1 (PL-1) criteria found in the American Association of State Highway and Transportation Official's (AASHTO's) *Guide Specification for Bridge Railings* (5).

The second pedestrian/bicycle railing or BR27C consisted of a single horizontal, tubular steel rail supported by vertical, tubular steel posts and was attached to a rectangular concrete parapet (2). The BR27C railing system was also constructed in two configurations - with and without a raised concrete sidewalk. For both configurations, the pedestrian/bicycle railing was evaluated using three full-scale crash tests and was determined to be acceptable according to the AASHTO PL-2 criteria (5).

The third pedestrian/bicycle railing consisted of two horizontal, tubular steel rails supported by vertical, tubular steel posts and was attached to the Illinois 2399-1 traffic railing system (4). The pedestrian/bicycle railing system was evaluated using one full-scale crash test and was determined to be acceptable according to the AASHTO PL-1 criteria (5). Only a small car test was performed.

The vandal protection fence consisted of chain-link fence supported by pipe posts and attached to a New Jersey safety shape bridge railing system (4). This vandal protection fence system was evaluated using one full-scale crash test and was determined to be acceptable according to the AASHTO PL-2 criteria (5). Small car and single-unit truck tests were not performed.

2.2 Concrete Parapets

From the literature review, it was evident that only a limited number of crash tests have been performed on bicycle railings and guard fences. Therefore, it was necessary to review the results of past crash tests on safety shape barriers and rectangular parapets in order to provide insight on how the impacting vehicles may potentially interact with the components of the combination traffic/bicycle railing system.

Recent crash tests on concrete barriers have revealed that the potential exists for a pickup truck or a single-unit truck to extend over the top of the parapet and make contact with any bicycle/pedestrian railing attached to the top of the existing bridge railing (6-10). Pickup truck crash tests have not been performed on safety shape barriers according to the TL-3 criteria of NCHRP Report No. 350 (1). However, it was believed that safety shape barriers would not exhibit the same magnitude of occupant compartment deformations that were found to occur during crash tests on rectangular parapets (9-11). Therefore, the researchers believed that a bicycle railing attached to a safety shape rather than a rectangular parapet would provide increased safety due to reduced occupant compartment deformations.

3 TEST REQUIREMENTS AND EVALUATION CRITERIA

3.1 Test Requirements

The safety performance objective of a bridge rail is to reduce injury to and eliminate deaths of occupants in errant vehicles and to protect lives and property on, adjacent to, or below a bridge (12). In order to prevent or reduce the severity of such accidents, special attention should be given to four major design factors. These factors are: (1) strength of the railing to resist impact forces; (2) effective railing height; (3) shape of the face of the railing; and (4) deflection characteristics of the railing (5).

Longitudinal barriers, such as a combination traffic/bicycle bridge rail, must satisfy the requirements provided in NCHRP Report No. 350 to be accepted for use on new construction projects or as a replacement for existing designs not meeting current safety standards. According to TL-4 of NCHRP Report No. 350, a combination bridge rail must be subjected to three full-scale vehicle crash tests: (1) a 8,000-kg single-unit truck impacting at a speed of 80 km/hr and at an angle of 15 degrees; (2) a 2,000-kg pickup truck impacting at a speed of 100 km/hr and at an angle of 25 degrees; and (3) an 820-kg small car impacting at a speed of 100 km/hr and at an angle of 20 degrees. The test conditions for TL-4 bridge railings are summarized in Table 1.

Although three full-scale crash tests are required for a TL-4 safety performance evaluation, the 820-kg small car crash test was deemed unnecessary for two reasons. First, rigid safety shape barriers when impacted by small cars have been shown to meet safety performance standards (13-16). Second, these crash tests have not revealed a potential for small cars to extend over the top of the barrier and make contact with the bicycle/pedestrian railing attached to the top of the existing bridge railing.

Table 1. NCHRP 350 Test Level 4 Crash Test Conditions (1).

Test Designation	Test Vehicle	Impact Conditions		Evaluation Criteria[1]
		Speed (km/hr)	Angle (degrees)	
4-10	820C	100	20	A,D,F,H,I,K,M
4-11	2000P	100	25	A,D,F,K,L,M
4-12	8000S	80	15	A,D,G,K,M

[1] - Evaluation criteria explained in Table 2.

3.2 Evaluation Criteria

Evaluation criteria for full-scale vehicle crash testing are based on three appraisal areas: (1) structural adequacy; (2) occupant risk; and (3) vehicle trajectory after collision. Criteria for structural adequacy are intended to evaluate the ability of the barrier to contain, redirect, or allow controlled vehicle penetration in a predictable manner. Occupant risk evaluates the degree of hazard to occupants in the impacting vehicle. Vehicle trajectory after collision is a measure of the potential for the post-impact trajectory of the vehicle to cause subsequent multi-vehicle accidents. It is also an indicator for the potential safety hazard for the occupants of other vehicles or the occupants of the impacting vehicle when subjected to secondary collisions with other fixed objects. These three evaluation criteria are defined in Table 2. The full-scale vehicle crash tests were conducted and reported in accordance with the procedures provided in NCHRP Report No. 350 (1).

Table 2. Relevant NCHRP 350 Evaluation Criteria (1).

Structural Adequacy	A.	Test article should contain and redirect the vehicle; the vehicle should not penetrate, underride, or override the installation although controlled lateral deflection of the test article is acceptable.
Occupant Risk	D.	Detached elements, fragments or other debris from the test article should not penetrate or show potential for penetrating the occupant compartment, or present an undue hazard to other traffic, pedestrians, or personnel in a work zone. Deformations of, or intrusions into, the occupant compartment that could cause serious injuries should not be permitted.
	F.	The vehicle should remain upright during and after collision although moderate roll, pitching and yawing are acceptable.
	G.	It is preferable, although not essential, that the vehicle remain upright during and after collision.
	H.	Longitudinal and lateral occupant impact velocities should fall below the preferred value of 9 m/s, or at least below the maximum allowable value of 12 m/s.
	I.	Longitudinal and lateral occupant ridedown accelerations should fall below the preferred value of 15 g's, or at least below the maximum allowable value of 20 g's.
Vehicle Trajectory	K.	After collision it is preferable that the vehicle's trajectory not intrude into adjacent traffic lanes.
	L.	The occupant impact velocity in the longitudinal direction should not exceed 12 m/s and the occupant ridedown acceleration in the longitudinal direction should not exceed 20 g's.
	M.	The exit angle from the test article preferably should be less than 60 percent of test impact angle, measured at time of vehicle loss of contact with test device.

4 BRIDGE RAIL SYSTEM DEVELOPMENT

4.1 AASHTO Design Considerations

As discussed previously in Section 3.1, combination traffic/bicycle railings must be designed to meet the NCHRP Report No. 350 impact safety standards. However, other design factors must be considered in order to promote a safe environment for bicyclists traversing the bridge and to provide an aesthetically pleasing railing that offers freedom of view. Guidelines addressing these design concerns are provided in three AASHTO publications - the *Guide Specifications for Bridge Railings* (5), the *AASHTO LRFD Bridge Design Specifications* (12), and the *Standard Specifications for Highway Bridges* (17). More specifically, recommendations are provided for the selection of bicycle railing materials, geometries, and design loading.

Material recommendations for bicycle railings include concrete, metal, timber, plastic, fiber reinforced plastic, or a combination thereof. Specific recommendations for the geometry of the bicycle railings are provided in each of the previously listed AASHTO publications. For example, the minimum height of the railing shall not be less than 1,372 mm, as measured from the top of the bicycle riding surface to the top of the upper rail. According to the *Guide Specifications* (5), within a band bordered by the riding surface and a line 1,372 mm above it, horizontal elements of the railing assembly shall have a maximum clear spacing of 381 mm. Vertical elements of the railing assembly shall have a maximum clear spacing of 203 mm. However, if a railing assembly uses both horizontal and vertical members, then the spacing requirements shall apply to one or the other, but not both. According to the *Standard Specifications for Highway Bridges* (17), within a band bordered by the riding surface and a line 686 mm above it, all members shall be spaced such that a 152-mm sphere will not pass through any opening. For a band bordered by lines at 686 and 1,372

mm, all members shall be spaced such that a 203-mm sphere will not pass through any opening. If both horizontal and vertical members are used, the spacing rule applies to one or the other, but not both. According to the AASHTO *LRFD Specifications* (12), the rail may consist of horizontal and/or vertical members. However, the clear opening between elements shall not exceed 152 mm. When both horizontal and vertical members are used, the 152-mm clear opening shall apply to the lower 686 mm of the railing, and the spacing of the upper region shall not be greater than 381 mm or that determined using figures provided by AASHTO (12). All three publications state that the rail spacing requirements shall not apply for chain link fence.

The design loading for the bicycle railing is stated to be 730 N/m transversely and vertically, acting simultaneously on each rail (5,17). However, according to the *LRFD Specifications* (12), the design live loading for the railing shall be the 730 N/m mentioned previously plus a 890-N concentrated load applied to any member and in any direction and acting simultaneously with the distributed load. The design load for chain link fence was also given as 718 N/m^2.

4.2 Design Concepts

Early in the research project, the Minnesota Department of Transportation (MnDOT) provided MwRSF with four combination traffic/bicycle bridge railing concepts that were currently included in their standard plans. Options one and two included a chain link fence railing supported by pipe posts which was attached to either a rectangular or safety shape concrete parapet and positioned in the middle of the top horizontal surface. Options three and four included a railing system consisting the two horizontal channel rails with vertical spindles placed within and supported by flat plate posts. This steel system was also attached to either a rectangular or safety shape concrete parapet and positioned in the middle of the top horizontal surface.

Following a review of Minnesota's combination traffic/bicycle railings as well as crash tests on other bridge railings, MwRSF engineers proposed several railing concepts to MnDOT that were constructed with flexible cables. These cable designs were initially selected since they would be less prone to extensive damage incurred by a truck extending over the parapet and snagging on the bicycle portion of the combination railing. It was also believed that the amount of hazardous debris could be significantly reduced by using a more flexible, bicycle railing system. Following MnDOT's review of the cable designs, it was proposed that MwRSF researchers consider using a railing system more closely resembling MnDOTs' options three and four as previously described.

Therefore, a bicycle railing concept, consisting of horizontal steel rails, vertical spindles, and steel posts, was selected. However, the researchers were concerned with the potential for hazardous debris becoming dislodged from the railing system and either penetrating the occupant compartment or causing undue hazard to traffic and pedestrians below. This hazardous debris could occur when an impacting vehicle contacts the bicycle rail and snags on the bridge rail components. During a vehicular impact, the railing system would likely deflect laterally backward as the posts fractured, allowing bridge railing members to breakaway from the barrier system. To address these concerns, it was necessary to move the bicycle rail to the back vertical face of the parapet and incorporate "weakened" posts that would reduce the potential for post snagging. It was also reasoned that continuous cables should be attached to the horizontal rails. These cables would reduce the potential for the rails to penetrate into the vehicle's occupant compartment or for rail elements to breakaway completely and present undue hazard below. Finally, it was believed that the bicycle railing could be constructed in a modular fashion in order to simplify construction, reduce the required labor costs, and facilitate the repair of the system following a vehicular impact.

5 STATIC POST TESTING

As mentioned previously in Section 4.2, it was deemed necessary to incorporate "weakened" posts into the design of the combination traffic/bicycle bridge railing system in order to reduce the potential for vehicle snagging or spearing of railing components into the vehicle's occupant compartment. Several mechanisms were considered for weakening the posts for the bicycle railing, such as drilling holes or placing cuts to reduce the moment of inertia. However, it should be noted that final post-weakening mechanism must, at a minimum, meet the minimum design load requirements provided in the AASHTO *LRFD Specifications* (12). Therefore, static post testing was performed on several posts to determine whether the weakened posts would provide the necessary structural capacity.

Tubular steel posts were tested under a static load to determine the force-deflection characteristics of several post-weakening alternatives. Each post was fabricated using TS 102 x 51 x 3.2 ASTM A500 Grade B steel and was welded to an 12.7-mm thick steel plate. The posts were attached to the back-side vertical face of the safety shape concrete barrier using four 22.2-mm diameter ASTM A307 bolts, as shown in Figure 1. As given in Figure 1, a load cell was attached to the back-side face of the post while a string potentiometer was attached to the traffic-side face of the post. Finally, various hole sizes and cut lengths were examined during the static testing phase to determine the optimum post weakening alternative. The distance between the applied load and the drilled hole or sawcut was 362 mm.

Eight static tests were performed and are summarized in Table 3. Typical damage to the tubular steel posts is shown in Figure 2. Following an analysis of the test results, a 34.9-mm diameter hole located 25.4 mm above the top of the steel mounting plate was selected for use in the

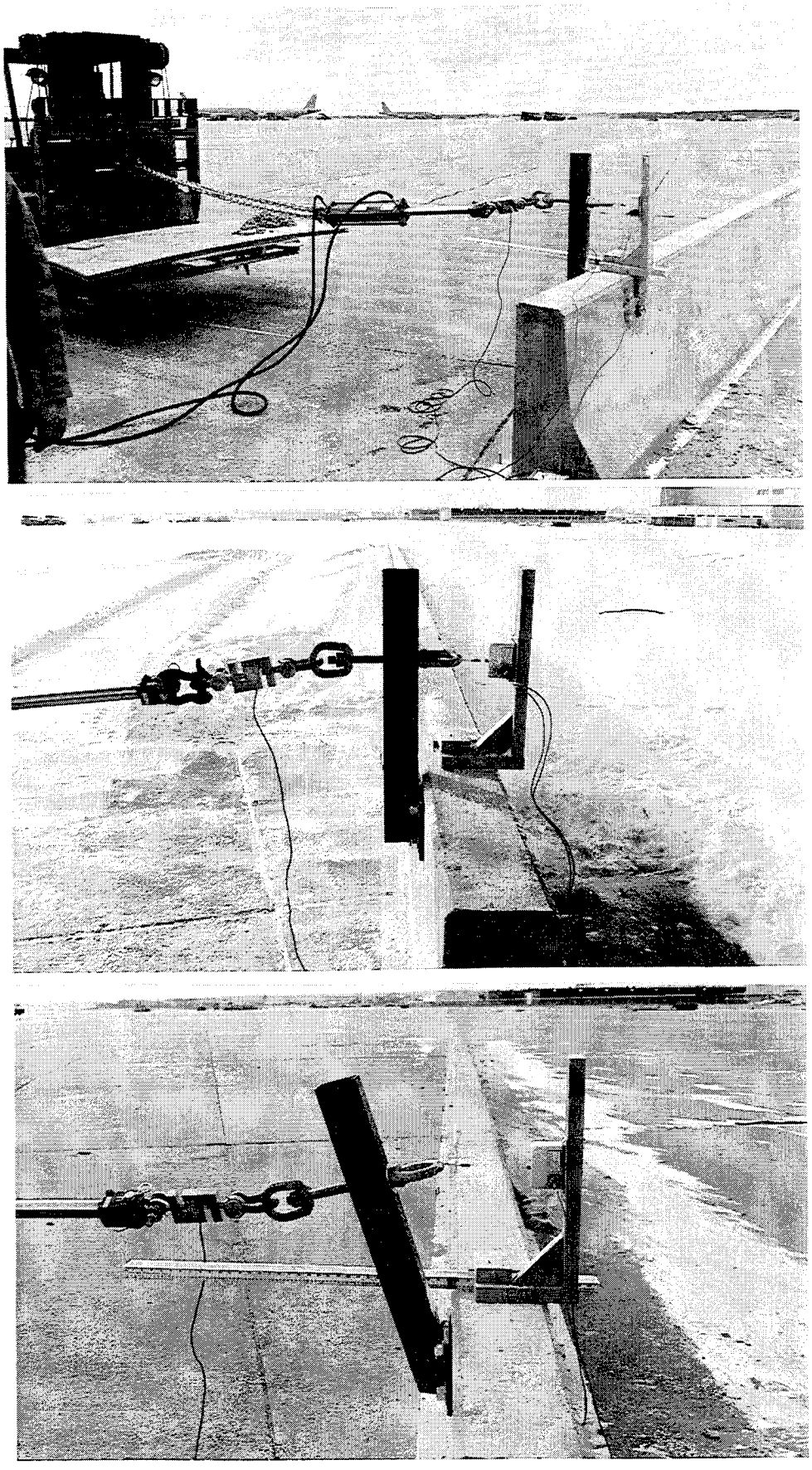

Figure 1. Static Testing Setup

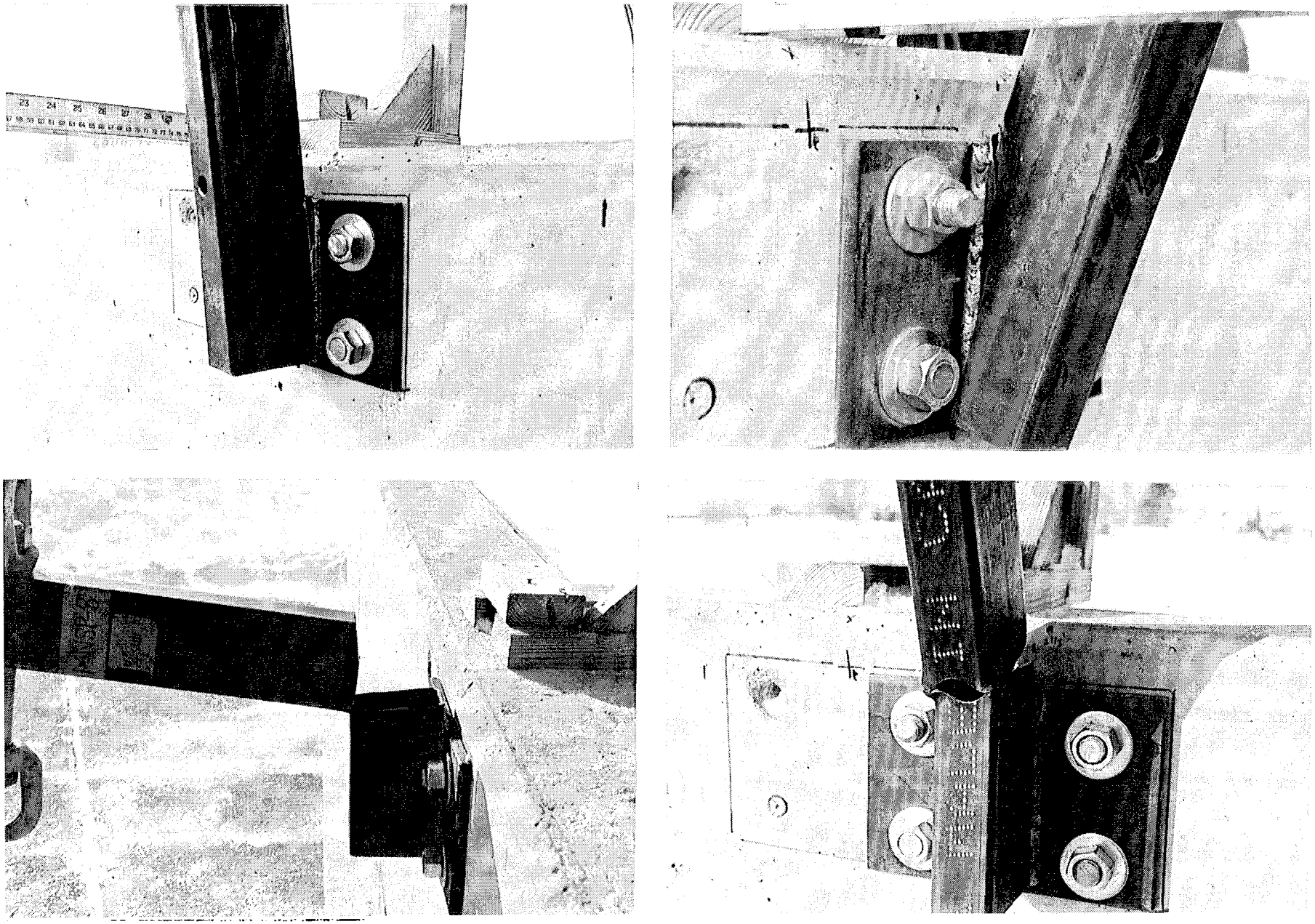

Figure 2. Static Testing Post Failures

because it provided the preferred failure characteristics without damage to the post-to-barrier attachment hardware but still maintained the necessary structural capacity. The maximum static force for the 34.9-mm diameter alternative was 22.0 kN, while all the other alternatives produced maximum static forces above that produced with the larger hole size, as shown in Table 3. The post with 34.9-mm diameter hole also had a maximum static moment of 7,943 kN-mm while the maximum static moment for the other alternatives was above 8,022 kN-mm.

Table 3. Static Post Testing Results.

Test No.	Weakening Alternative	Peak Load (kN)	Deflection at Peak Load (mm)	Maximum Moment (kN-mm)	Failure Location
MNSP-1	15.9-mm ϕ hole	26.7	45.7	10349	base material of post at weld
MNSP-2	19.2-mm ϕ hole	28.8	35.6	11163	base material of post at weld
MNSP-3	25.5-mm ϕ hole	28.3	33.0	10248	through hole
MNSP-4	30.5-mm ϕ hole	25.4	25.4	9186	through hole
MNSP-5	31.8-mm ϕ hole	23.0	21.1	8316	through hole
MNSP-6	34.9-mm ϕ hole	22.0	21.1	7943	through hole
MNSP-7	3.2-mm cut[1]	25.0	22.1	9050	along cut
MNSP-8	6.4-mm cut[1]	22.2	23.1	8022	along cut

[1] - The cut was placed on the tension side of the post.

6 COMBINATION TRAFFIC/BICYCLE RAILING DESIGN DETAILS

The total length of the combination bridge railing installation was 36.58 m. The test installation, as shown in Figures 3 through 9, consisted of two major components: (1) the traffic railing; and (2) the bicycle railing. The traffic railing consisted of a 36.58-m long New Jersey shape concrete parapet. The bicycle railing consisted of three major components: (1) steel rail panels; (2) steel posts; and (3) cables for containing hazardous debris.

6.1 Traffic Rail

Due to past crash testing of the standard New Jersey shape concrete bridge rail, it was deemed unnecessary to construct the concrete parapet on a simulated, cantilevered bridge deck. Therefore, the concrete bridge rail was rigidly attached to the existing concrete apron using Grade 60 epoxy coated rebar. The vertical rebar were placed into holes drilled vertically in the surface and filled with an epoxy adhesive. The spacing and size of both the longitudinal and vertical steel reinforcement is shown in Figure 3.

The 810-mm high concrete bridge rail was configured with the New Jersey safety shape on the front face and a flat vertical surface on the back-side face, as shown in Figure 3. The top and bottom widths of the concrete parapet were 230 and 460 mm, respectively. The concrete bridge was constructed with two separate pours, each 18.29-m long. In addition, vertical deflection joints were placed in the upper regions of the concrete rail and spaced 6.10 m on-center, as shown in Figure 3. All concrete (30 percent limestone and 70 percent sand-gravel mix) had minimum 28-day concrete compressive strengths of 41.37 MPa.

6.2 Bicycle Rail

The combination traffic/bicycle bridge rail design details are shown in Figures 4 through 7. Additional photographs of the bridge railing system are shown in Figures 8 and 9.

Eleven steel railing panels were fabricated from two horizontal steel tubular rails with solid steel spindles placed vertically between the tubular rails, as shown in Figures 3 through 9. Five of the railing panels included expansion joints while six of the panels were continuous. The railing panels were supported by twelve, tubular steel posts. Each steel post was welded to a steel plate which bolted to the back-side vertical face of the concrete bridge railing. Steel wire rope cables, with nominal strengths of 43.59 kN, were placed within each of the tubular rails and horizontally through each of the steel posts. At each end of the test installation, the tubular railing system was sloped downward. This was done for several reasons, such as to reduce the potential for vehicular snagging on the end of the tubes, shield the 7.9-mm diameter wire rope cables (type 7x19) from vehicle contact, and allow for the anchorage of the cables behind the concrete barrier. The cable anchorage hardware and attachment details are shown in Figures 3 through 4, 7, and 9.

The horizontal rails were fabricated with TS 76-mm x 51-mm x 3.2-mm ASTM A500 Grade B structural steel tubing. Vertical spindles, consisting of 15.9-mm ASTM A36 square bars spaced 168-mm on-centers, were welded between the upper and lower rails, thereby forming the modular panel sections, as shown in Figures 4 and 8 through 9. Expansion tubes for the panels were fabricated using TS 64-mm x 38-mm x 6.4-mm ASTM A500 Grade B steel members, as shown in Figures 4, 6, and 9. The ASTM A500 Grade B steel posts, TS 102 mm x 51 mm x 3.2 mm, were fabricated 800-mm long and spaced 3,048 m on centers, as shown in Figures 4, 5, and 7 through 9. A 12.7-mm thick ASTM A36 steel plate was welded to the base of the post to allow for a rigid

attachment to the concrete bridge rail, as shown in Figures 4, 5, and 7 through 9. In addition, four bent steel plates were welded to the sides of each post to provide a mechanism for supporting the modular railing panels between posts. As shown in Figures 4 and 5, the mounting height of the upper rail was 1.38 m, as measured from the concrete surface to the top of the upper rail.

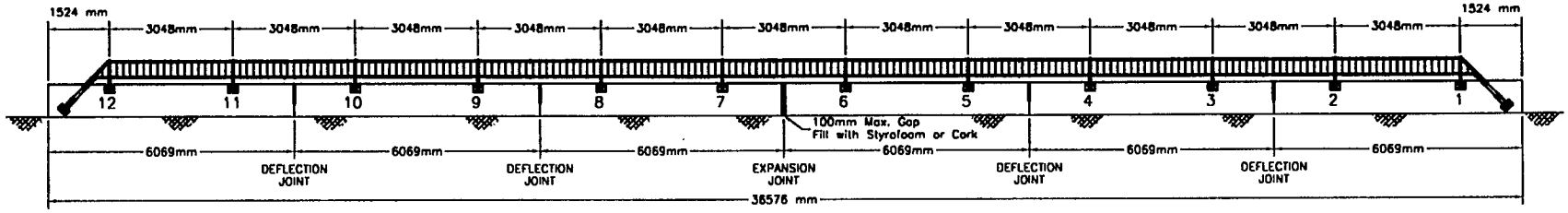

ELEVATION VIEW

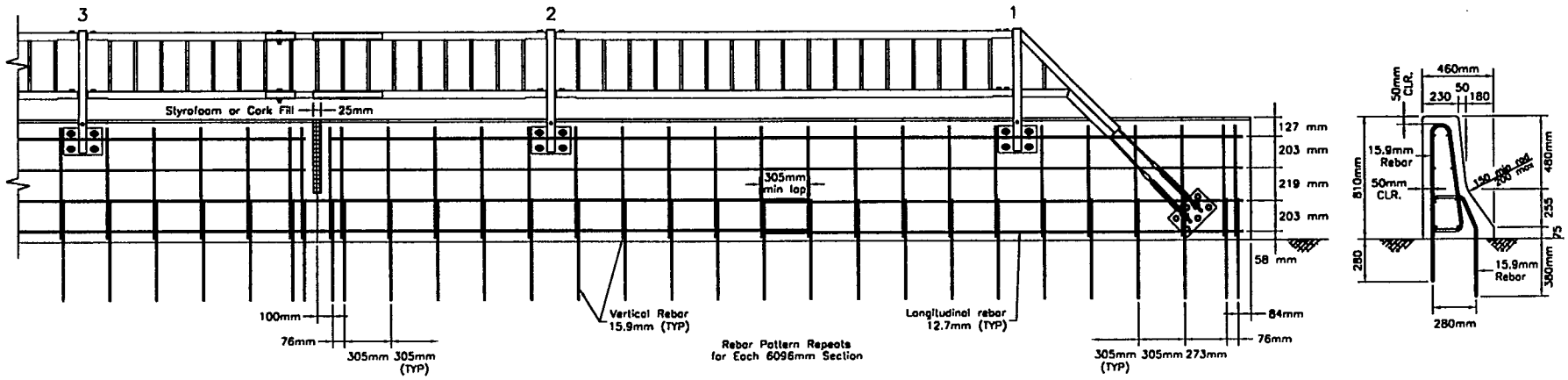

REBAR DETAILS

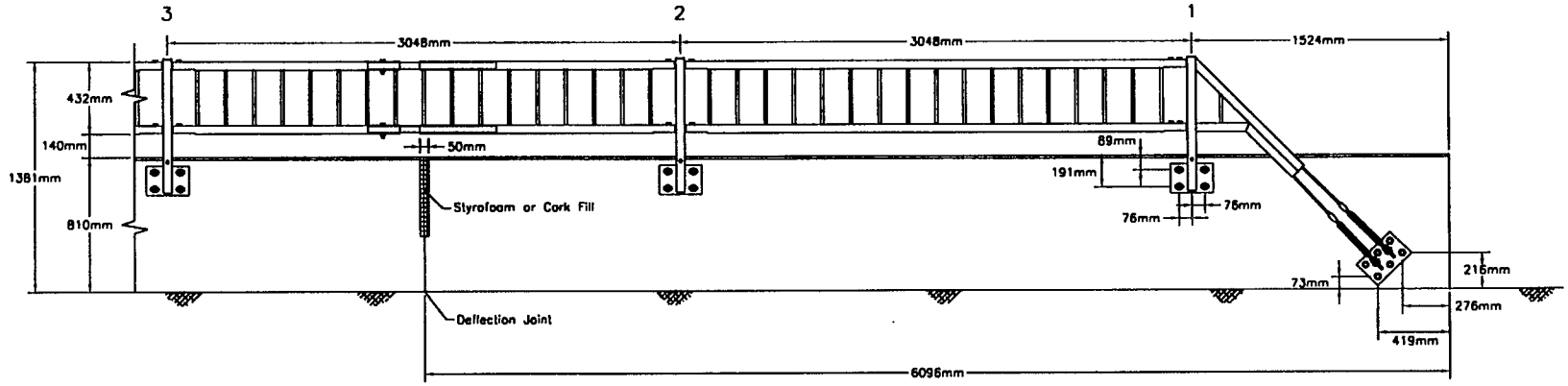

RAIL CONNECTION DETAILS

Figure 3. New Jersey Shape Concrete Bridge Rail Details

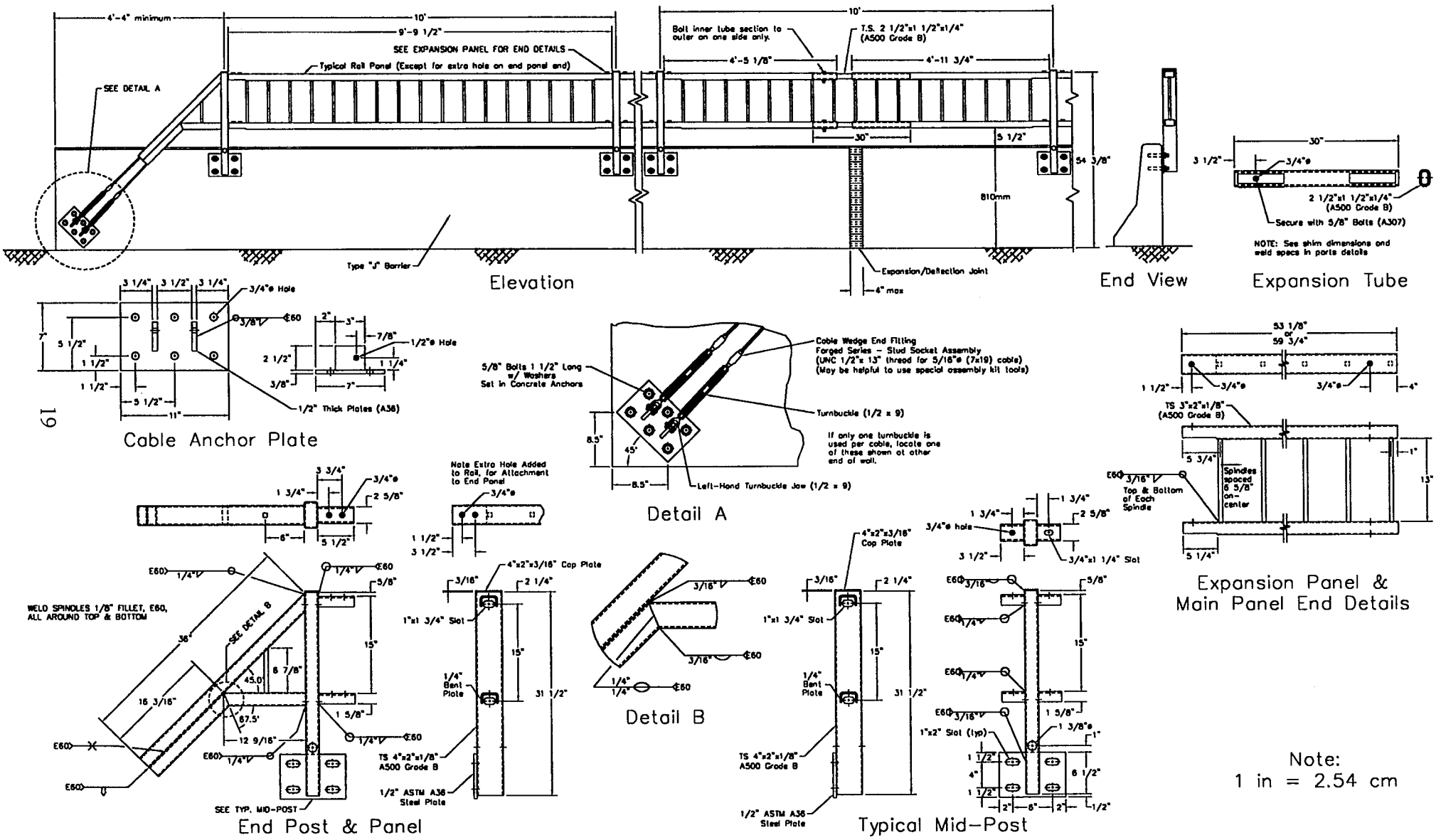

Figure 4. Combination Traffic/Bicycle Bridge Rail Design Details

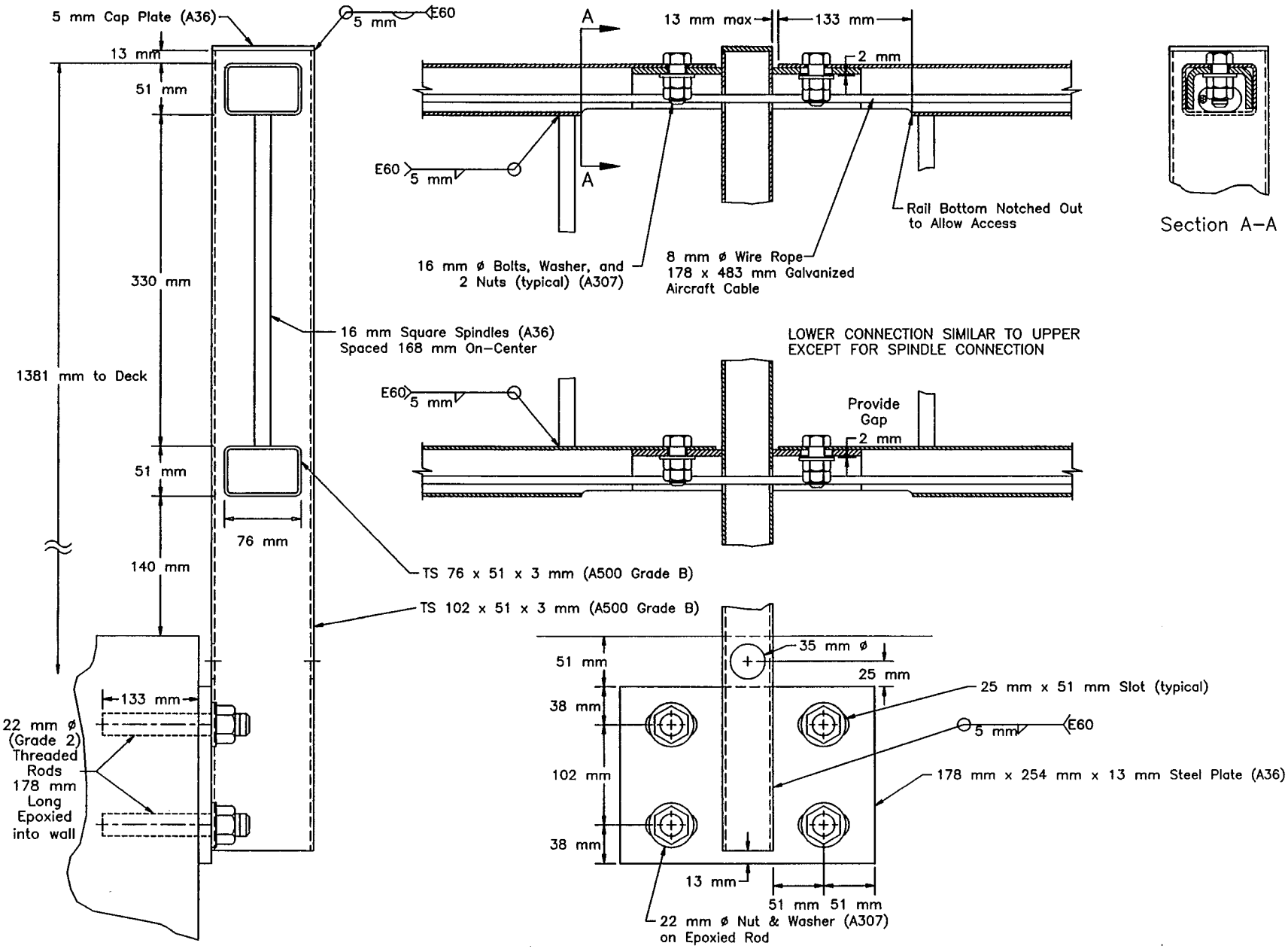

Figure 5. Combination Traffic/Bicycle Bridge Rail Design Details (Continued)

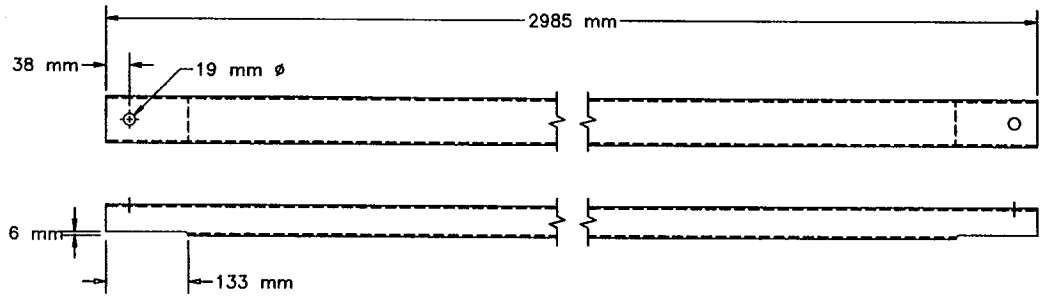

MAIN RAIL (12) T.S. 76 mm x 51 mm x 3 mm
(A500 Grade B)

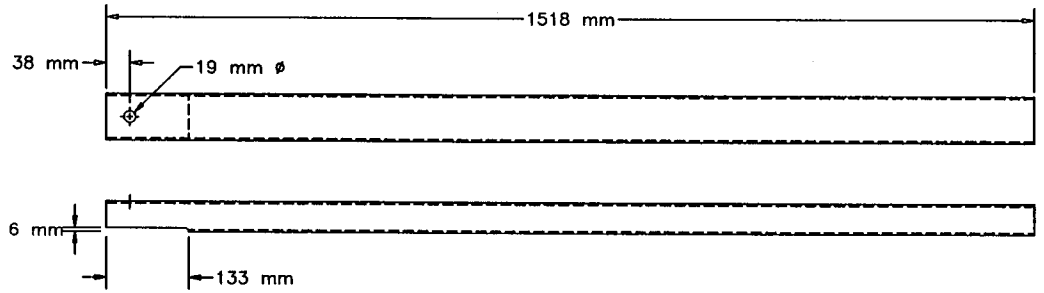

LEFT SPLICE RAIL (10) T.S. 76 mm x 51 mm x 3 mm
(A500 Grade B)

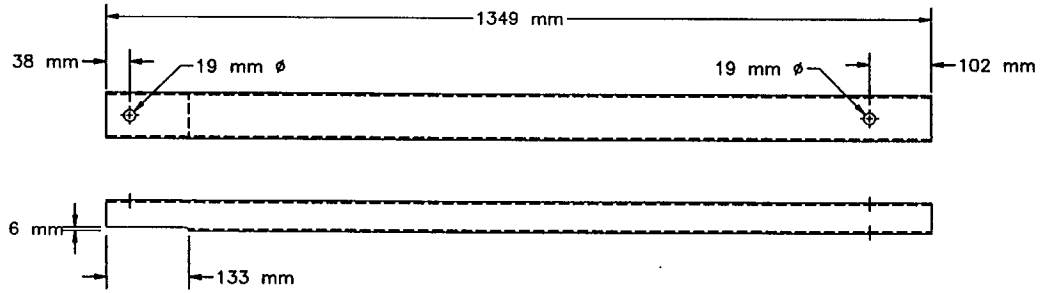

RIGHT SPLICE RAIL (10) T.S. 76 mm x 51 mm x 3 mm
(A500 Grade B)

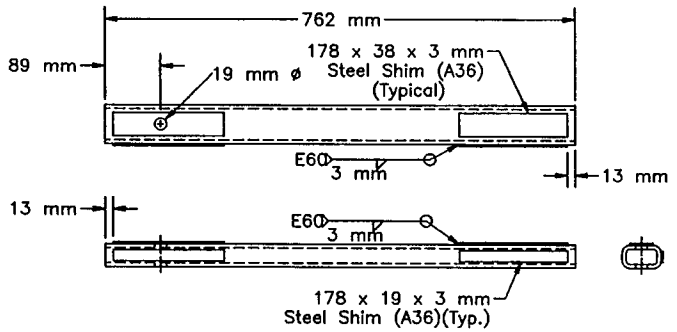

EXPANSION TUBE (10)
T.S. 64 mm x 38 mm x 6 mm
(A500 Grade B)

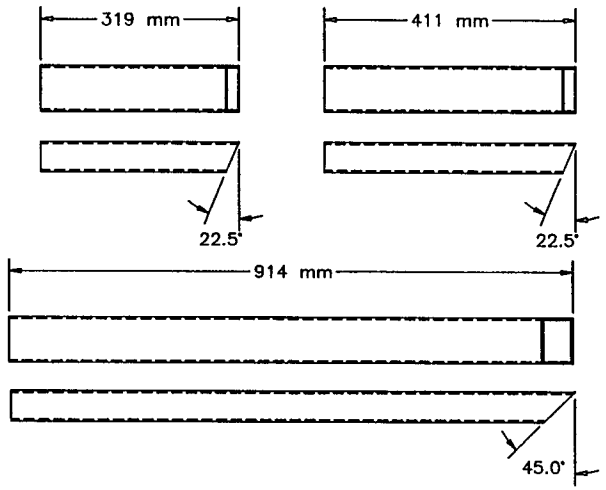

END PANEL RAILS (2 EACH)
T.S. 76 mm x 51 mm x 3 mm
(A500 Grade B)

Figure 6. Combination Traffic/Bicycle Bridge Rail - Railing Components

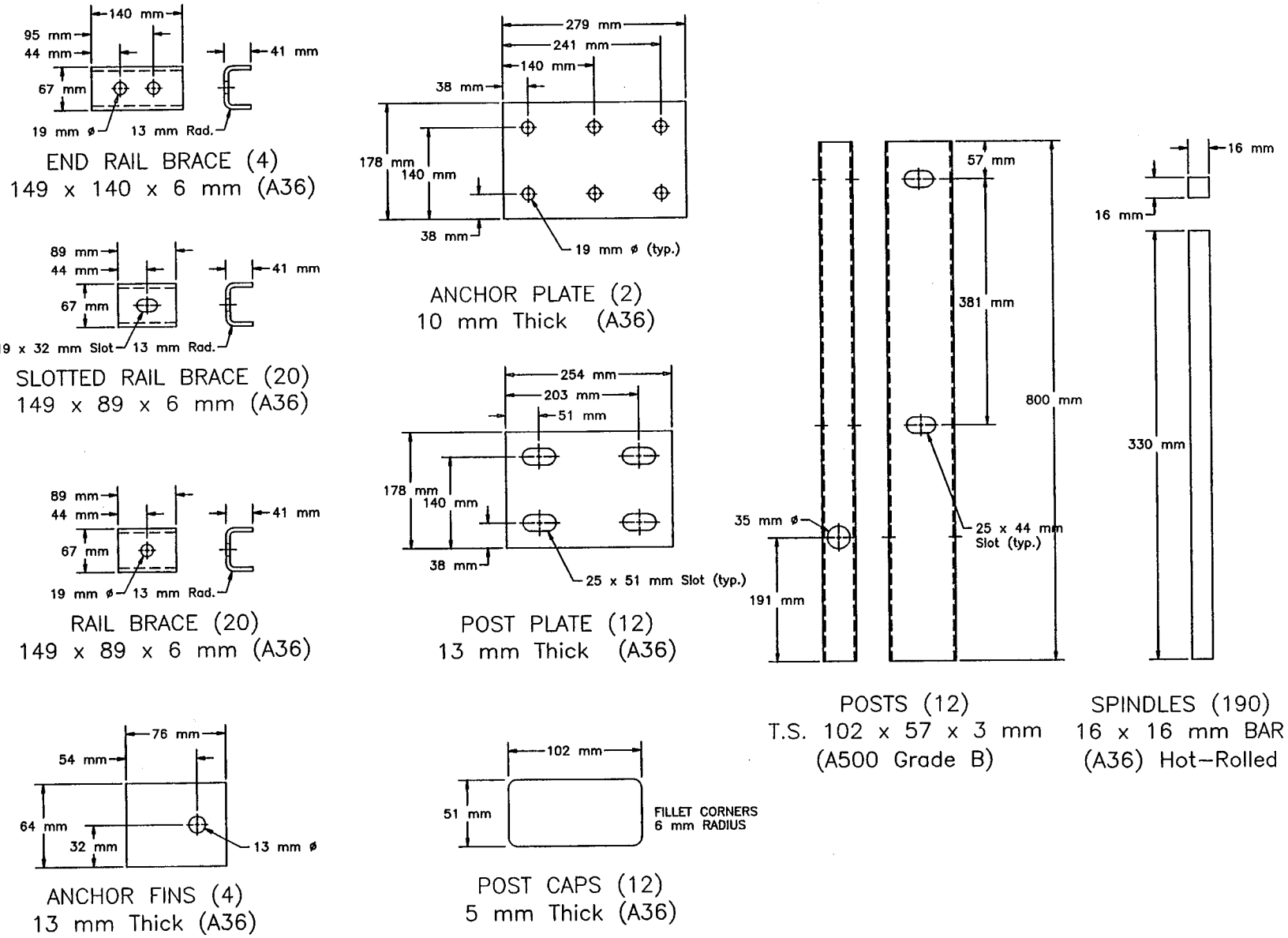

Figure 7. Combination Traffic/Bicycle Bridge Rail - Post Components

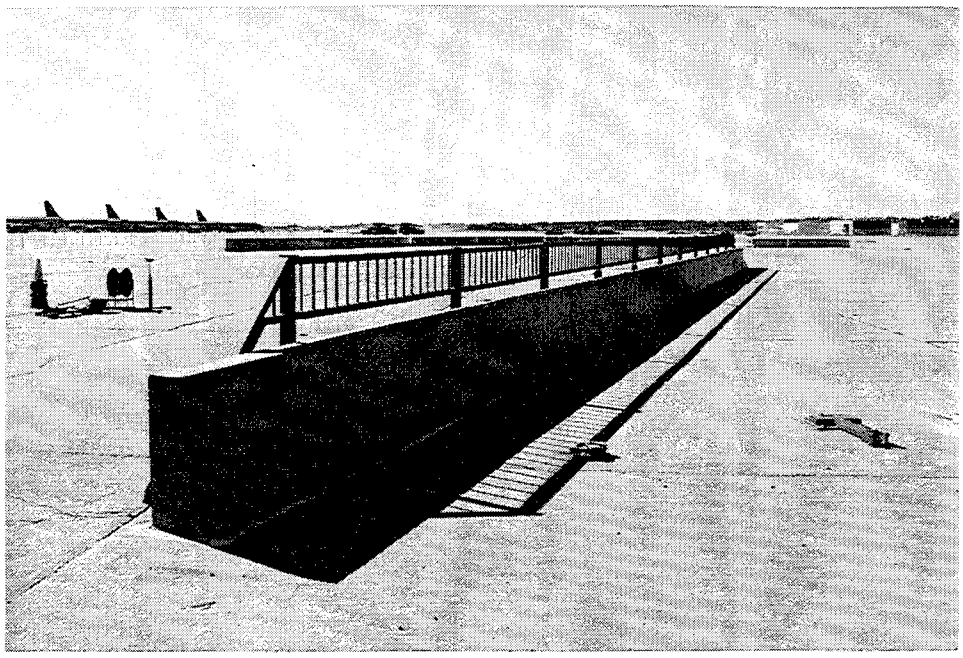

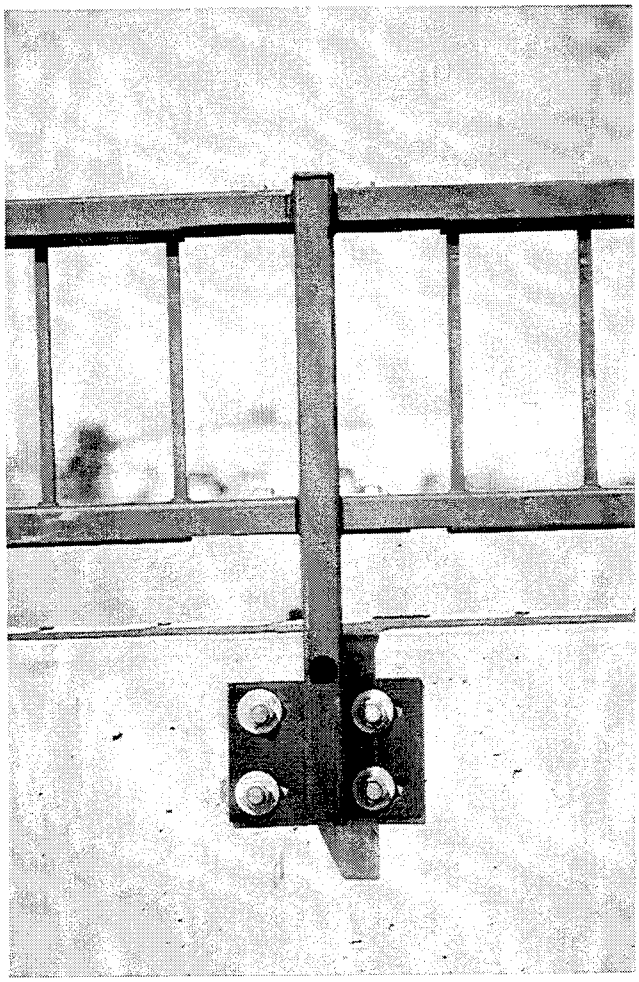

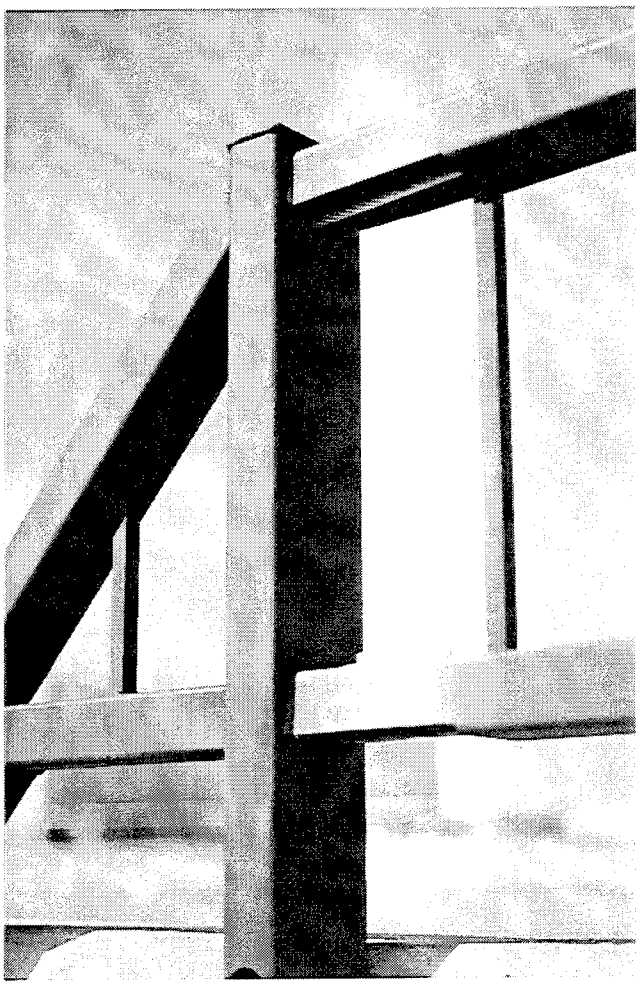

Figure 8. Combination Traffic/Bicycle Bridge Rail

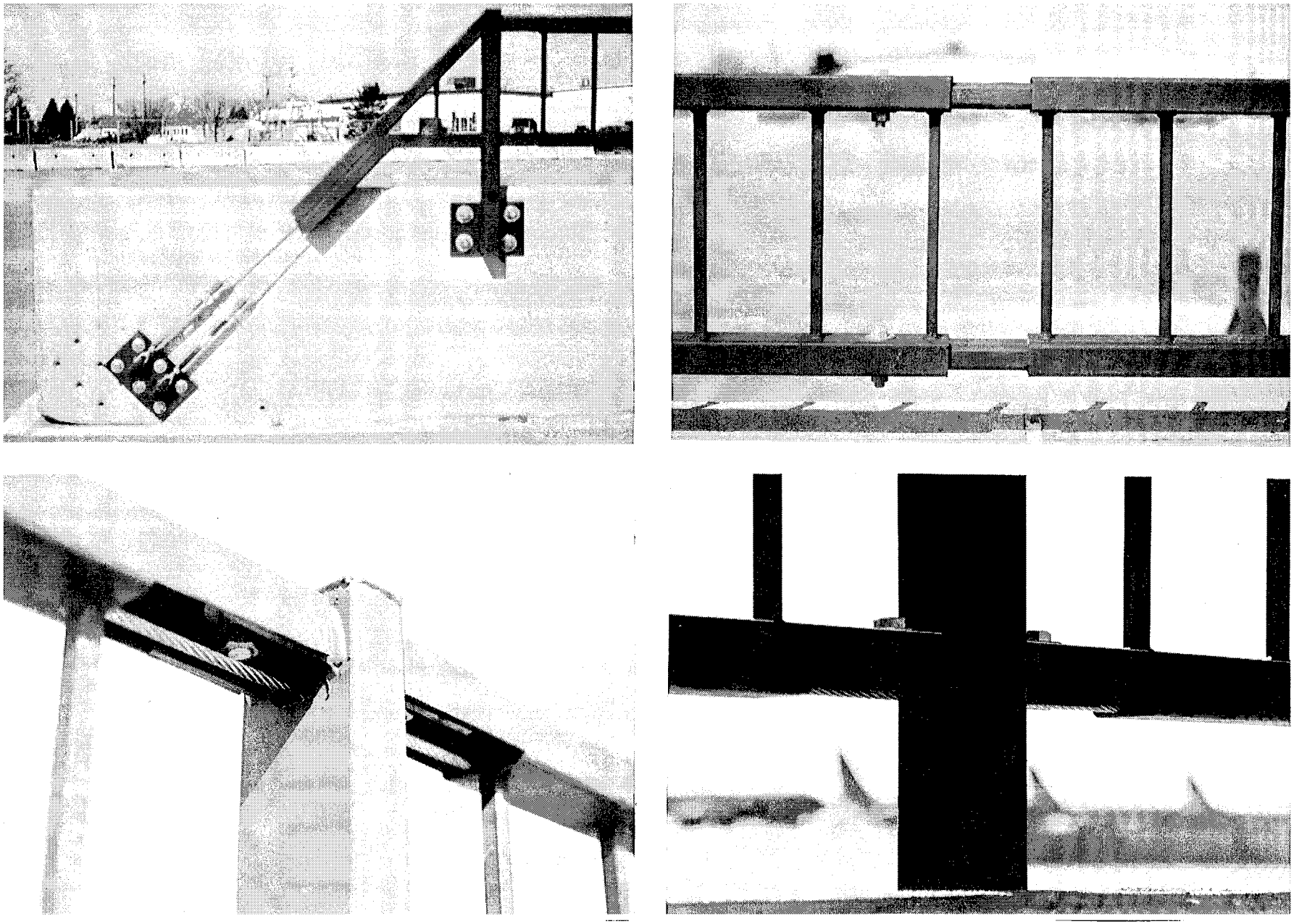

Figure 9. Combination Traffic/Bicycle Bridge Rail

7 TEST CONDITIONS

7.1 Test Facility

The testing facility is located at the Lincoln Air-Park on the NW end of the Lincoln Municipal Airport and is approximately 8.0 km NW of the University of Nebraska-Lincoln. The site is protected by an 2.44-m high chain-link security fence.

7.2 Vehicle Towing and Guidance System

A reverse cable tow system with a 1:2 mechanical advantage was used to propel the test vehicles. The distance traveled and the speed of the tow vehicle are one-half that of the test vehicle. The test vehicle was released from the tow cable before impact with the bridge rail. A fifth wheel, built by the Nucleus Corporation, was located on the tow vehicle and used in conjunction with a digital speedometer to increase the accuracy of the test vehicle impact speed.

A vehicle guidance system developed by Hinch (18) was used to steer the test vehicle. A guide-flag, attached to the front-left wheel and the guide cable, was sheared off before impact. The 9.5-mm diameter guide cable was tensioned to approximately 13.3 kN, and supported laterally and vertically every 30.48-m by hinged stanchions. The hinged stanchions stood upright while holding up the guide cable, but as the vehicle was towed down the line, the guide-flag struck and knocked each stanchion to the ground. The vehicle guidance system was approximately 457-m long for test MNPD-1 and 610-m long for test MNPD-2.

7.3 Test Vehicles

For test MNPD-1, a 1988 Ford F-250 ¾-ton pickup truck, test vehicle designation 2000P, was used as the test vehicle. The test inertial and gross static weights were 2,001 kg. The test vehicle is shown in Figure 10, and vehicle dimensions are shown in Figure 11.

Figure 10. Test Vehicle, Test MNPD-1

Date: 4/3/97 Test Number: MNPD-1 Model: F-250/WHITE

Make: FORD Vehicle I.D.#: 1FTHF25HXJNA86305

Tire Size: 235/85 R16 Year: 1988 Odometer: 96513

*(All Measurements Refer to Impacting Side)

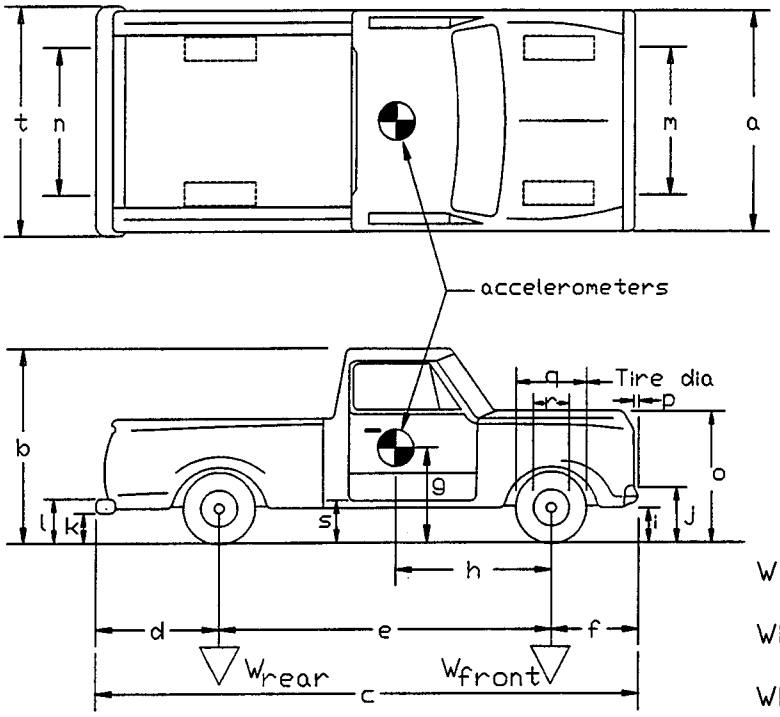

Vehicle Geometry - mm

a	1943	b	1880
c	5410	d	1308
e	3340	f	794
g	715	h	1422
i	406	j	708
k	546	l	711
m	1676	n	1638
o	1219	p	108
q	768	r	445
s	505	t	1930

Wheel Center Height Front 378

Wheel Center Height Rear 381

Wheel Well Clearance (FR) 860

Wheel Well Clearance (RR) 946

Engine Type V-8

Engine Size 302-5.0L

Transmission Type:

(Automatic) or Manual

FWD or (RWD) or 4WD

Weights

- kg	Curb	Test Inertial	Gross Static
W_{front}	1141	1149	1149
W_{rear}	888	852	852
W_{total}	2029	2001	2001

Note any damage prior to test: _____

Figure 11. Vehicle Dimensions, Test MNPD-1

For test MNPD-2, a 1988 Ford F-800 single unit truck, test vehicle designation 8000S, was used as the test vehicle. The test inertial and gross static weights were 8,002 kg. The test vehicle is shown in Figure 12, and vehicle dimensions are shown in Figure 13.

The Suspension Method (19) was used to determine the vertical component of the center of gravity for the 2000P test vehicle. This method is based on the principle that the center of gravity of any freely suspended body is in the vertical plane through the point of suspension. The vehicle was suspended successively in three positions, and the respective planes containing the center of gravity were established. The intersection of these planes pinpointed the location of the center of gravity. The Elevated Axle Method (20) was used to determine the vertical component of the center of gravity for the 8000S test vehicle. This method converts measured wheel weights at different elevations to the location of the vertical component of the center of gravity. The longitudinal component of the center of gravity for both test vehicles, and the vertical component of the 8000S test vehicle, were determined using measured axle weights. The location of the final centers of gravity are shown in Figures 11 and 13.

Square, black and white-checkered targets were placed on the vehicle to aid in the viewing and analysis of the high-speed film, as shown in Figures 10, 12, and 14 through 15. Round, checkered targets were placed on the center of gravity on the driver's side, the passenger's side, and on the roof of the vehicle. The other square targets were located at convenient reference locations for viewing from the high-speed cameras for film analysis.

The front wheels of the test vehicle were aligned for camber, caster, and toe-in values of zero so that the vehicles would track properly along the guide cable. Two 5B flash bulbs were mounted on both the hood and roof of the vehicles to pinpoint the time of impact with the bridge railing on

the high-speed film. The flash bulbs were fired by a pressure tape switch mounted on the front face of the bumper. A remote controlled brake system was installed in the test vehicle so the vehicle could be brought safely to a stop after the test.

7.4 Data Acquisition Systems

7.4.1 Accelerometers

One triaxial piezoresistive accelerometer system with a range of ±200 G's was used to measure the acceleration in the longitudinal, lateral, and vertical directions at a sample rate of 10,000 Hz. The environmental shock and vibration sensor/recorder system, Model EDR-4M6, was developed by Instrumented Sensor Technology (IST) of Okemos, Michigan and includes three differential channels as well as three single-ended channels. The EDR-4 was configured with 6 Mb of RAM memory and a 1,500 Hz lowpass filter. Computer software, "DynaMax 1 (DM-1)" and "DADiSP" were used to digitize, analyze, and plot the accelerometer data.

A backup triaxial piezoresistive accelerometer system with a range of ±200 G's was also used to measure the acceleration in the longitudinal, lateral, and vertical directions at a sample rate of 3,200 Hz. The environmental shock and vibration sensor/recorder system, Model EDR-3, was developed by Instrumented Sensor Technology (IST) of Okemos, Michigan. The EDR-3 was configured with 256 Kb of RAM memory and a 1,120 Hz lowpass filter. Computer software, "DynaMax 1 (DM-1)" and "DADiSP" were used to digitize, analyze, and plot the accelerometer data.

7.4.2 Rate Transducer

A Humphrey 3-axis rate transducer with a range of 250 deg/sec in each of the three directions (pitch, roll, and yaw) was used to measure the rates of motion of the test vehicle. The rate transducer was rigidly attached to the vehicles near the center of gravity of the test vehicle. Rate transducer

Figure 12. Test Vehicle, Test MNPD-2

Date: 4/15/97 Test Number: MNPD-2 Model: F-800/BLUE

Tire Sz FR: 11R 22.5 Odometer: 139545 Make: FORD

Tire Sz RR: 11R 22.5 V.I.N. #: 1FDPF708XJVA39576 Year: 1986

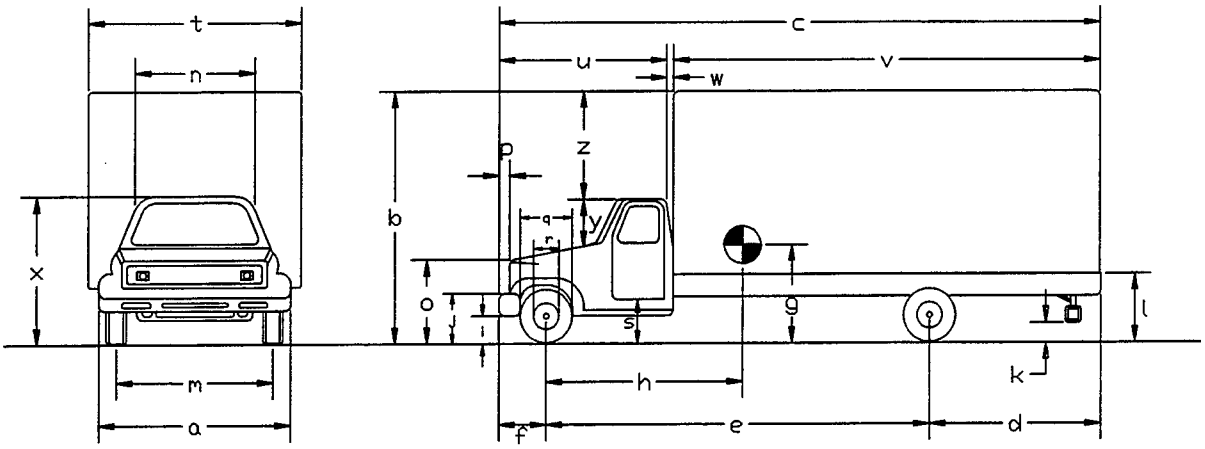

Vehicle Geometry (mm)

a> front bumper width 2375 j> fr. bump. top 787 s> bot. door hieght 864

b> overall height 3702 k> rr. bump. bot. 546 t> overall width 2426

c> overall length 7899 l> rr. frame top 1283 u> cab length 2527

d> rear overhang 2223 m> front track width 2032 v> trailer/box width 4921

e> wheel base 4794 n> roof width 1549 w> gap width 140

f> front overhang 902 o> hood height 1549 x> overall front height 2223

g> C.G. height 1250 p> bump. extension 76 y> roof-hood dist. 521

h> C.G. hor. distance 2972 q> fr. tire width 1016 z> roof height dif. 1448

i> fr. bump. bot. 483 r> fr. wheel width 610

wheel center height front 495

wheel center height rear 502

wheel well clearance (FR) 1143

wheel well clearance (RR) 1124

Engine Type V-8 (GAS)

Engine Size 429 CID

Transmission Type:

Automatic or (Manual)

FWD or (RWD) or 4WD

Weights (kg)

	Curb	Test Inertial	Gross Static
$W_{front\ axel}$	2232	3044	3044
$W_{rear\ axel}$	3022	4959	4959
W_{TOTAL}	5254	8002	8002

Ballast 2879

Note any damage prior to test: REAR FRAME DUE TO BOGIE TESTS

Figure 13. Vehicle Dimensions, MNPD-2

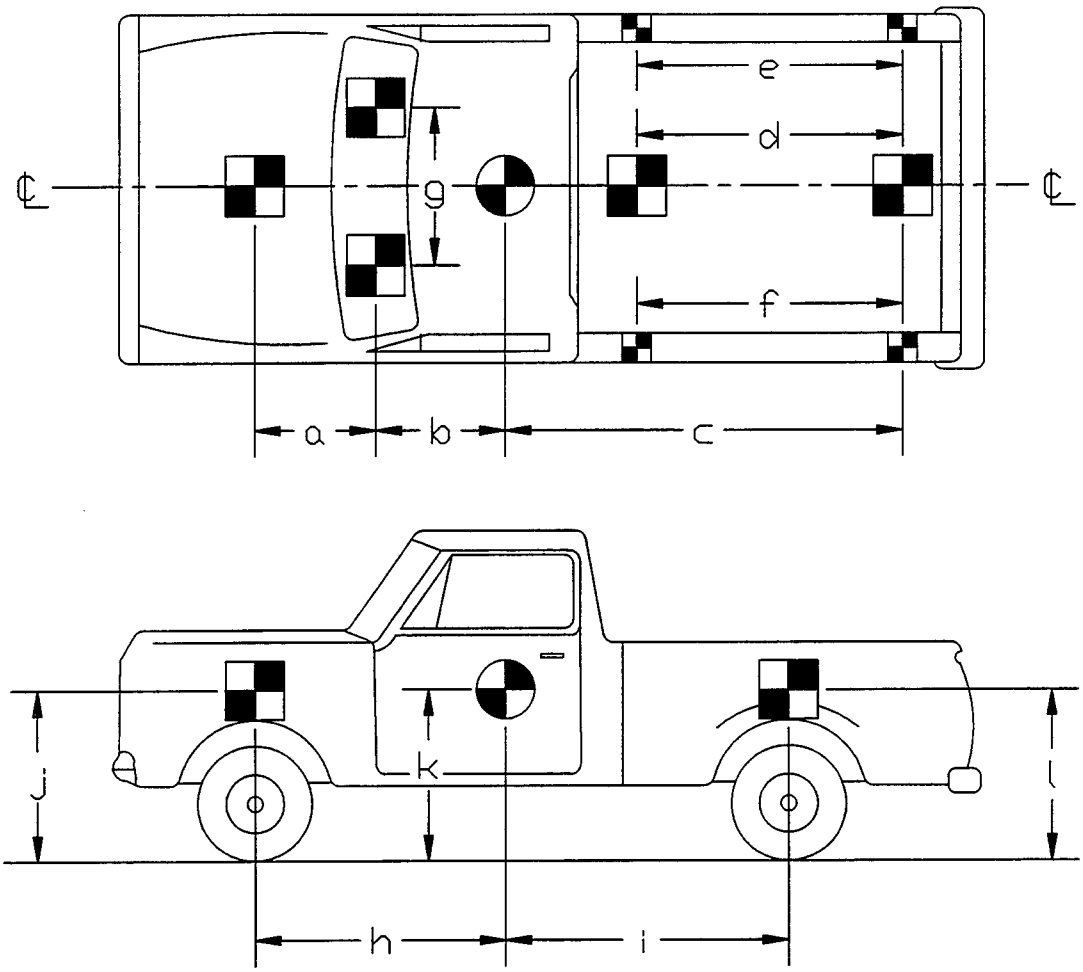

TEST #: MNPD-1

TARGET GEOMETRY (mm)

a 1130	b 584	c 2731	d 1638
e 2197	f 2197	g 889	h 1422
i 1918	j 1118	k 715	l 1168

Figure 14. Vehicle Target Locations, Test MNPD-1

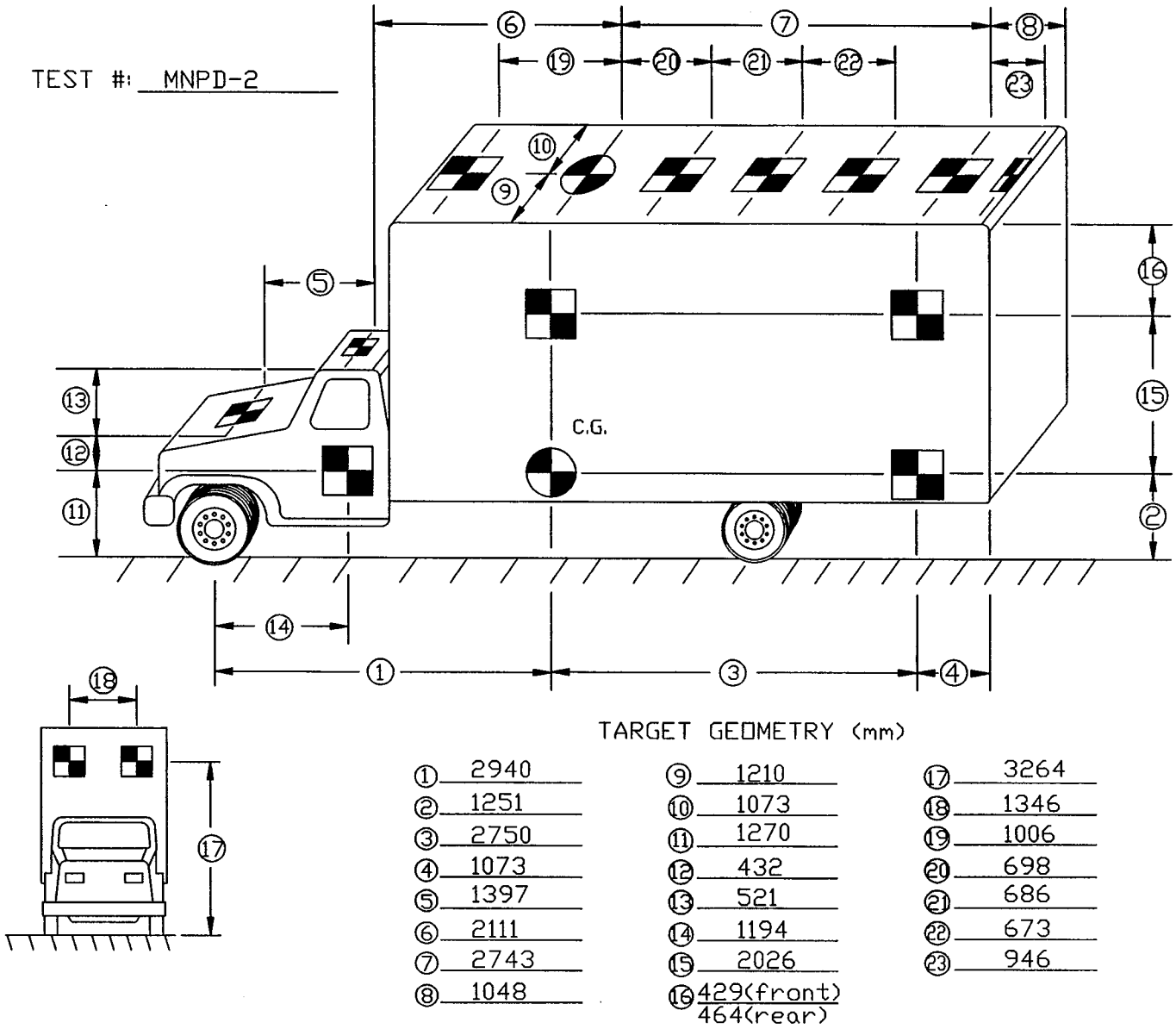

Figure 15. Vehicle Target Locations, Test MNPD-2

signals, excited by a 28 volt DC power source, were received through the three single-ended channels located externally on the EDR-4M6 and stored in the internal memory. The raw data measurements were then downloaded for analysis and plotting. Computer software, "DynaMax 1 (DM-1)" and "DADiSP" were used to digitize, analyze, and plot the rate transducer data.

7.4.3 High-Speed Photography

For test MNPD-1, five high-speed 16-mm Red Lake Locam cameras, with operating speeds of approximately 500 frames/sec, were used to film the crash test. A Locam, with a wide-angle 12.5-mm lens, was placed above the test installation to provide an overhead field of view perpendicular to the ground. A Locam, with a 76-mm lens, a SVHS video camera, and a 35-mm still camera were placed downstream from the impact point and had a field of view parallel to the barrier. A Locam, with a zoom lens, was placed on the traffic side of the barrier and had a field of view perpendicular to the barrier. A Locam, with a zoom lens, and a SVHS video camera were placed downstream and behind the barrier. A Locam, with a zoom lens, was located behind the barrier and upstream of impact. A schematic of all eight camera locations for test MNPD-1 is shown in Figure 16.

For test MNPD-2, four high-speed 16-mm Red Lake Locam cameras, with operating speeds of approximately 500 frames/sec, were used to film the crash test. A Locam, with a wide-angle 12.5-mm lens, was placed above the test installation to provide an overhead field of view perpendicular to the ground. A Locam, with a 76-mm lens, a SVHS video camera, and a 35-mm still camera were placed downstream from the impact point and had a field of view parallel to the barrier. A Locam, with a zoom lens, was placed downstream and behind the barrier. A Locam, with a zoom lens, was placed on the traffic side and had a field of view perpendicular to the barrier. A SVHS video camera was placed upstream of impact and behind the barrier. A schematic of all seven camera locations for test MNPD-2 is shown in Figure 17.

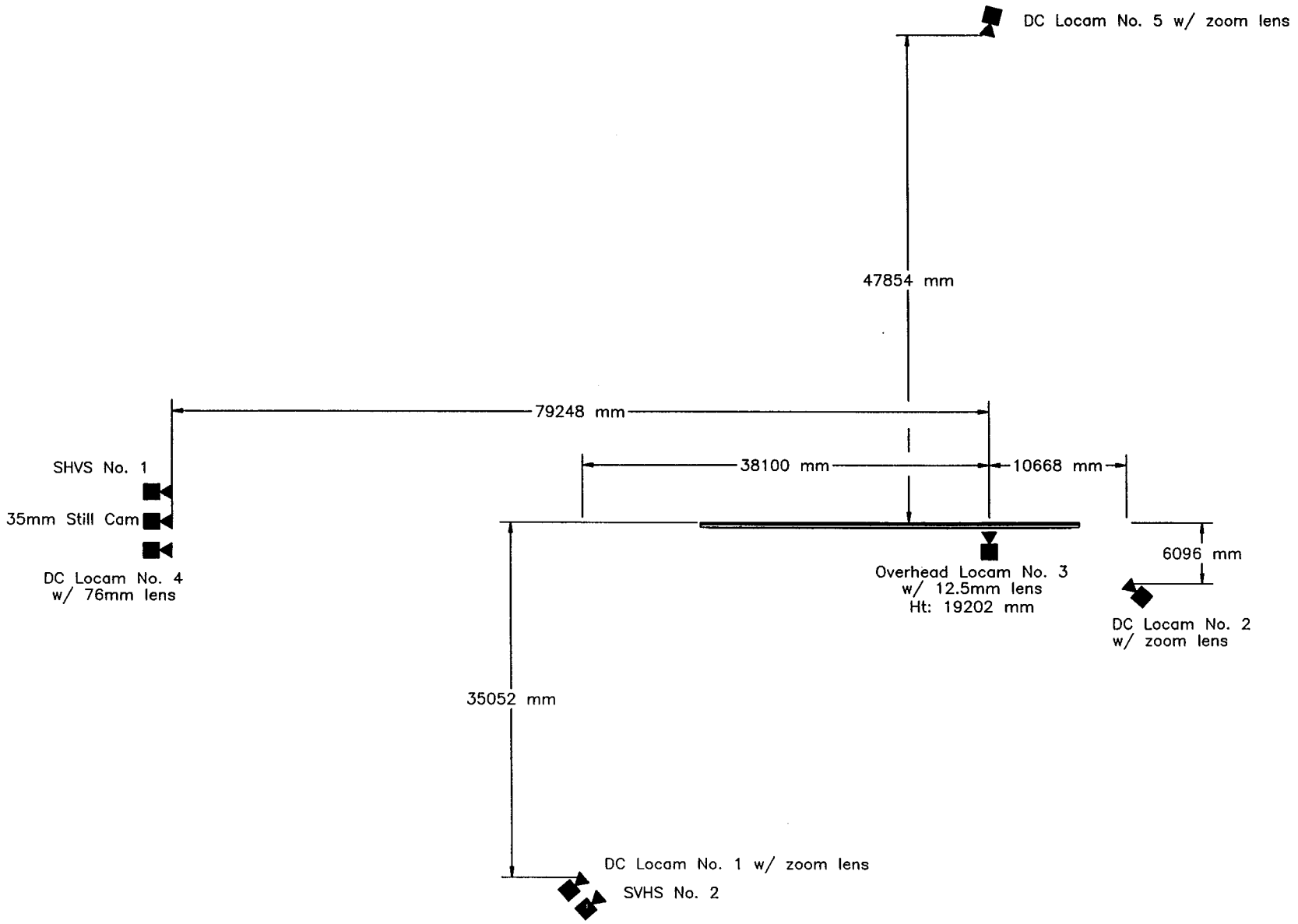

Figure 16. Location of High-Speed Cameras, Test MNPD-1

The film was analyzed using the Vanguard Motion Analyzer. Actual camera speed and camera divergence factors were considered in the analysis of the high-speed film.

7.4.4 Pressure Tape Switches

For tests MNPD-1 and MNPD-2, five pressure-activated tape switches, spaced at 2-m intervals, were used to determine the speed of the vehicle before impact. Each tape switch fired a strobe light which sent an electronic timing signal to the data acquisition system as the left front tire of the test vehicle passed over it. Test vehicle speeds were determined from electronic timing mark data recorded on "EGAA" software. Strobe lights and high-speed film analysis are used only as a backup in the event that vehicle speeds cannot be determined from the electronic data.

7.4.5 Guardrail Instrumentation

7.4.5.1 Strain Gauges

For test MNPD-1, eight strain gauges were installed on the two critical posts, nos. 4 and 5, to measure post strain at selected regions. The four gauges on each critical post were centered on each side at 38-mm above the top of the breakaway hole in the post. Two additional gauges were mounted on the cable turnbuckles to measure cable tension. The strain gauge positions are shown in Figure 18. For test MNPD-2, two strain gauges were installed on the turnbuckles to monitor the cable tension. The strain gauge positions are shown in Figure 18.

For both tests, weldable strain gauges were used and consisted of gauge type LWK-06-W250B-350. The nominal resistance of the gauges was 350.0 ± 1.4 ohms with a gauge factor equal to 2.02. The operating temperature limits of the gauges was -195 to +260 degrees Celsius. The strain limits of the gauges were 0.5% (5000 $\mu\varepsilon$) in tension or compression. The strain gauges were manufactured by the Micro-Measurements Division of Measurements Group, Inc. of Raleigh, North

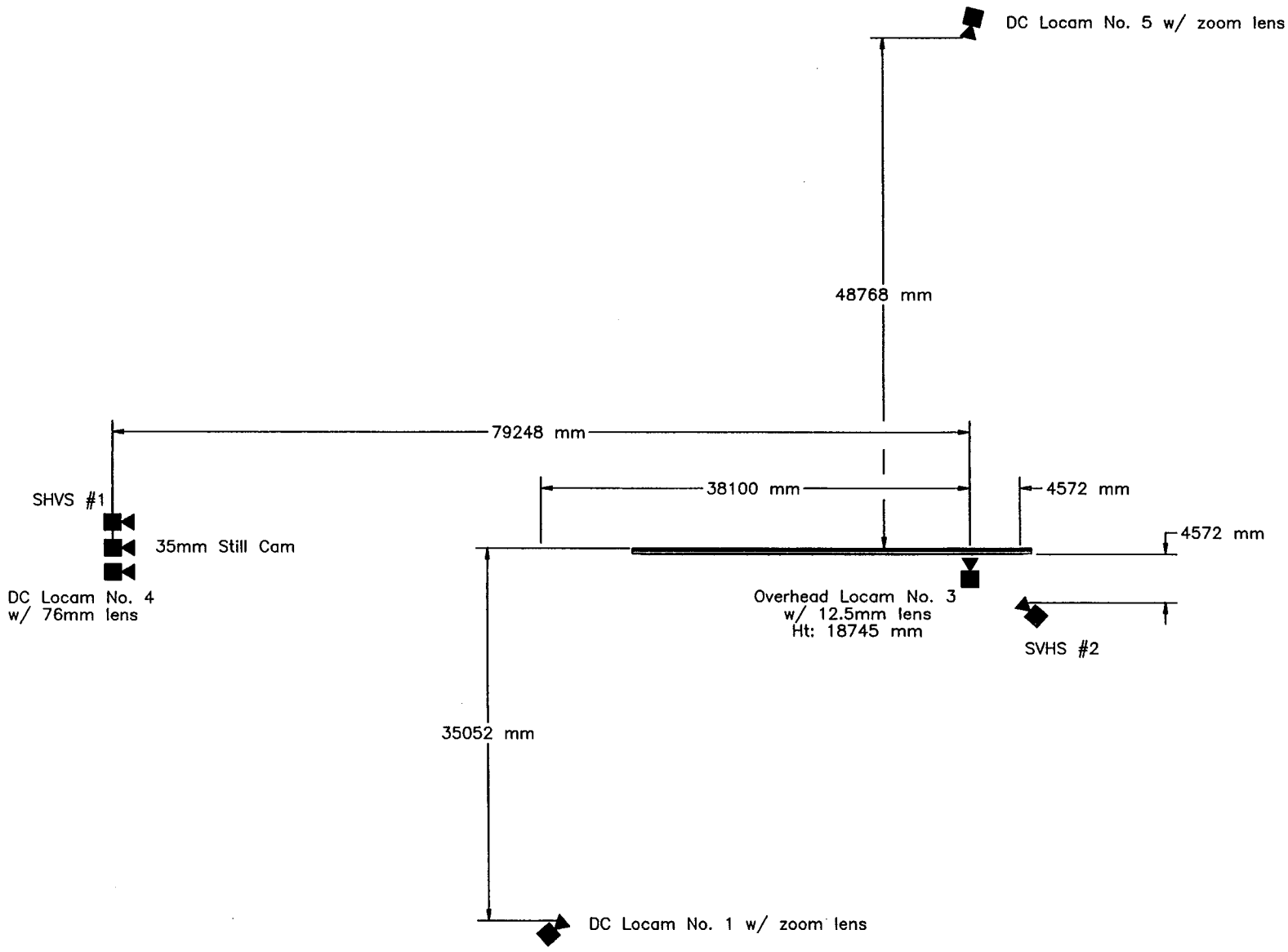

Figure 17. Location of High-Speed Cameras, Test MNPD-2

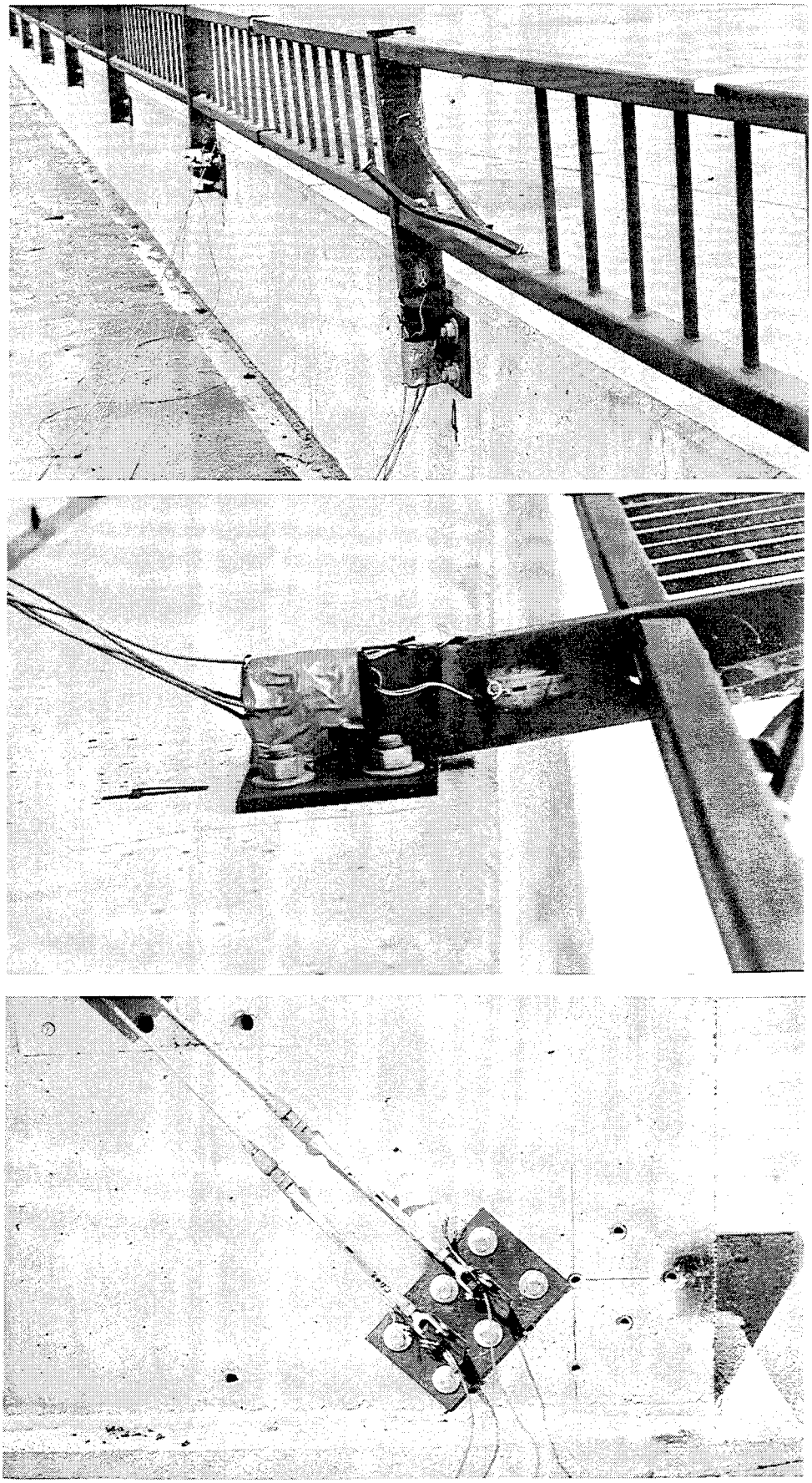

Figure 18. Strain Gauge Locations, Tests MNPD-1 and MNPD-2

Carolina. The installation procedure required that the metal surface be clean and free from debris and oxidation. Once the surface had been prepared, the gauges were spot welded to the test surface.

A Measurements Group Vishay Model 2310 signal conditioning amplifier was used to condition and amplify the low-level signals to high-level outputs for multichannel, simultaneous dynamic recording on "Test Point" software. After each signal was amplified, it was sent to a Keithley Metrabyte DAS-1802HC data acquisition board, and then stored permanently on the portable computer. The sample rate for all gauges was 10,000 samples per second (10,000 Hz), and the duration of sampling was 8 seconds.

8 CRASH TEST NO. 1

8.1 Test MNPD-1

The 2,001-kg pickup truck impacted the combination traffic/bicycle bridge rail at a speed of 105.2 km/hr and an angle of 25.5 degrees. A summary of the test results and the sequential photographs are shown in Figure 19. Additional sequential photographs are shown in Figure 20. Documentary photographs of the crash test are shown in Figures 21 and 22.

8.2 Test Description

Initial impact occurred 2-m upstream from the center of post no. 4, as shown in Figure 23. Upon impact with the bridge rail, the left-front corner of the pickup crushed inward, except for the engine hood which protruded over the top of the bridge rail. At 0.038 sec after impact, the left-front tire climbed up the face of the concrete rail, and the hood protruded into the plane of the bicycle portion of the bridge rail. At 0.056 sec, the engine hood snagged on post no. 4. This contact twisted the hood and pushed it back into the windshield, thus causing it to crack. After 0.112 sec into the crash event, the top of the driver's side door opened, and the left-rear tire impacted the bridge rail and became airborne. At 0.226 sec, the truck was parallel with the bridge rail and had a velocity of 40.91 km/hr. At that same instance, the right-rear tire became airborne, resulting in the entire truck being airborne. At 0.360 sec, the pickup truck reached a maximum height above the concrete surface with the hood popped open and rotated upward. At this same time, the truck exited the bridge rail at a speed of 15.34 km/hr and an angle of 1.7 degrees. By 0.620 sec, both front tires landed on the ground, and at 0.888 sec the rear of the truck contacted the ground. At 1.024 sec, the truck reached its maximum roll angle of 7.2 degrees. The vehicle's post-impact trajectory is shown in Figure 19. The vehicle came to rest 63.8 m downstream from impact and 9.8 m laterally behind a line projected parallel to the traffic side of the bridge rail.

8.3 Barrier Damage

Damage to the combination traffic/bicycle bridge rail was minimal, as shown in Figures 24 and 25. Damage to the concrete rail consisted of tire marks and minor gouging. No concrete cracking was found to have occurred during the crash test. The damage to the bicycle rail included light contact marks on the rail between the downstream side of post nos. 3 to the downstream side of post no. 4. Plastic deformations were observed in post nos. 3 and 4. Damage to spindles on the upstream side of post no. 4 ranged from moderate deformations to complete fracture of the welds at the top and bottom of one spindle. The cables inside the upper and lower rails of the bicycle rail did not fracture during the crash test and were found to be taut. The maximum dynamic deflections for posts and rail were 69 mm at post no. 4 and 55 mm at the midspan between post nos. 4 and 5, respectively.

8.4 Vehicle Damage

Vehicle damage was moderate, as shown in Figures 26 and 27. The front bumper, left-front quarter panel, and left-front inner fender well were crushed inward. The engine was twisted and shoved toward the right side of the vehicle. During impact, the left-front wheel assembly became dislodged as the outer steel rim fractured away from the inner region attached to the wheel hub. The tire was ripped and deflated. The left door bent outward at the top, causing a crease near the keyhole. The hood disengaged at the right-side attachment, was crushed severely on the left side, and shoved into the left side of the windshield which cracked. Longitudinal deformations, due to vehicle-rail interlock, were observed along the vehicle's left side. The steel frame was bent and twisted along its entire length, causing the box to contact and crease at the right rear of the cab. Maximum occupant compartment deformations to the floorboard and/or firewall in the lateral, longitudinal, and vertical directions were 203 mm, 146 mm, and 108 mm, respectively, as shown in Figure 26.

8.5 Occupant Risk Values

The normalized longitudinal and lateral occupant impact velocities were determined to be 6.58 m/sec and 7.83 m/sec, respectively. The maximum 0.010-sec average occupant ridedown decelerations in the longitudinal and lateral directions were 5.06 g's and 7.57 g's, respectively. It is noted that the occupant impact velocities (OIV) and occupant ridedown decelerations (ORD) were within the suggested limits provided in NCHRP Report No. 350. The results of the occupant risk, determined from the accelerometer data, are summarized in Figure 19. Results are shown graphically in Appendix A. The results from the rate transducer are shown graphically in Appendix B.

8.6 Discussion

The analysis of the MNPD-1 test results showed that the combination bridge rail adequately contained and redirected the vehicle with controlled lateral displacement of the bridge rail. Minor deformations to the occupant compartment were evident but not considered excessive enough to cause serious injuries to the occupants. The vehicle remained upright both during and after the collision. Vehicle roll, pitch, and yaw angular displacements were noted, but they were deemed acceptable because they did not adversely influence occupant safety criteria or cause rollover. After collision, the vehicle's trajectory intruded slightly into adjacent traffic lanes but was determined to be acceptable. In addition, the vehicle's exit angle was less than 60 percent of the impact angle. Therefore, test MNPD-1 conducted on the Minnesota Combination Traffic/Bicycle Bridge Rail was determined to be acceptable according to the NCHRP Report 350 criteria.

8.7 Barrier Instrumentation Results

For test MNPD-1, strain gauges were located on the cable anchor turnbuckles and post nos. 4 and 5. The results of the strain gauge analysis are provided in Table 4. The maximum turnbuckle

load was determined to be 4.79 kN, while the maximum measured post strain was found to be 2,383 μ stain. Results are also shown graphically in Appendix C.

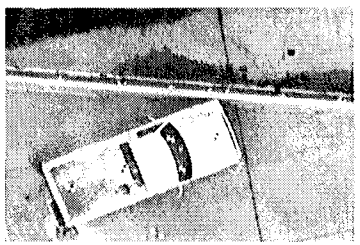

0.000 sec

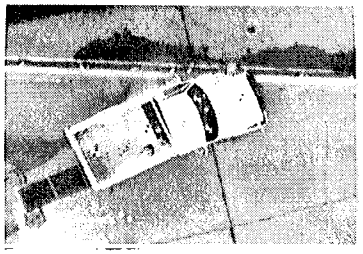

0.065 sec

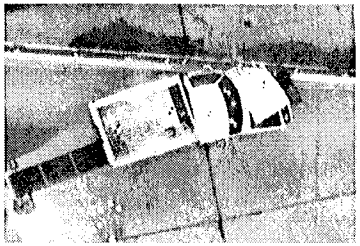

0.102 sec

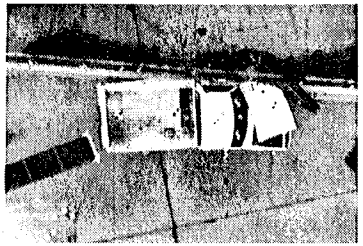

0.172 sec

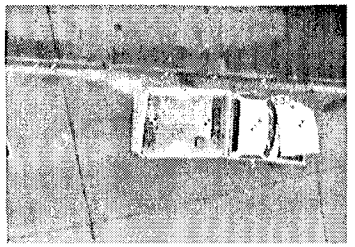

0.309 sec

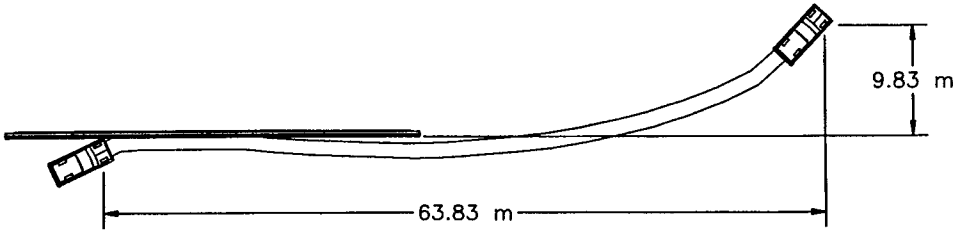

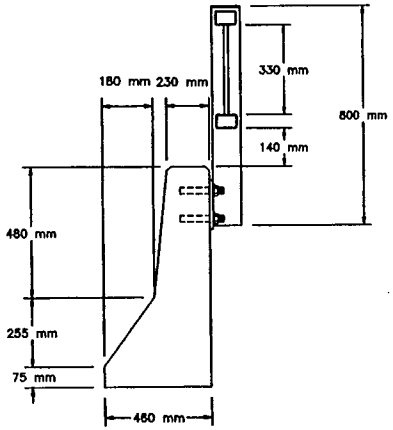

- Test Number MNPD-1
- Date 4/3/97
- Appurtenance . . . . . Minnesota Combination Traffic/Bicycle Bridge Rail
- Total length . . . . . 36.6 m
- Concrete Traffic Rail . . . . . New Jersey Safety Shape
  - Length . . . . . 6.1 m
  - Height . . . . . 810 mm
  - Base Width . . . . . 460 mm
  - Top Width . . . . . 230 mm
- Steel Rail . . . . . TS 76 x 51 x 3 mm - A500 Grade B
- Steel Spindles . . . . . 16 mm Square Bars - A36
- Steel Posts . . . . . TS 102 x 51 x 3 mm - A500 Grade B
- Vehicle Model . . . . . 1988 Ford F-250 ¾-Ton Pickup
  - Curb . . . . . 2,020 kg
  - Test Inertia . . . . . 2,001 kg
  - Gross Static . . . . . 2,001 kg
- Vehicle Speed
  - Impact . . . . . 105.2 km/hr
  - Exit . . . . . 15.3 km/hr
- Vehicle Angle
  - Impact . . . . . 25.5 deg
  - Exit . . . . . 1.7 deg
- Vehicle Stability . . . . . Satisfactory
- Occupant Ridedown Deceleration (10 msec avg.)
  - Longitudinal . . . . . 5.06 G's < 20 G's
  - Lateral (not required) . . . . . 7.57 G's
- Occupant Impact Velocity (Normalized)
  - Longitudinal . . . . . 6.58 m/s < 12 m/s
  - Lateral (not required) . . . . . 7.83 m/s
- Vehicle Damage . . . . . Moderate
  - TAD[21] 11-LFQ-6
  - SAE[22] 11-LDAW4
- Vehicle Stopping Distance . . . . . 63.8 m downstream 9.8 m lateral behind
- Bridge Rail Damage . . . . . Minimal
- Maximum Deflections
  - Permanent Set . . . . . NA
  - Dynamic . . . . . 69 mm

Figure 19. Summary of Test Results, Test MNPD-1.

0.000 sec

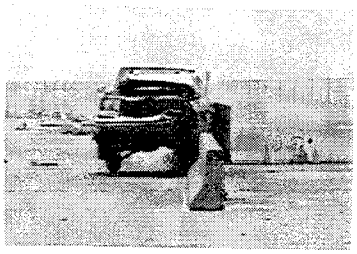

0.226 sec

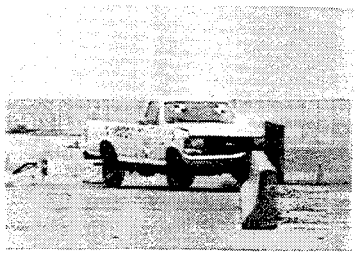

0.038 sec

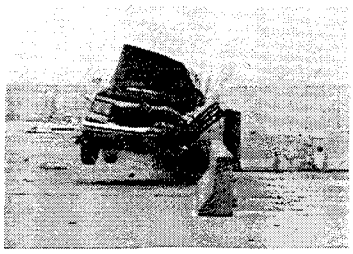

0.360 sec

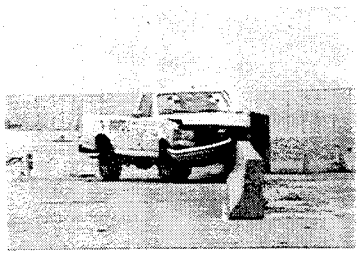

0.056 sec

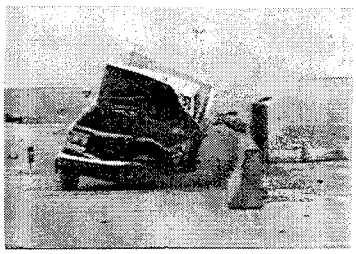

0.620 sec

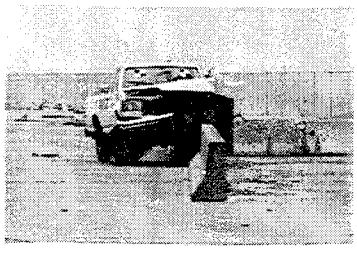

0.112 sec

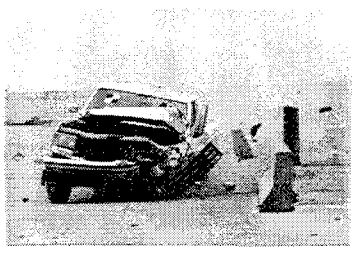

0.888 sec

Figure 20. Additional Sequential Photographs, Test MNPD-1.

Figure 21. Documentary Photographs, Test MNPD-1

Figure 22. Documentary Photographs, Test MNPD-1

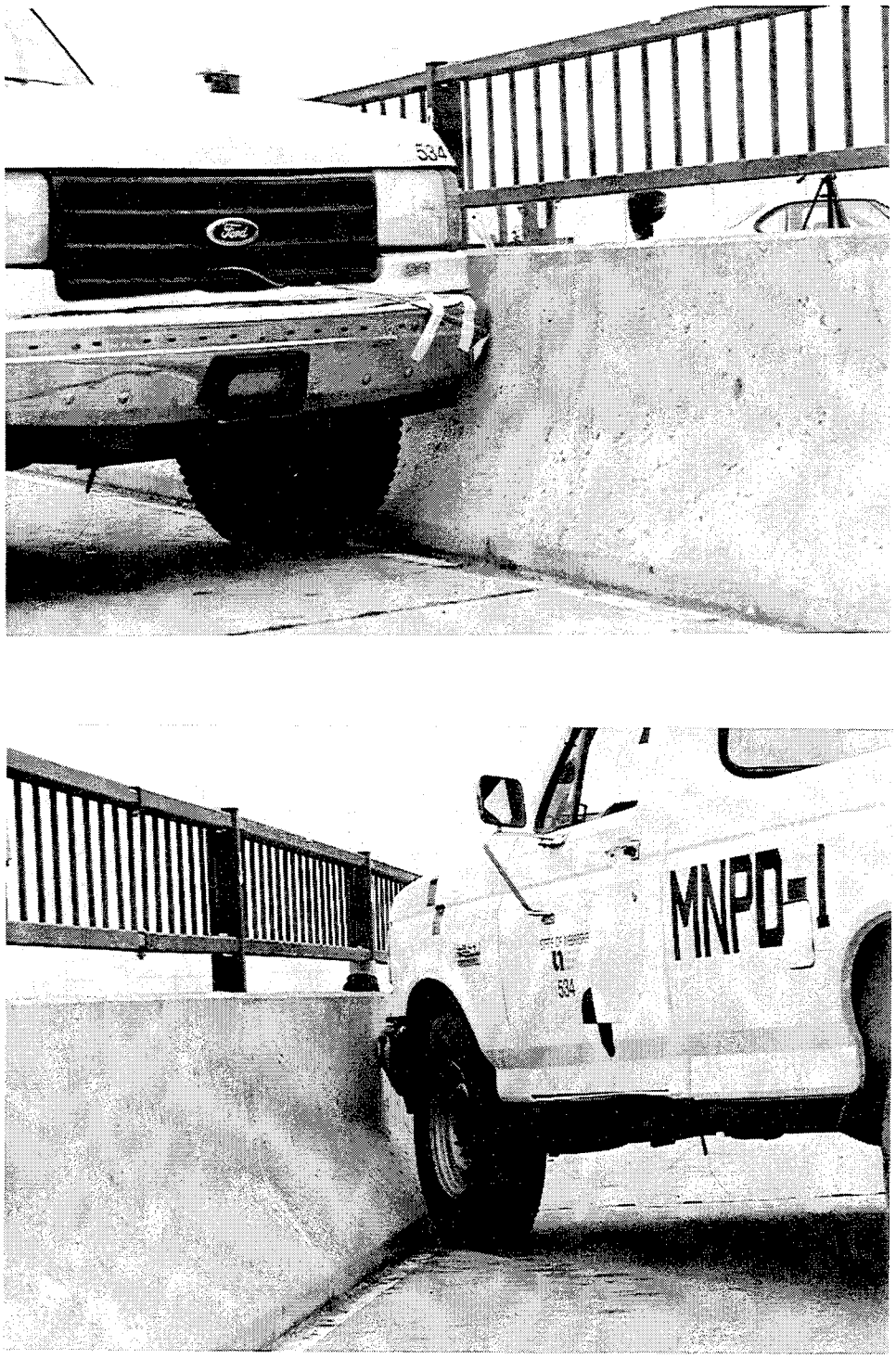

Figure 23. Impact Location, Test MNPD-1

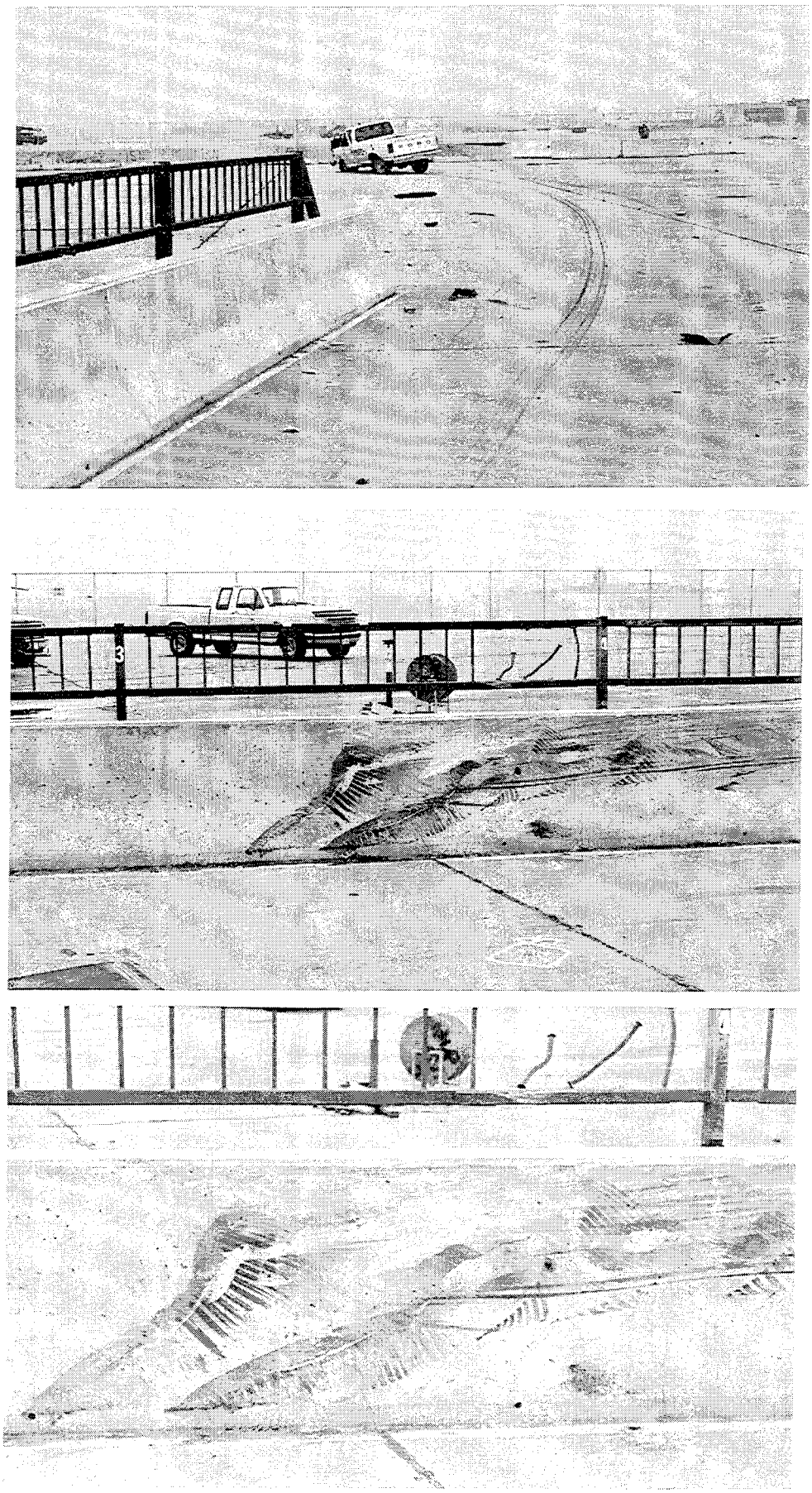

Figure 24. Barrier Damage, Test MNPD-1

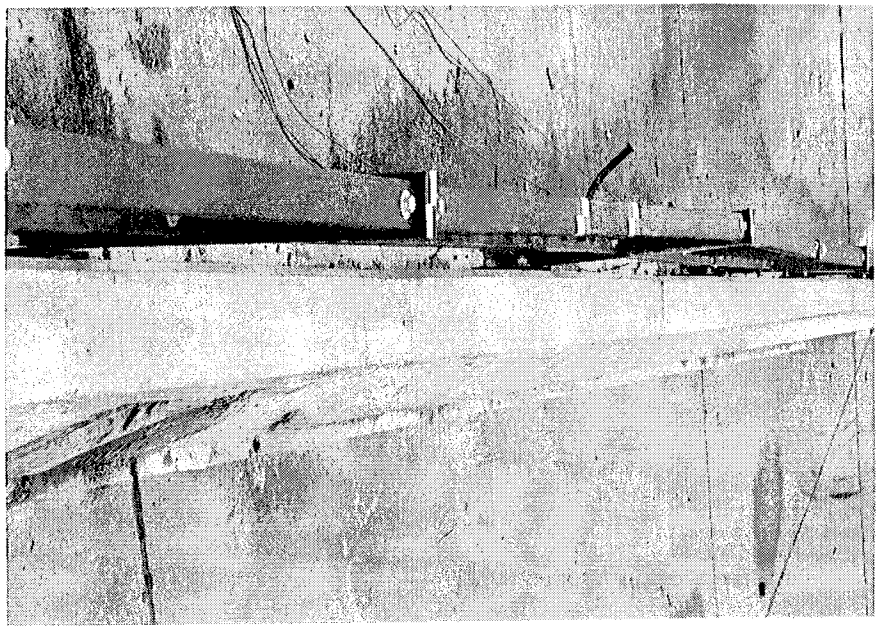

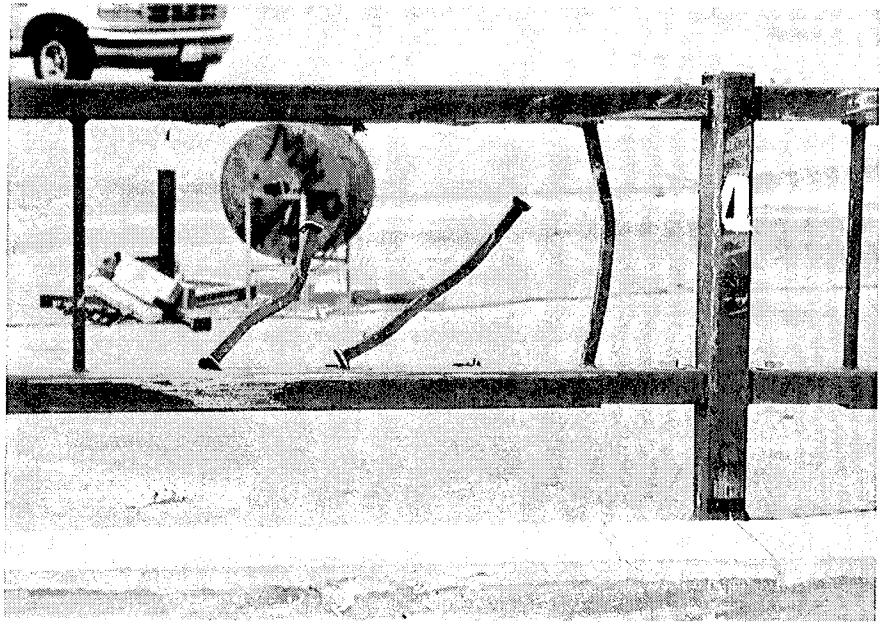

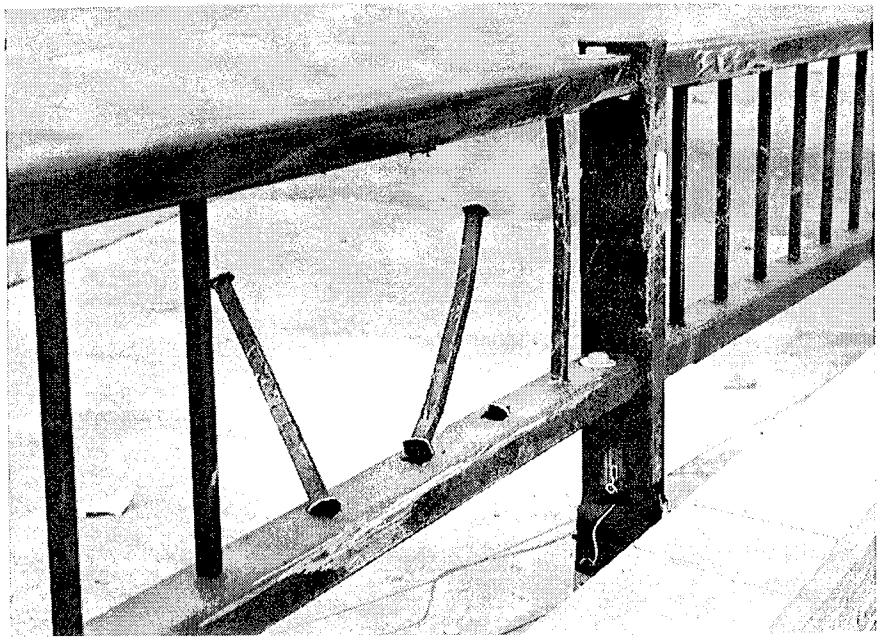

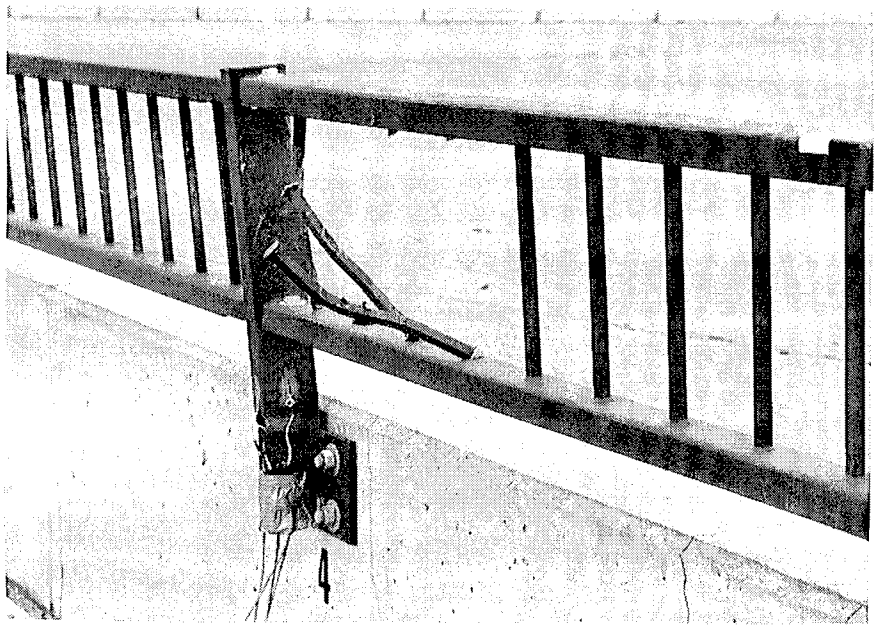

Figure 25. Barrier Damage, Test MNPD-1 (Continued)

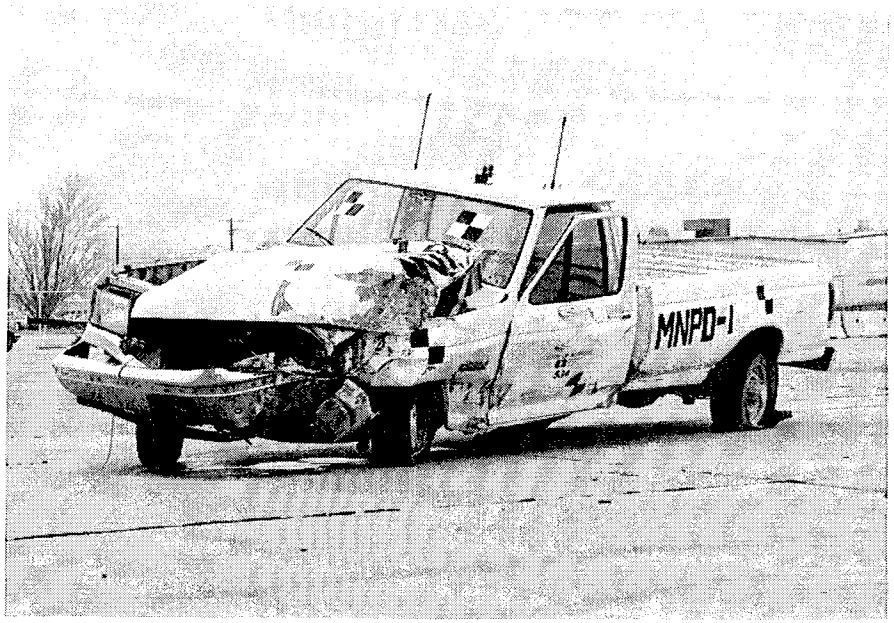

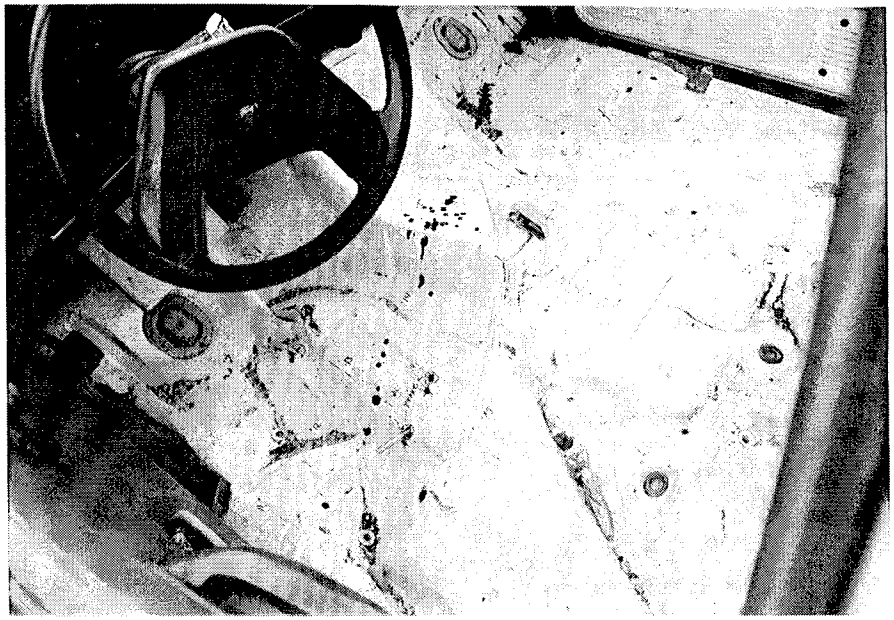

Figure 26. Vehicle Damage, Test MNPD-1

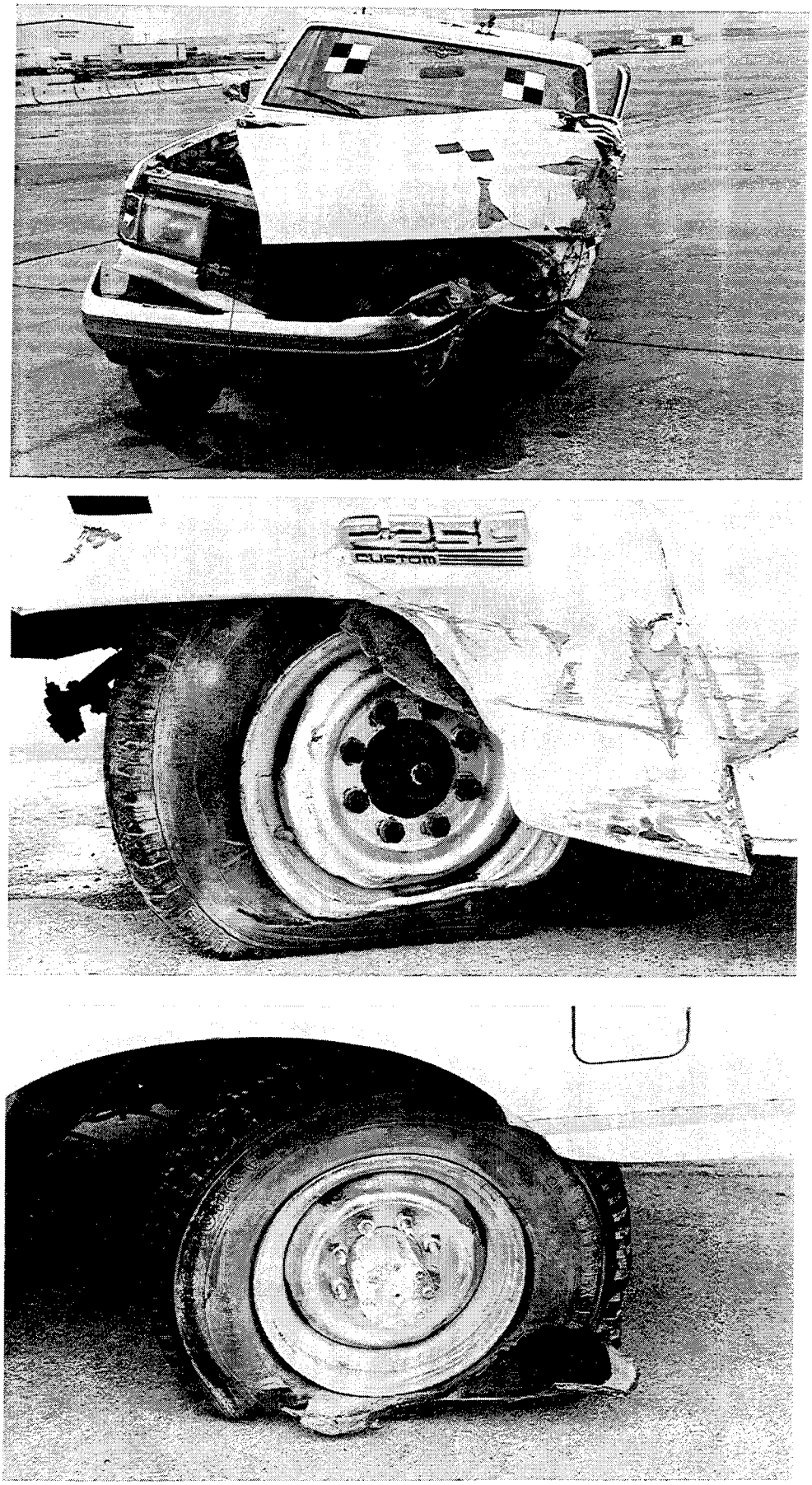

Figure 27. Vehicle Damage, Test MNPD-1 (Continued)

Table 4. Strain Gauge Results, Test MNPD-1

Hardware Type	Strain Gauge No.	Strain Gauge Location	Maximum μ Strain[1] (mm/mm)	Maximum Stress[2] (MPa)	Maximum Load[3] (kN)	Comments
Cable Turnbuckle	1	Note[4]	NA	NA	4.79	Upstream end- Upper rail cable
	2	Note[5]	NA	NA	3.55	Upstream end- Lower rail cable
Post	3	Post 4	1533	317.0	NA	Upstream-side[6]
	4	Post 4	2383	NA	NA	Traffic-side[6]
	5	Post 4	953	197.1	NA	Downstream-side[6]
	6	Post 4	1656	NA	NA	Back-side[6]
	7	Post 5	258	53.4	NA	Upstream-side[6]
	8	Post 5	686	142.0	NA	Traffic-side[6]
	9	Post 5	263	54.4	NA	Downstream-side[6]
	10	Post 5	746	154.4	NA	Back-side[6]

[1] - All strain values are shown in the absolute value only.
[2] - All elastic stress values are shown as the absolute value only and calculated by multiplying the strain by the modulus of elasticity equal to 207,000 MPa. Minimum yield stress for the post is 317 MPa.
[3] - All load values are shown in the absolute value only.
[4] - Strain gauge location is the cable turnbuckle on the upstream end of the upper rail cable.
[5] - Strain gauge location is the cable turnbuckle on the upstream end of the lower rail cable.
[6] - Strain gauge location is 559 mm from the top of the post.
NA - Not Available

9 CRASH TEST NO. 2

9.1 Test MNPD-2

The 8,002-kg single-unit truck impacted the combination traffic/bicycle bridge rail at a speed of 82.1 km/hr and an angle of 14.7 degrees. A summary of the test results and the sequential photographs are shown in Figure 28. Additional sequential photographs are shown in Figure 29. Documentary photographs of the crash test are shown in Figures 30 through 32.

9.2 Test Description

Initial impact occurred 2-m upstream from the center of post no.3, or 0.56-m upstream from the first bridge rail splice, as shown in Figure 33. Upon impact, the left-front tire and bumper corner began to deform. After 0.043 sec after impact, the left-front tire climbed to its maximum height on the face of the concrete bridge rail, and the left-front fender rode on top of the concrete bridge rail as the front bumper crushed inward. At 0.118 sec, the front of the truck pitched upward, the left-front fender raised off the top of the bridge rail, and the right-front tire became airborne. At the same time, the left-front fender began to contact the bicycle railing. At 0.204 sec after impact, the left-rear tire contacted the bridge rail while the truck box rolled toward the rail, thus causing the right-front tire to become airborne. At 0.212 sec, the right-front fender was elevated to a height above the top of the bicycle rail. At that time, the left-front corner of the box impacted and deformed the bicycle rail, thereby causing most of the damage to the bicycle rail. At 0.427 sec, the truck rolled counterclockwise toward the rail while the right-rear tire came off the ground. Simultaneously, the left-front tire was pushed back and inward, twisting the front axle and turning the right-front tire nearly perpendicular to the truck's path of travel. At 0.702 sec, the twisted right-front tire struck the ground, and at 0.756 sec the truck box reached its maximum roll angle of 26.9 degrees while leaning

over the top of the bridge rail. At 1.058 sec, the right-rear tires contacted the ground as the truck began to roll away from the bridge rail. At 1.504 sec after impact, the truck exited the bridge rail. At 2.351 sec, the left-front corner of the truck contacted the ground, and the truck continued in a stable upright position. The vehicle's post-impact trajectory is shown in Figure 28. The vehicle came to rest 68.3 m downstream from impact and 4.39 m away from the traffic side of the bridge rail.

9.3 Barrier Damage

Damage to the combination traffic/bicycle bridge rail was moderate, as shown in Figures 34 through 38. The damage consisted of tire and gouge marks on the concrete bridge rail, permanent deformations in the steel bicycle rail, and permanent set in the steel posts. Contact marks were found on both the concrete and the steel rail. Deformation to the steel rail included spindle deformations, fracture of the spindles away from the rail tubes, and extension of the gaps between rail splices. As measured in the field, the maximum gaps between rail splices in the top and bottom rails were 241 mm and 203 mm, respectively.

Post damage occurred to all posts, except nos. 1, 2, 11, and 12. Contact marks were found on the bicycle rail between post no. 3 through 11. Post no. 3 fractured on the traffic-side face near the breakaway hole. Post no. 4 also fractured on the traffic-side at the breakaway hole and was bent backward. Post nos. 5 and 6 ruptured almost through the entire depth and bent nearly 90 degrees from the vertical. Post no. 7 sustained the most damage as it was completely broken off. Post no. 8 ruptured along the welds connecting the post to the steel plate. Post no. 9 fractured halfway through the breakaway hole while post no. 10 bent at the breakaway hole. The cables inside the upper and lower steel rails exhibited no damage and constrained the large pieces of loose steel rail. A total of nineteen spindles were detached from the bicycle railing - seventeen on the back side and two on the

traffic side of the bridge railing. The maximum dynamic post and rail deflections were 415 mm at post no. 4 and 456 mm at the midspan between post nos. 4 and 5, respectively.

9.4 Vehicle Damage

Vehicle damage was moderate, as shown in Figure 39. Most of the vehicle damage occurred near the left-front corner of the vehicle, consisting primarily of damage to the fender, hood, bumper, and running board. This damage also included disengagement of the front axle assembly, resulting in the vehicle coming to a stop on the front springs. The left-front corner of the truck box was severely worn due to contact with the bridge rail. The truck rail under the left side of the box was twisted and bent. In addition, the truck box was pushed forward against the cab. There was no occupant compartment deformations to the interior of the cab nor fracture of the windshield.

9.5 Occupant Risk Values

The normalized longitudinal and lateral occupant impact velocities were determined to be 2.37 m/sec and 2.69 m/sec, respectively. The maximum 0.010-sec average occupant ridedown decelerations in the longitudinal and lateral directions were 5.18 g's and 4.30 g's, respectively. It is noted that the occupant impact velocities (OIV) and occupant ridedown decelerations (ORD) were within the suggested limits provided in NCHRP Report No. 350. The results of the occupant risk, determined from the accelerometer data, are summarized in Figure 28. Results are shown graphically in Appendix D. The results from the rate transducer are shown graphically in Appendix E.

9.6 Discussion

The analysis of the MNPD-2 test results showed that the combination bridge rail adequately contained and redirected the vehicle with controlled lateral displacement of the bridge rail. No deformations were found to have occurred to the occupant compartment. The vehicle remained

upright both during and after the collision. Vehicle roll, pitch, and yaw angular displacements were noted, but they were deemed acceptable because they did not adversely influence occupant safety criteria or cause rollover. After collision, the vehicle's trajectory intruded slightly into adjacent traffic lanes but was determined to be acceptable. In addition, the vehicle's exit angle was less than 60 percent of the impact angle. Therefore, test MNPD-2 conducted on the Minnesota Combination Traffic/Bicycle Bridge Rail was determined to be acceptable according to the NCHRP Report 350 criteria.

9.7 Barrier Instrumentation Results

For test MNPD-2, strain gauges were located on the cable anchor turnbuckles. The results of the strain gauge analysis are provided in Table 5. The maximum turnbuckle load was determined to be 46.74 kN. Results are shown graphically in Appendix F.

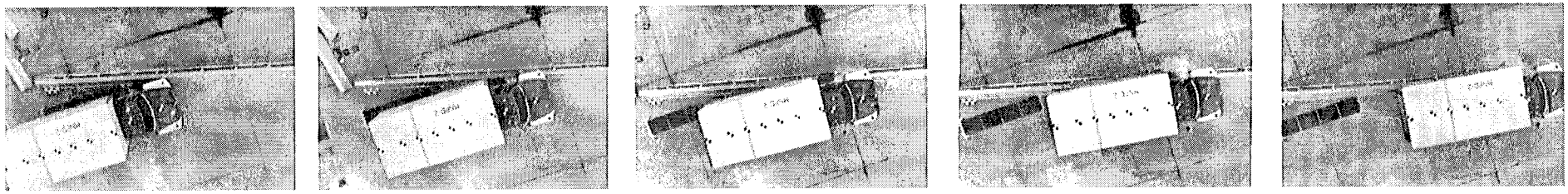

0.000 sec 0.115 sec 0.205 sec 0.273 sec 0.340 sec

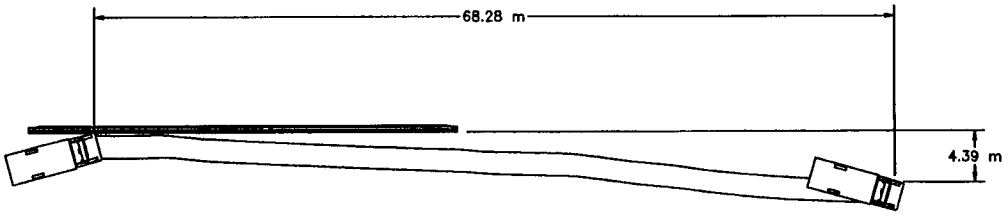

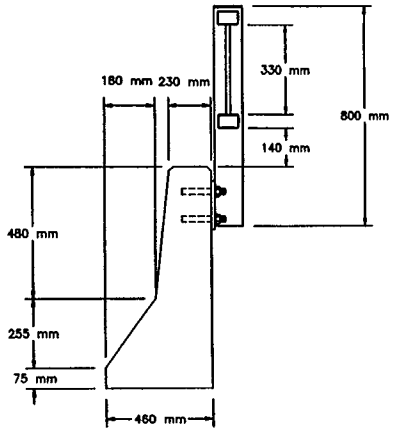

- Test Number MNPD-2
- Date 4/15/97
- Appurtenance ..... Minnesota Combination Traffic/Bicycle Bridge Rail
- Total length ..... 36.6 m
- Concrete Traffic Rail ..... New Jersey Safety Shape
  - Length ..... 6.1 m
  - Height ..... 810 mm
  - Base Width ..... 460 mm
  - Top Width ..... 230 mm
- Steel Rail ..... TS 76 x 51 x 3 mm - A500 Grade B
- Steel Spindles ..... 16 mm Square Bars - A36
- Steel Posts ..... TS 102 x 51 x 3 mm - A500 Grade B
- Vehicle Model ..... 1986 Ford F-800 Single-Unit Truck
  - Curb ..... 5,254 kg
  - Test Inertia ..... 8,002 kg
  - Gross Static ..... 8,002 kg
- Vehicle Speed
  - Impact ..... 82.1 km/hr
  - Exit ..... NA
- Vehicle Angle
  - Impact ..... 14.7 deg
  - Exit ..... NA
- Vehicle Stability ..... Satisfactory
- Occupant Ridedown Deceleration (10 msec avg.)
  - Longitudinal ..... 5.18 G's < 20 G's
  - Lateral (not required) ..... 4.30 G's
- Occupant Impact Velocity (Normalized)
  - Longitudinal ..... 2.37 m/s < 12 m/s
  - Lateral (not required) ..... 2.69 m/s
- Vehicle Damage ..... Moderate
  - TAD[21] 11-LFQ-3
  - SAE[22] 11-LFWL2
- Vehicle Stopping Distance ..... 68.3 m downstream 4.39 m lateral
- Bridge Rail Damage ..... Moderate
- Maximum Deflections
  - Permanent Set ..... NA
  - Dynamic ..... 456 mm

Figure 28. Summary of Test Results, Test MNPD-2.

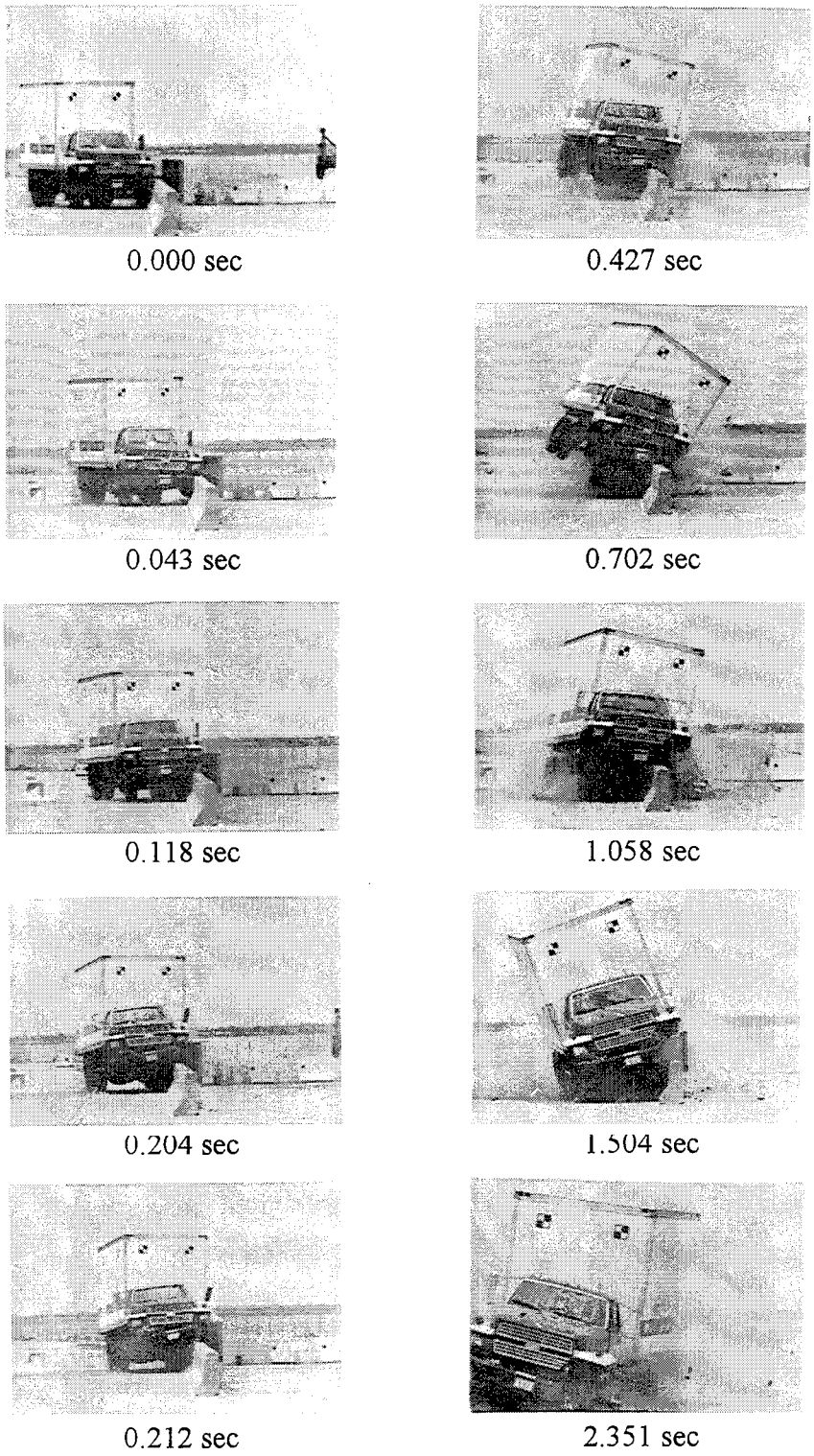

Figure 29. Additional Sequential Photographs, Test MNPD-2.

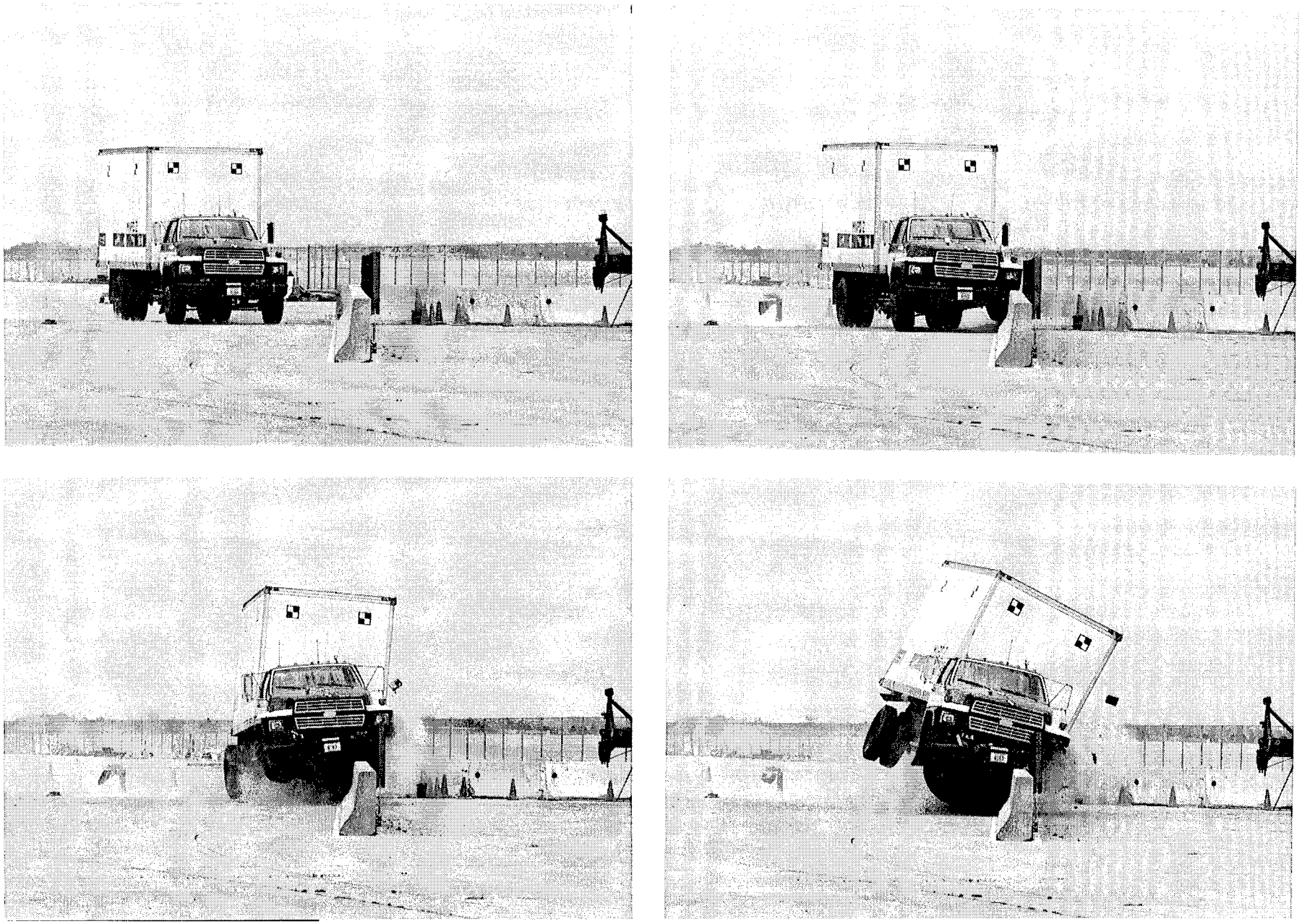

Figure 30. Documentary Photographs, Test MNPD-2

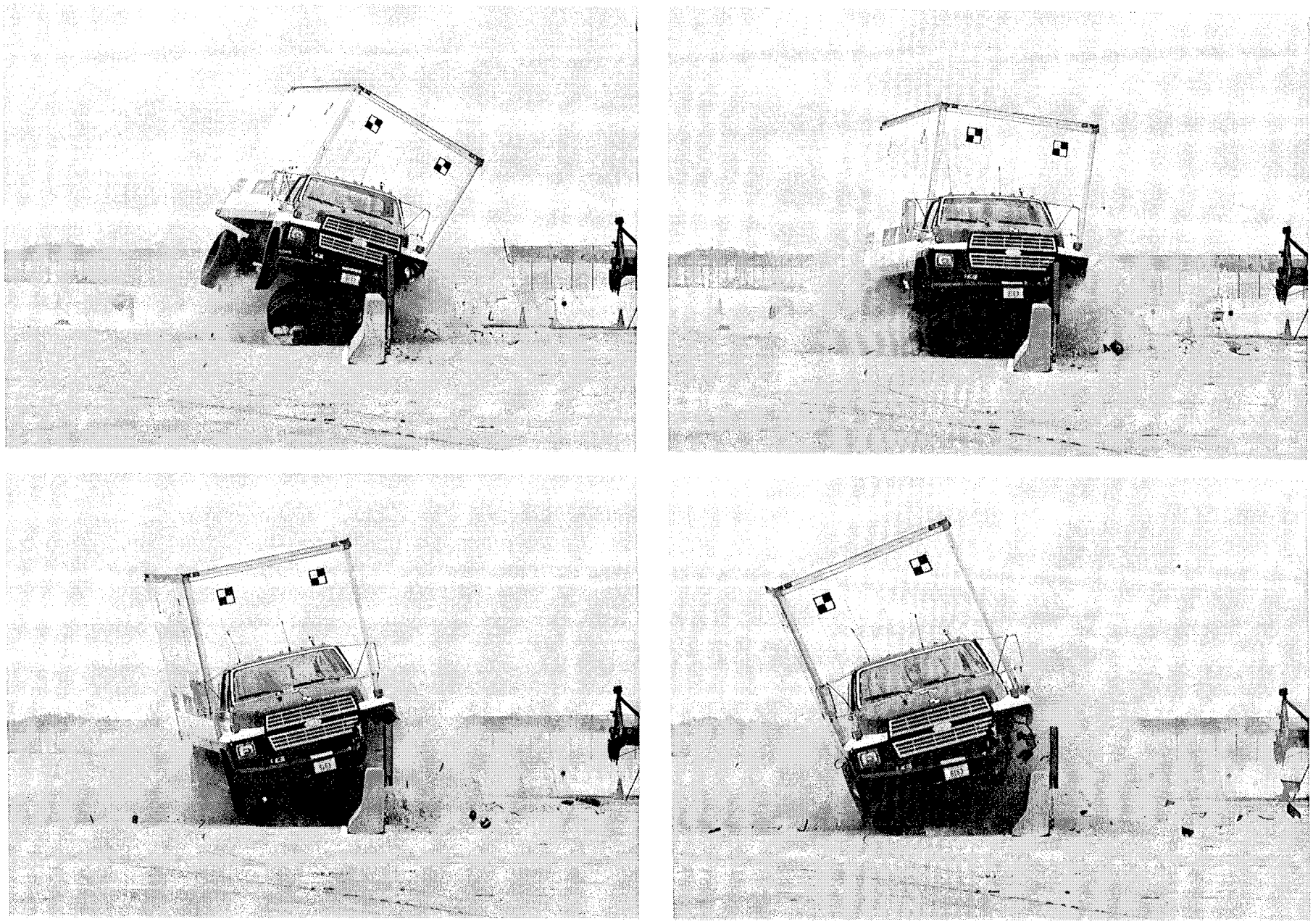

Figure 31. Documentary Photographs, Test MNPD-2

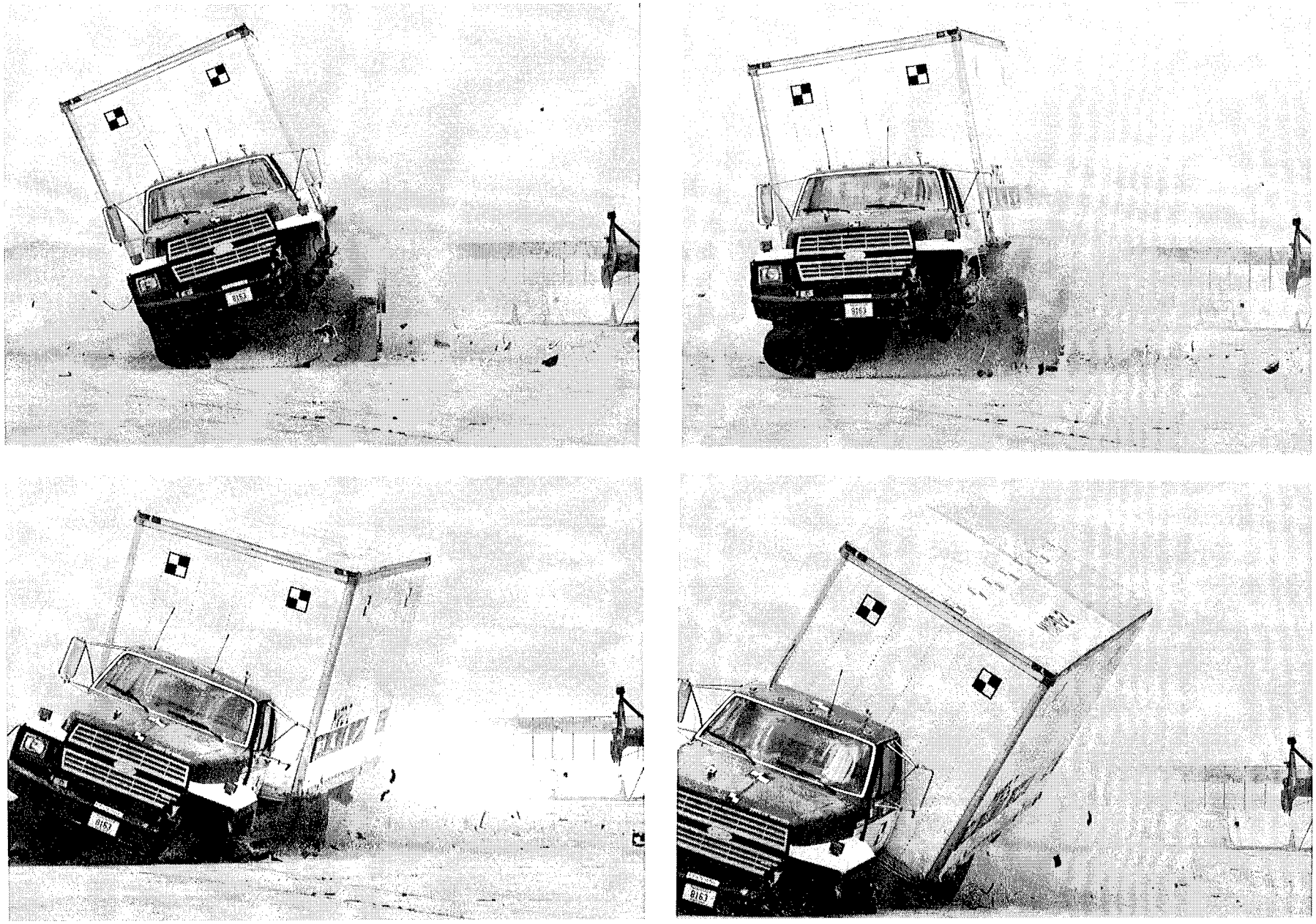

Figure 32. Documentary Photographs, Test MNPD-2

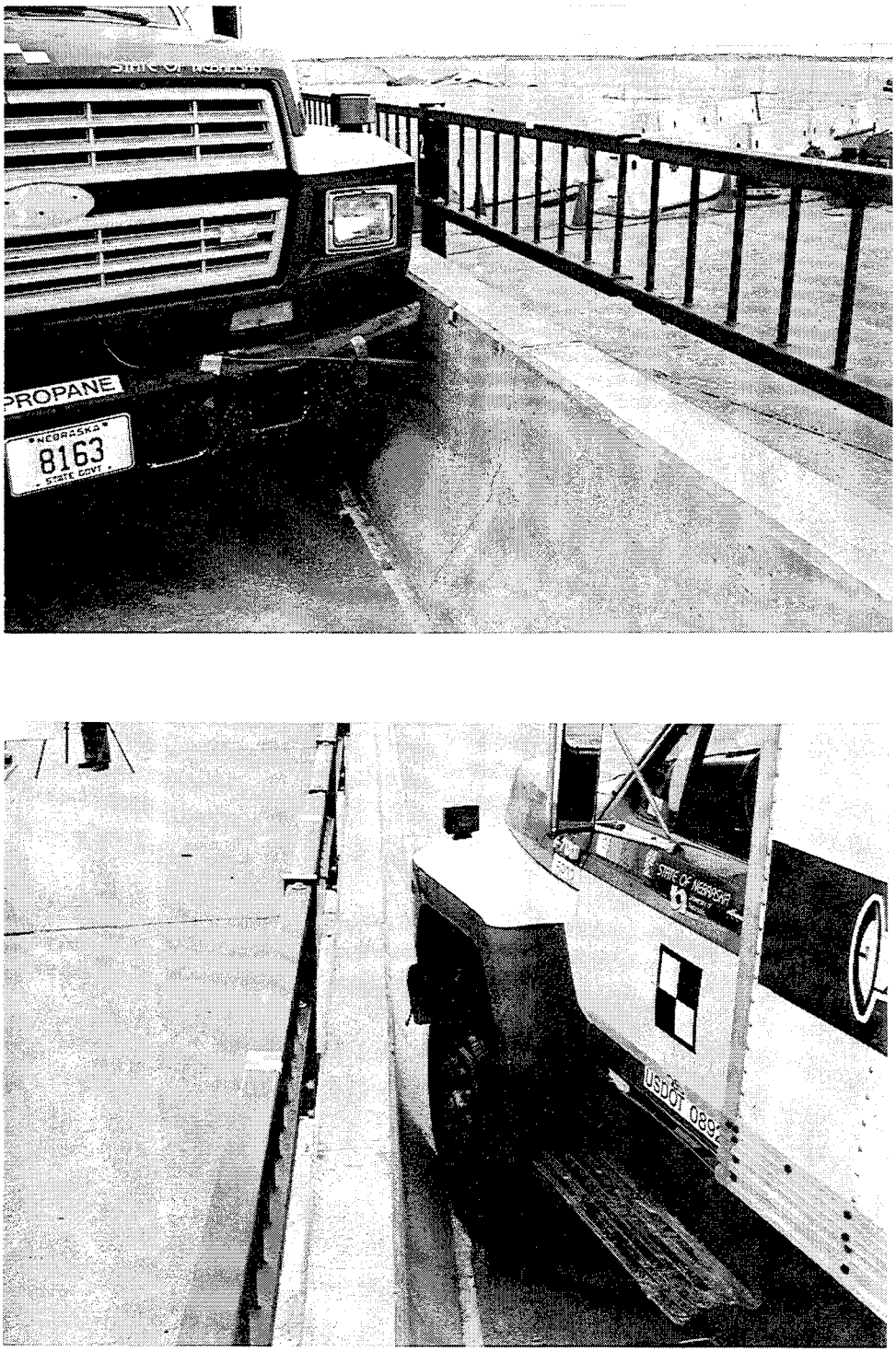

Figure 33. Impact Location, Test MNPD-2

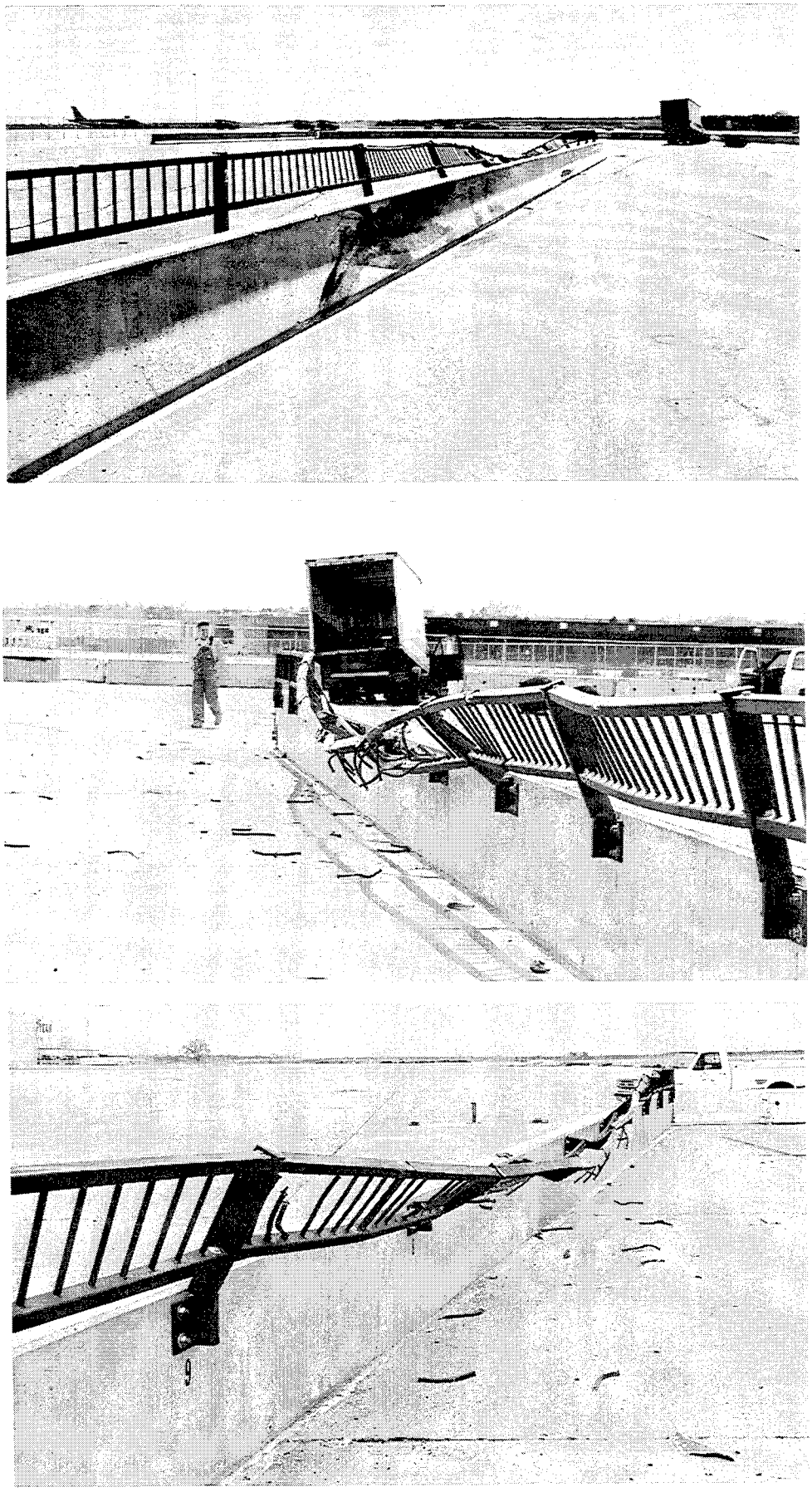

Figure 34. Barrier Damage, Test MNPD-2

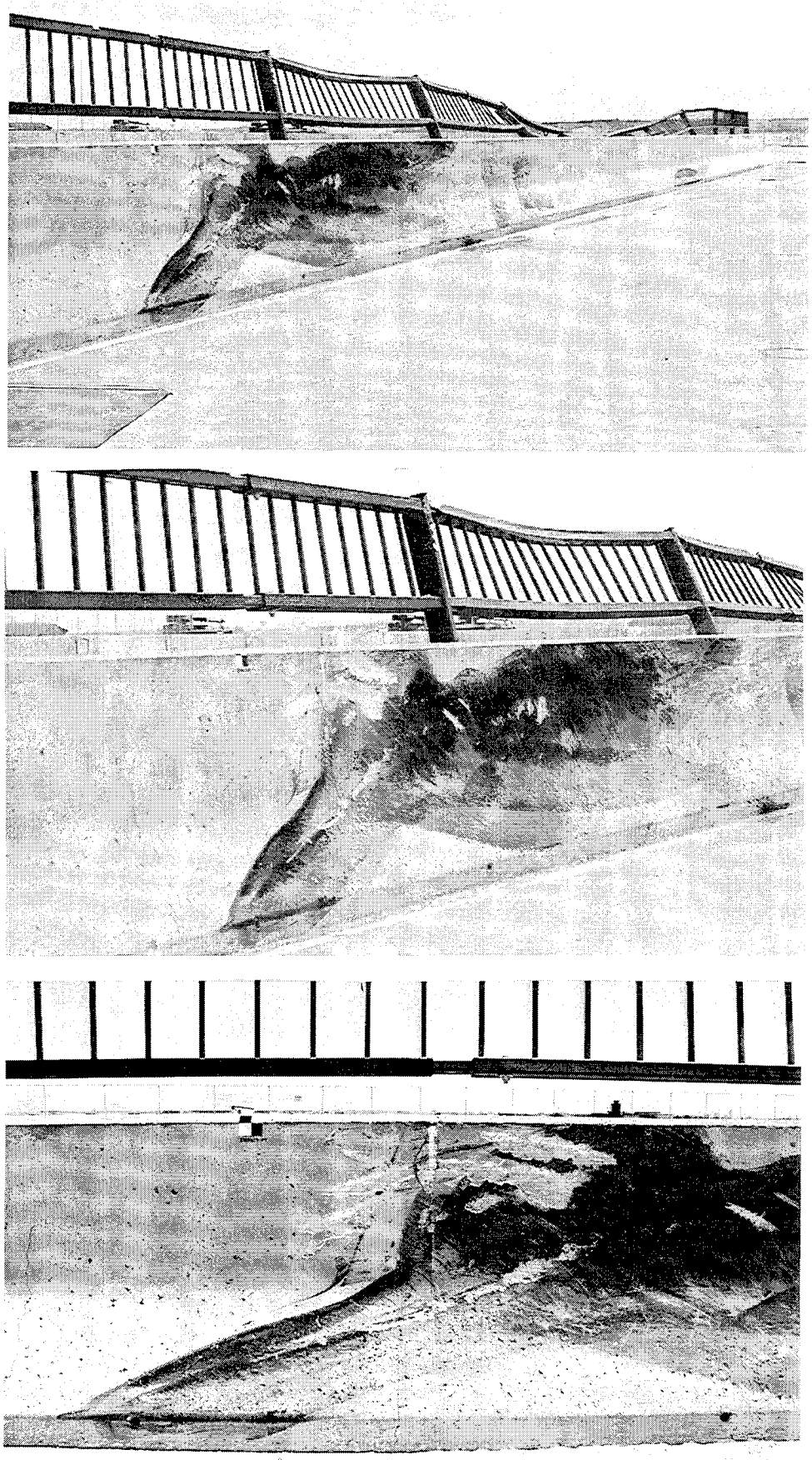

Figure 35. Barrier Damage, Test MNPD-2 (Continued)

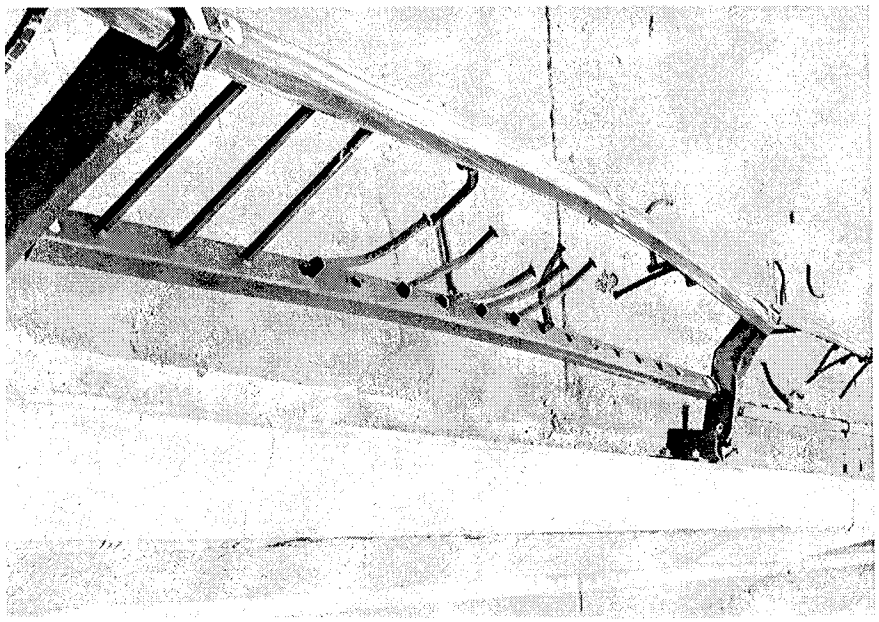

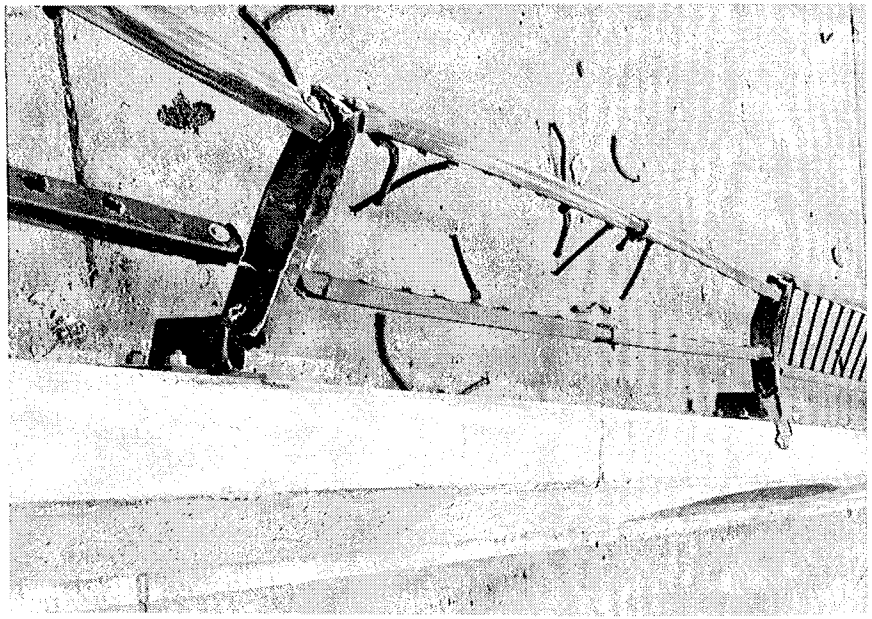

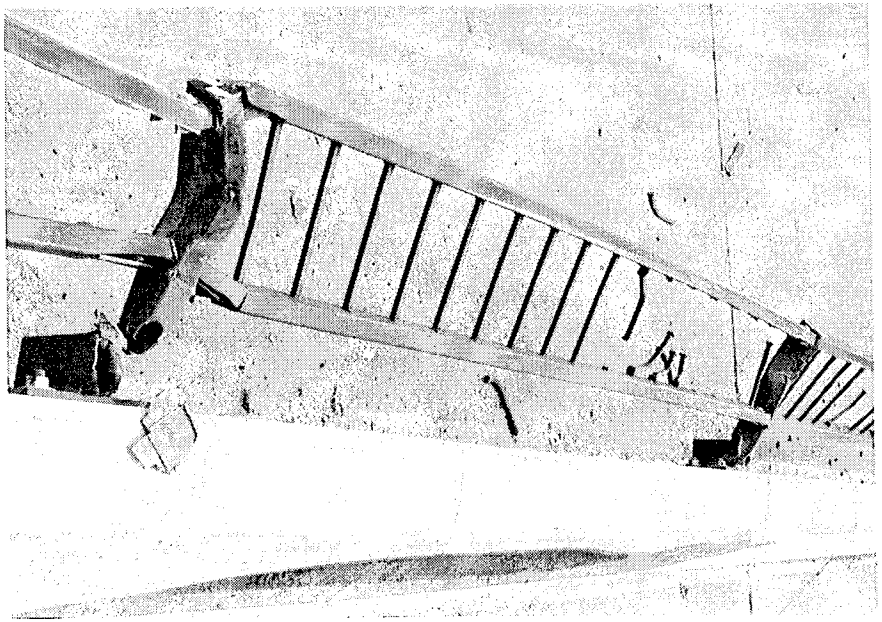

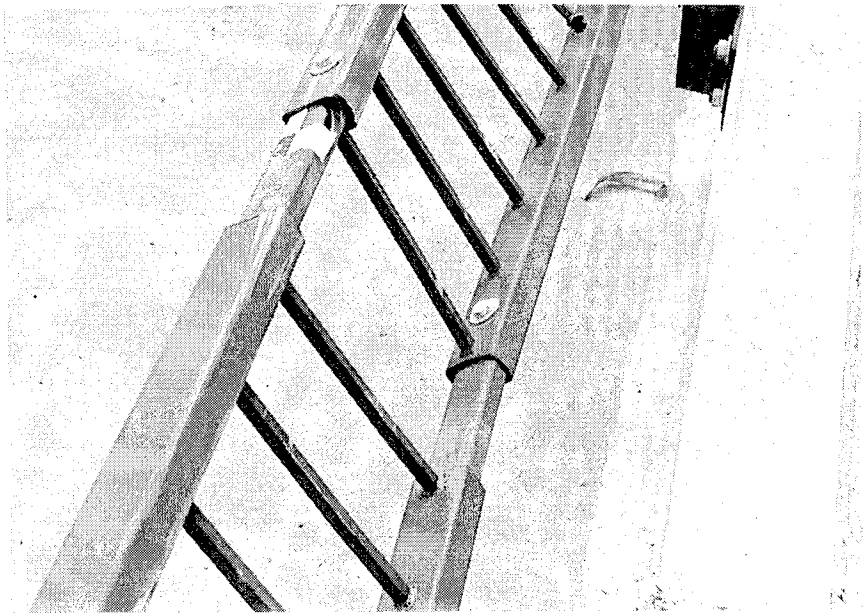

Figure 36. Barrier Damage, Test MNPD-2 (Continued)

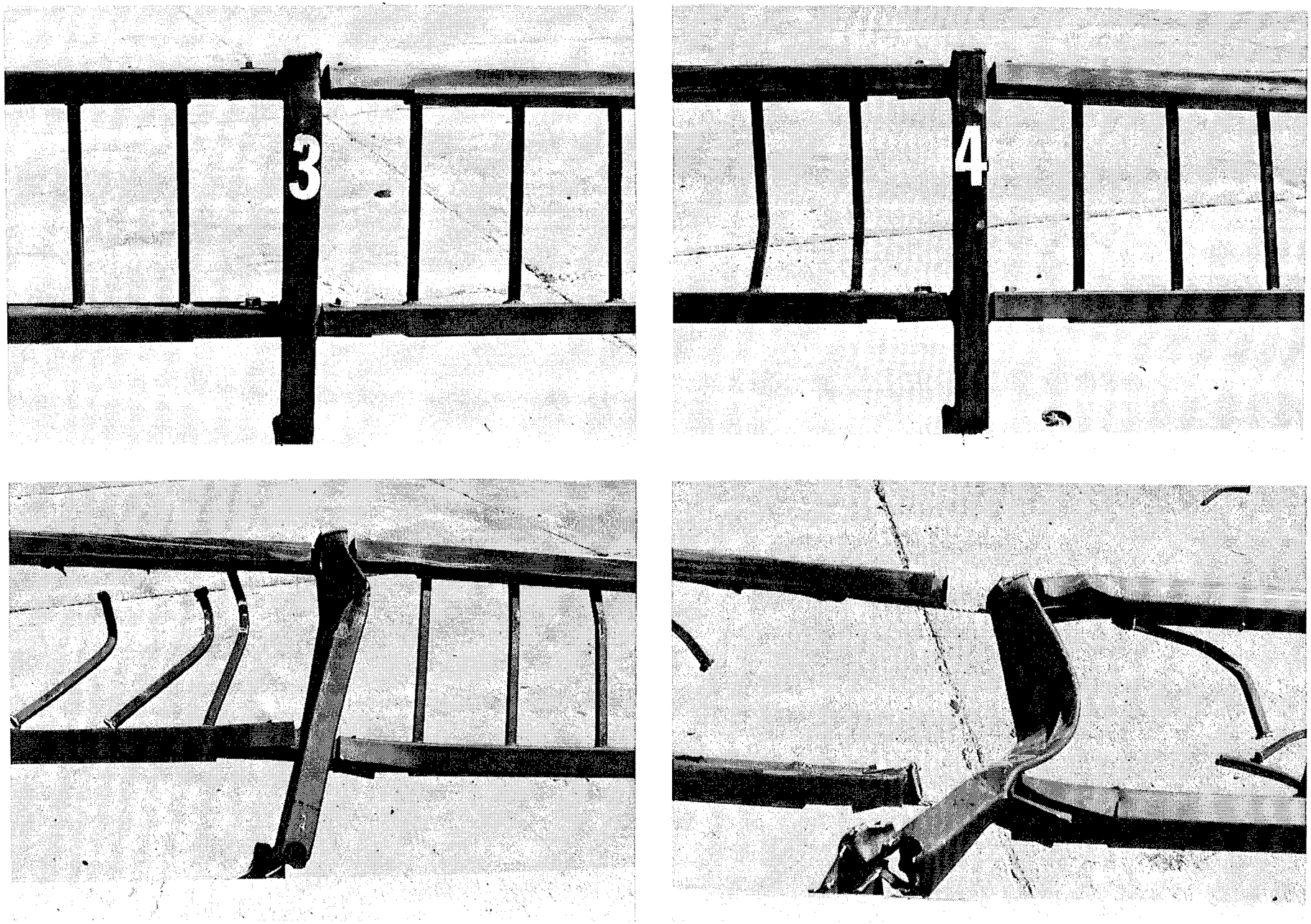

Figure 37. Post Damage, Test MNPD-2

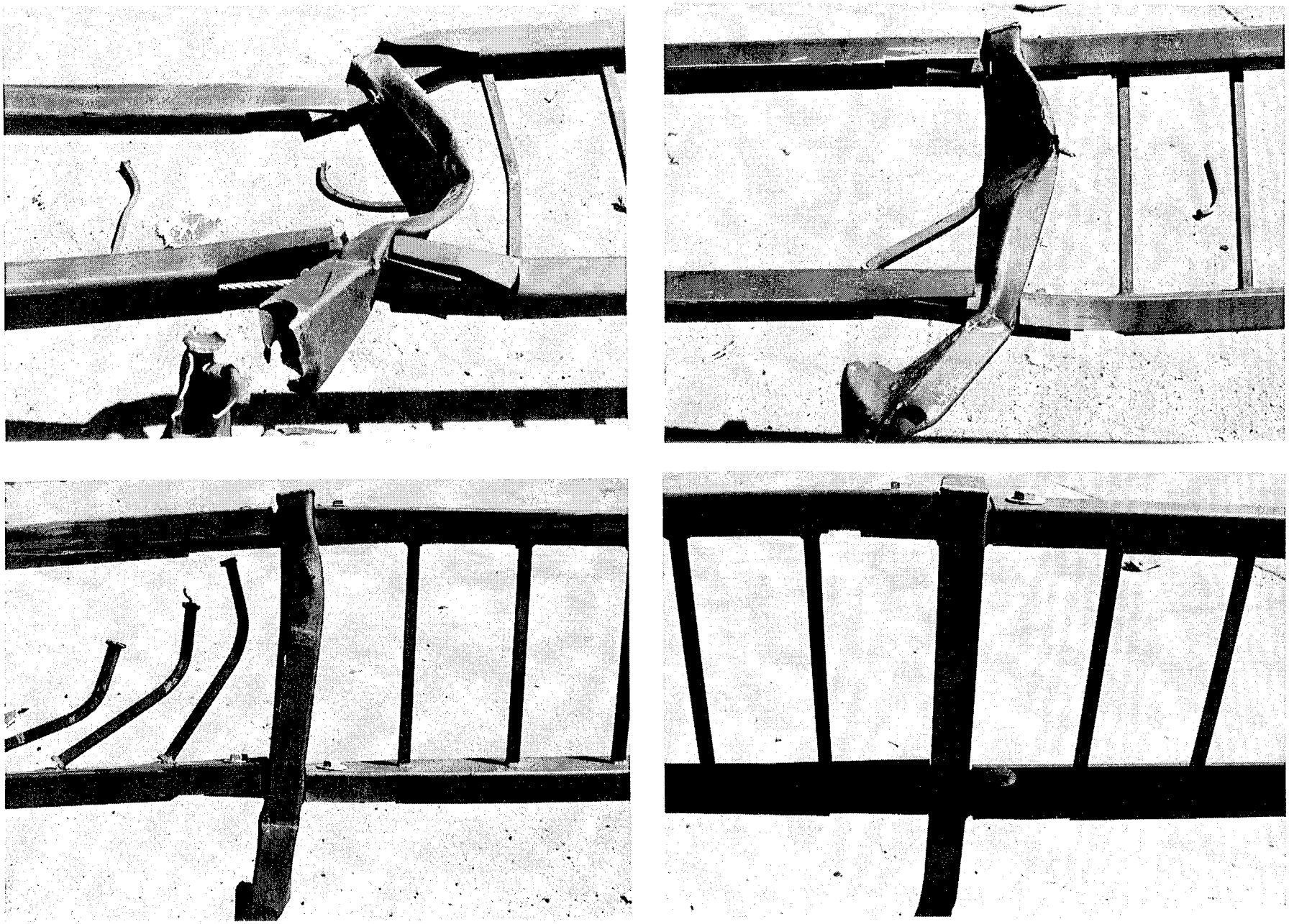

Figure 38. Post Damage, Test MNPD-2 (Continued)

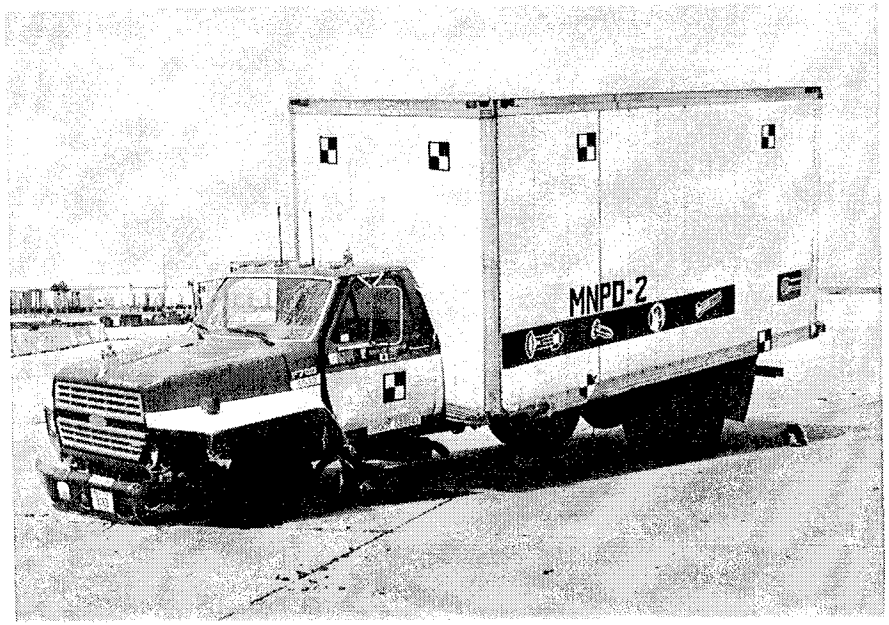

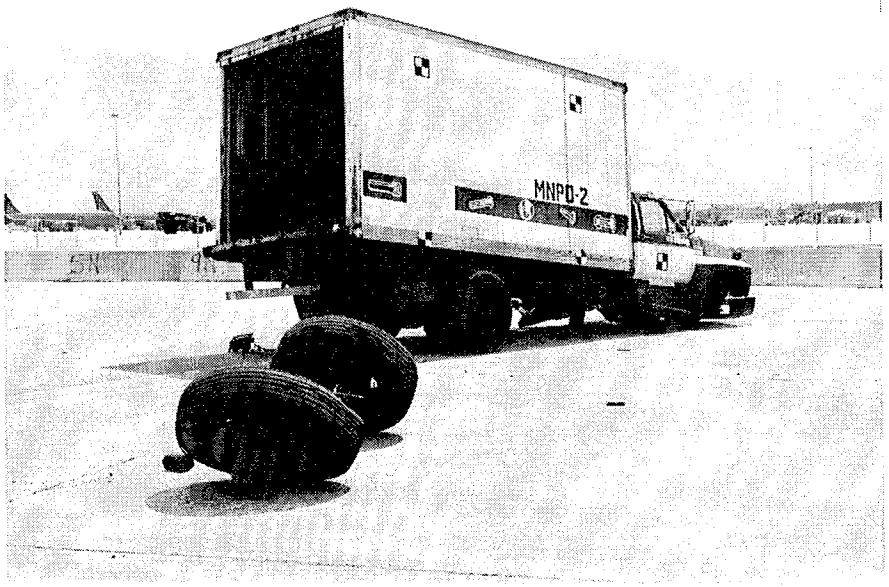

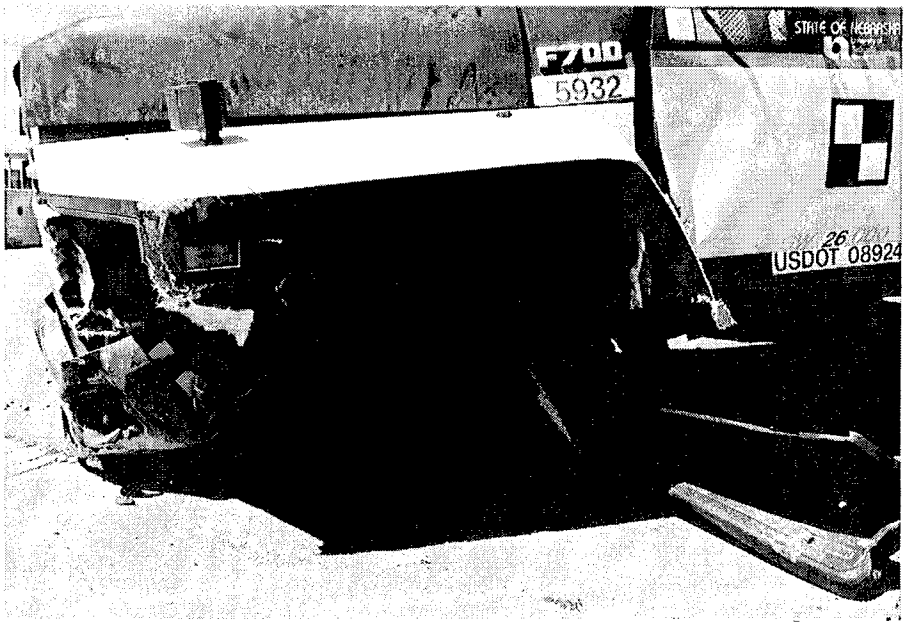

Figure 39. Vehicle Damage, Test MNPD-2

Table 5. Strain Gauge Results, Test MNPD-2

Hardware Type	Strain Gauge No.	Strain Gauge Location	Maximum Load[1] (kN)	Comments
Cable Turnbuckle	1	Note[2]	46.74	Upstream end of cable for lower rail
	2	Note[3]	18.24	Upstream end of cable for upper rail

[1] - All load values are shown in the absolute value only.
[2] - Strain gauge location is the cable turnbuckle on the upstream end of the lower rail cable.
[3] - Strain gauge location is the cable turnbuckle on the upstream end of the upper rail cable.

10 SUMMARY AND CONCLUSIONS

The combination traffic/bicycle bridge railing system described in this report was developed and successfully evaluated according to current impact safety standards. The bridge railing system was configured with a standard New Jersey safety shape bridge rail, tubular steel rails, tubular steel posts with breakaway mechanism, and solid vertical spindle bars. Two longitudinal wire rope cables were also incorporated into the design to prevent the bicycle railing from falling below after impact and to eliminate the potential for penetration of the vehicle's occupant compartment by dislodged railing members.

Two full-scale vehicle crash tests were performed according to the TL-4 criteria found in NCHRP Report No. 350. Test MNPD-1, performed with a pickup truck impacting the railing system, was determined to be acceptable according to the safety performance criteria presented in NCHRP Report 350. Following this crash test, the steel bicycle railing was repaired and made ready for the second crash test. Test MNPD-2, performed with a single-unit truck impacting the railing system, was also determined to be acceptable according to the TL-4 safety performance criteria. A summary of the safety performance evaluations for the two crash tests is provided in Table 6.

Therefore, a combination traffic/bicycle bridge rail has been successfully developed and meets current safety standards. Full-scale crash testing has indicated that acceptable impact performance is possible; although, large dynamic rail and post deflections can occur when impacted by single-unit trucks. However, it is noted that the combination traffic/bicycle bridge railing can easily be repaired due to its modular-type construction.

Table 6. Summary of Safety Performance Evaluation Results

Evaluation Criteria		Test MNPD-1	Test MNPD-2
A.	Test article should contain and redirect the vehicle; the vehicle should not penetrate, underride, or override the installation although controlled lateral deflection of the test article is acceptable.	S	S
D.	Detached elements, fragments or other debris from the test article should not penetrate or show potential for penetrating the occupant compartment, or present an undue hazard to other traffic, pedestrians, or personnel in a work zone. Deformations of, or intrusions into, the occupant compartment that could cause serious injuries should not be permitted.	S	M
F.	The vehicle should remain upright during and after collision although moderate roll, pitching and yawing are acceptable.	S	S[1]
G.	It is preferable, although not essential, that the vehicle remain upright during and after collision.	S[1]	S
H.	Longitudinal and lateral occupant impact velocities should fall below the preferred value of 9 m/s, or at least below the maximum allowable value of 12 m/s.	S[1]	S[1]
I.	Longitudinal and lateral occupant ridedown accelerations should fall below the preferred value of 15 g's, or at least below the maximum allowable value of 20 g's.	S[1]	S[1]
K.	After collision it is preferable that the vehicle's trajectory not intrude into adjacent traffic lanes.	M	M
L.	The occupant impact velocity in the longitudinal direction should not exceed 12 m/s and the occupant ridedown acceleration in the longitudinal direction should not exceed 20 g's.	S	S[1]
M.	The exit angle from the test article preferably should be less than 60 percent of test impact angle, measured at time of vehicle loss of contact with test device.	S	S

S - Satisfactory
M - Marginally passed
U - Unsatisfactory
[1] Results of evaluation reported here even though it is not required by NCHRP Report No. 350 (1)

11 RECOMMENDATIONS

For combination traffic/bicycle railing systems, such as the one developed and described in this report, significant contact can occur between the impacting vehicle and the bicycle railing components. For example, when the single-unit truck struck the attached bicycle rail, several vertical spindle bars became dislodged from the railing system. Therefore, it is recommended that consideration be given to modifying the design in order to reduce the potential for the vertical spindle bars from releasing from the system and decrease any hazard from flying debris. These design considerations may include the following: (1) increasing the strength of the connection between the tubular rails and the spindle bars; (2) attaching a longitudinal railing member to the traffic-side face of the spindle bars and at the mid-height between the two rails; (3) reducing the mass of the spindle bars by using small tubes; and (4) moving the spindle bars to the back side of the tubular rails to increase the strength of the welded connection.

The researchers believe that other combination traffic/bicycle bridge railing concepts may be developed to meet the NCHRP Report No. 350 and AASHTO LRFD criteria. However, those concepts may not provide the same level of aesthetic appeal as provided by this system. In addition, newly developed combination traffic/bicycle bridge railing systems can only be verified through the use of full-scale vehicle crash testing.

Finally, the authors believe that this combination traffic/bicycle bridge railing can be adapted to other safety shape bridge railings (i.e., F-shape and single slope) or vertical parapets of similar height and top width with only minor modifications. Additionally, it is believed that no further testing will be required since the F-shape and single-slope barriers are considered to behave slightly better than the New Jersey shape in crash testing (6,8,23).

12 REFERENCES

1. Ross, H.E., Sicking, D.L., Zimmer, R.A. and Michie, J.D., *Recommended Procedures for the Safety Performance Evaluation of Highway Features*, National Cooperative Research Program (NCHRP) Report No. 350, Transportation Research Board, Washington, D.C., 1993.

2. Bullard, D.L., Jr., Menges, W.L., and Buth, C.E., *Development of Combination Pedestrian-Traffic Bridge Railings*, Transportation Research Record No. 1468, Transportation Research Board, National Research Council, Washington D.C., December 1994.

3. Alberson, D.C., Menges, W.L., and Buth, C.E., *Performance Level 1 Bridge Railings*, Transportation Research Record No. 1500, Transportation Research Board, National Research Council, Washington D.C., July 1995.

4. Buth, C.E. and Menges, W.L., *Crash Testing and Evaluation of Retrofit Bridge Railings and Transition*, Report No. FHWA-RD-96-032, Submitted to the Office of Safety and Traffic Operations R&D, Federal Highway Administration, Performed by Texas Transportation Institute, Texas A&M University, College Station, Texas, January 1997.

5. *Guide Specifications for Bridge Railings*, American Association of State Highway and Transportation Officials (AASHTO), Washington, D.C., 1989.

6. Buth, C.E., Hirsch, T.J., and McDevitt, C.F., *Performance Level 2 Bridge Railings*, Transportation Research Record No. 1258, Transportation Research Board, National Research Council, Washington D.C., 1990.

7. Holloway, J.C., Faller, R.K., Pfeifer, B.G., Post, E.R., and Davidson, D.E., *Performance Level 2 Tests on the Missouri 30-in. New Jersey Safety-Shape Bridge Rail*, Transportation Research Record No. 1367, Transportation Research Board, National Research Council, Washington D.C., 1992.

8. Mak, K.K., Gripne, D.J., McDevitt, C.F., *Single-Slope Concrete Bridge Rail*, Transportation Research Record No. 1468, Transportation Research Board, National Research Council, Washington D.C., December 1994.

9. Holloway, J.C., Faller, R.K., Wolford, D.F., Dye, D.L., and Sicking, D.L., *Performance Level 2 Tests on a 29-in. Open Concrete Bridge Rail*, Final Report to the Nebraska Department of Roads, Transportation Report No. TRP-03-51-95, Midwest Roadside Safety Facility, University of Nebraska-Lincoln, June 1996.

10. Holloway, J.C., Sicking, D.L., and Faller, R.K., *Reduced-Height Performance Level 2 Bridge Rail*, Transportation Research Record No. 1528, Transportation Research Board, National Research Council, Washington D.C., September 1996.

11. Pfeifer, B.G., Holloway, J.C., Faller, R.K., and Rosson, B.T., *Test Level 4 Evaluation of the Minnesota Combination Bridge Rail*, Final Report to the Minnesota Department of Transportation, Transportation Research Record No. TRP-03-53-96, Midwest Roadside Safety Facility, University of Nebraska-Lincoln, March 1996.

12. *AASHTO LRFD Bridge Design Specifications*, Customary U.S. Units - First Edition, American Association of State Highway and Transportation Officials (AASHTO), 1994.

13. Bronstad, M.E., Calcote, L.R., and Kimball, C.E., Jr., *Concrete Median Barrier Research - Volume 2 Research Report*, Report No. FHWA-RD-77-4, Submitted to the Offices of Research and Development, Federal Highway Administration, Performed by Southwest Research Institute, March 1976.

14. Davis, S., Baczynski, R., Garn, R., and Bjork, T., *Test and Evaluation of Heavy Vehicle Barrier Concepts - Technical Report*, Final Report to Office of Research and Development, Federal Highway Administration, Performed by Dynamic Science, Inc., Phoenix, Arizona, July 1981.

15. Buth, C.E., Campise, W.L., Griffin III, L.I., Love, M.L., and Sicking, D.L., *Performance Limits of Longitudinal Barrier Systems - Volume I: Summary Report*, FHWA/RD-86/153, Final Report to the Federal Highway Administration, Office of Safety and Traffic Operations R&D, Performed by Texas Transportation Institute, Texas A&M University, May 1986.

16. Beason, W.L., Ross, H.E., Jr., Perera, H.S., and Marek, M., *Single-Slope Concrete Median Barrier*, Transportation Research Record No. 1302, Transportation Research Board, National Research Council, Washington, D.C., 1991.

17. *Standard Specifications for Highway Bridges*, Fifteenth Edition, American Association of State Highway and Transportation Officials (AASHTO), Washington, D.C., 1992.

18. Hinch, J., Yang, T-L, and Owings, R., *Guidance Systems for Vehicle Testing*, ENSCO, Inc., Springfield, VA 1986.

19. *Center of Gravity Test Code - SAE J874 March 1981*, SAE Handbook Vol. 4, Society of Automotive Engineers, Inc., Warrendale, Pennsylvania, 1986.

20. Taborck, J.J., "*Mechanics of Vehicle - 7*", Machine Design Journal, May 30, 1957.

21. *Vehicle Damage Scale for Traffic Investigators*, Second Edition, Technical Bulletin No. 1, Traffic Accident Data (TAD) Project, National Safety Council, Chicago, Illinois, 1971.

22. *Collision Deformation Classification - Recommended Practice J224 March 1980*, Handbook Volume 4, Society of Automotive Engineers (SAE), Warrendale, Pennsylvania, 1985.

23. Mak, K.K., and Sicking, D.L., *Rollover Caused by Concrete Safety Shape Barrier - Volume I: Technical Report and Volume II: Appendices*, Report Nos. FHWA-RD-88-219/220, Performed for the Office of Safety and Traffic Operations R&D, Federal Highway Administration, Performed by the Texas Transportation Institute, Texas A&M University, January 1989.

13 APPENDICES

APPENDIX A

Accelerometer Data Analysis - Test MNPD-1

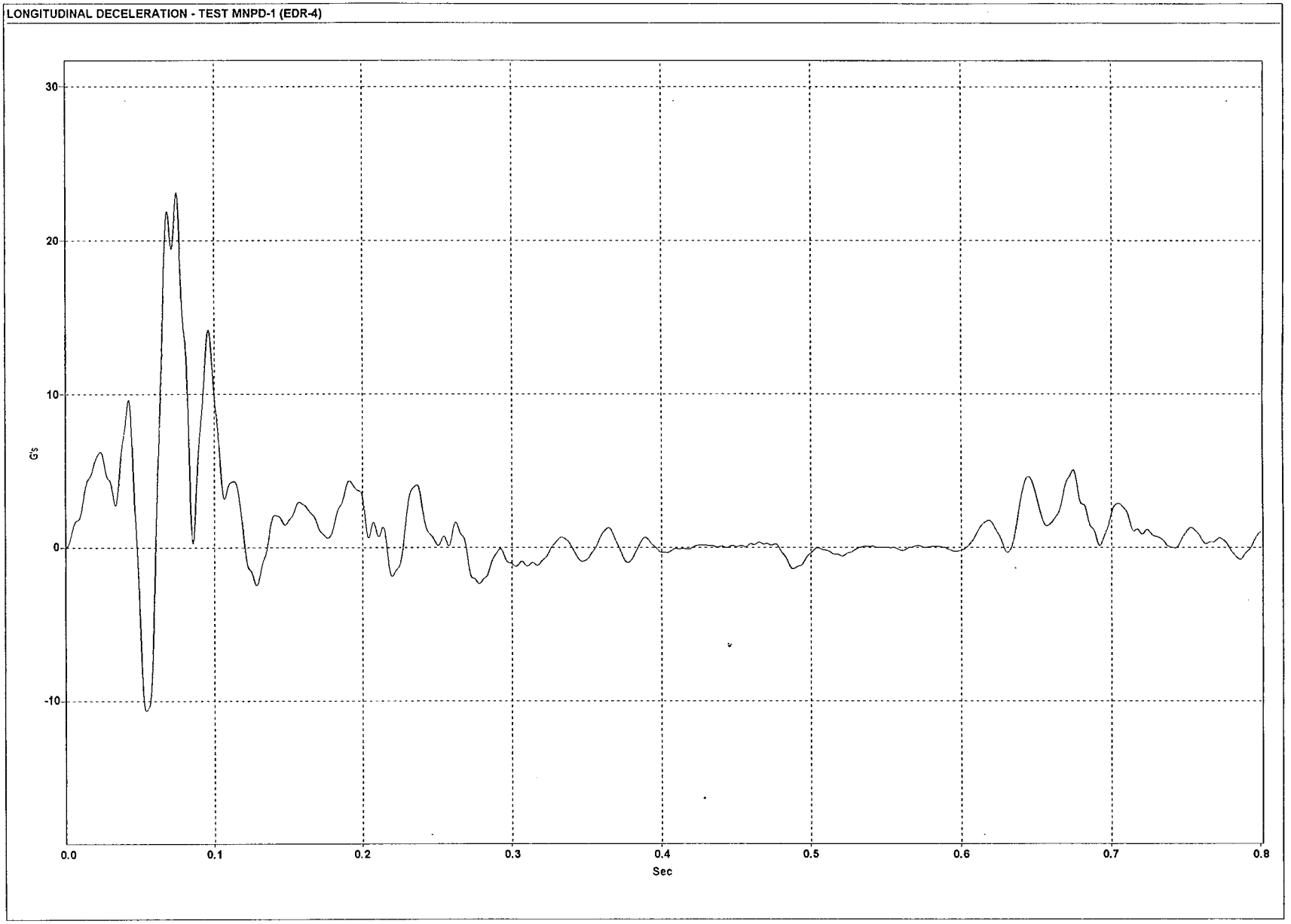

Figure A-1. Graph of Longitudinal Deceleration, Test MNPD-1

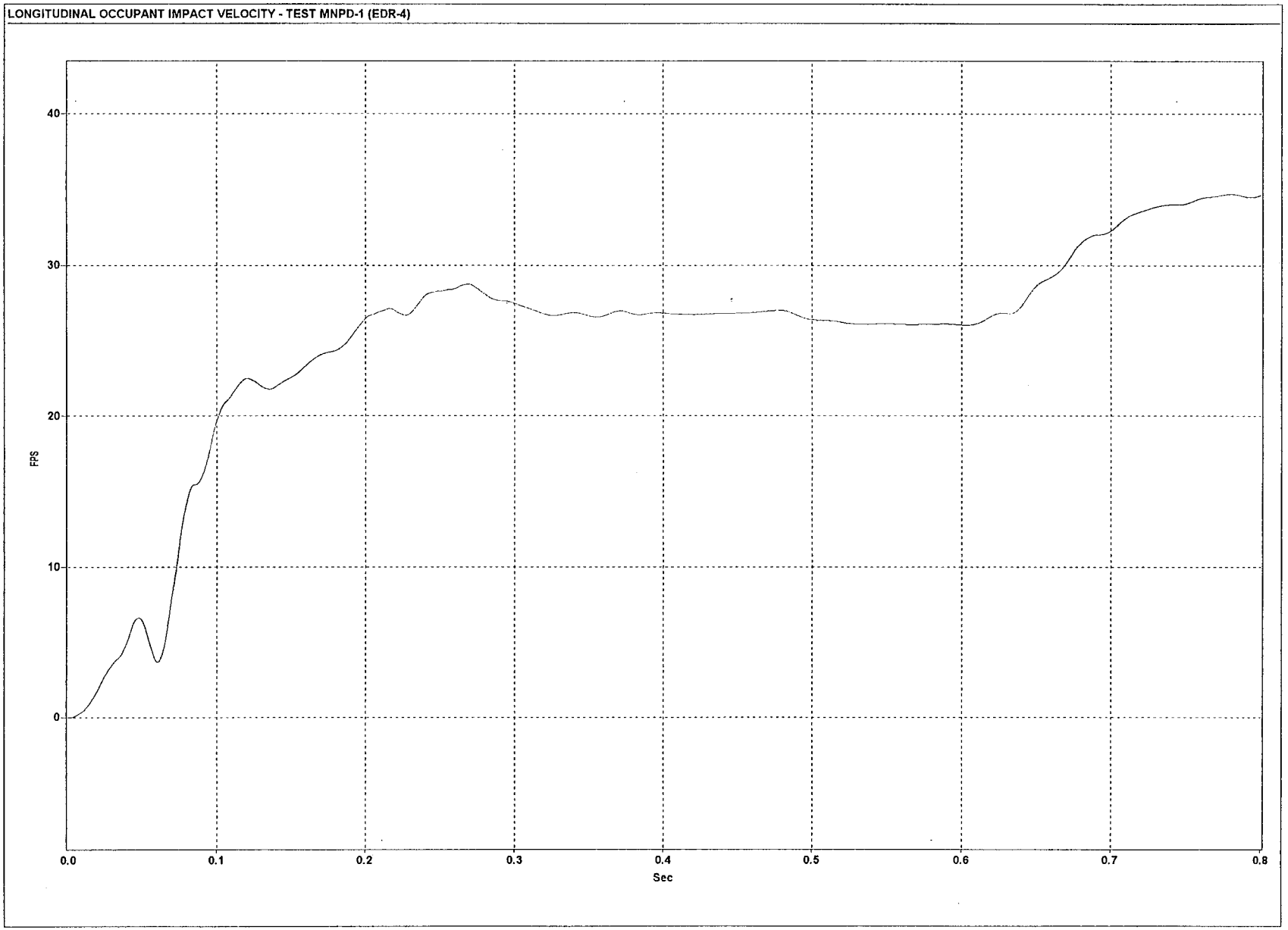

Figure A-2. Graph of Longitudinal Occupant Impact Velocity, Test MNPD-1

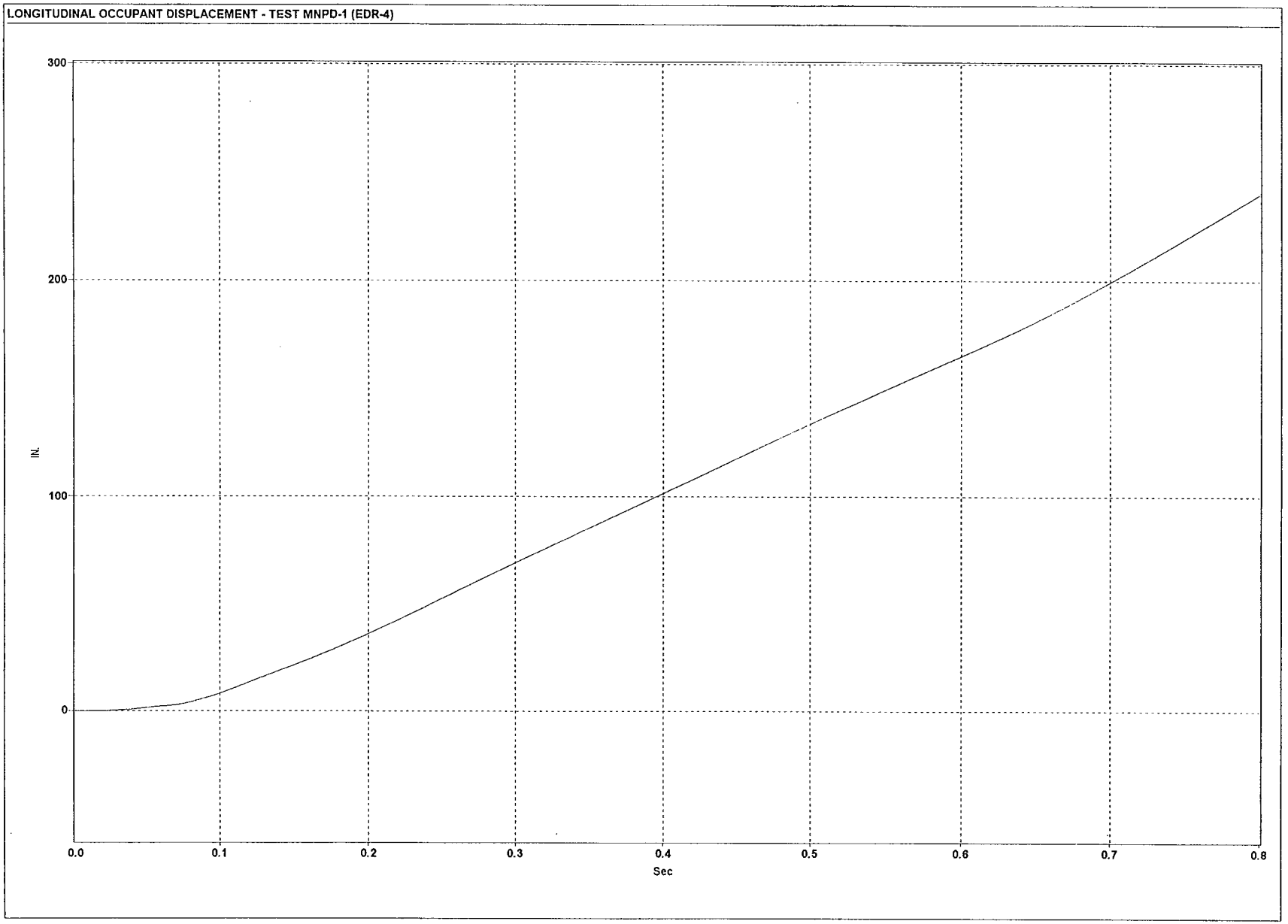

Figure A-3. Graph of Longitudinal Occupant Displacement, Test MNPD-1

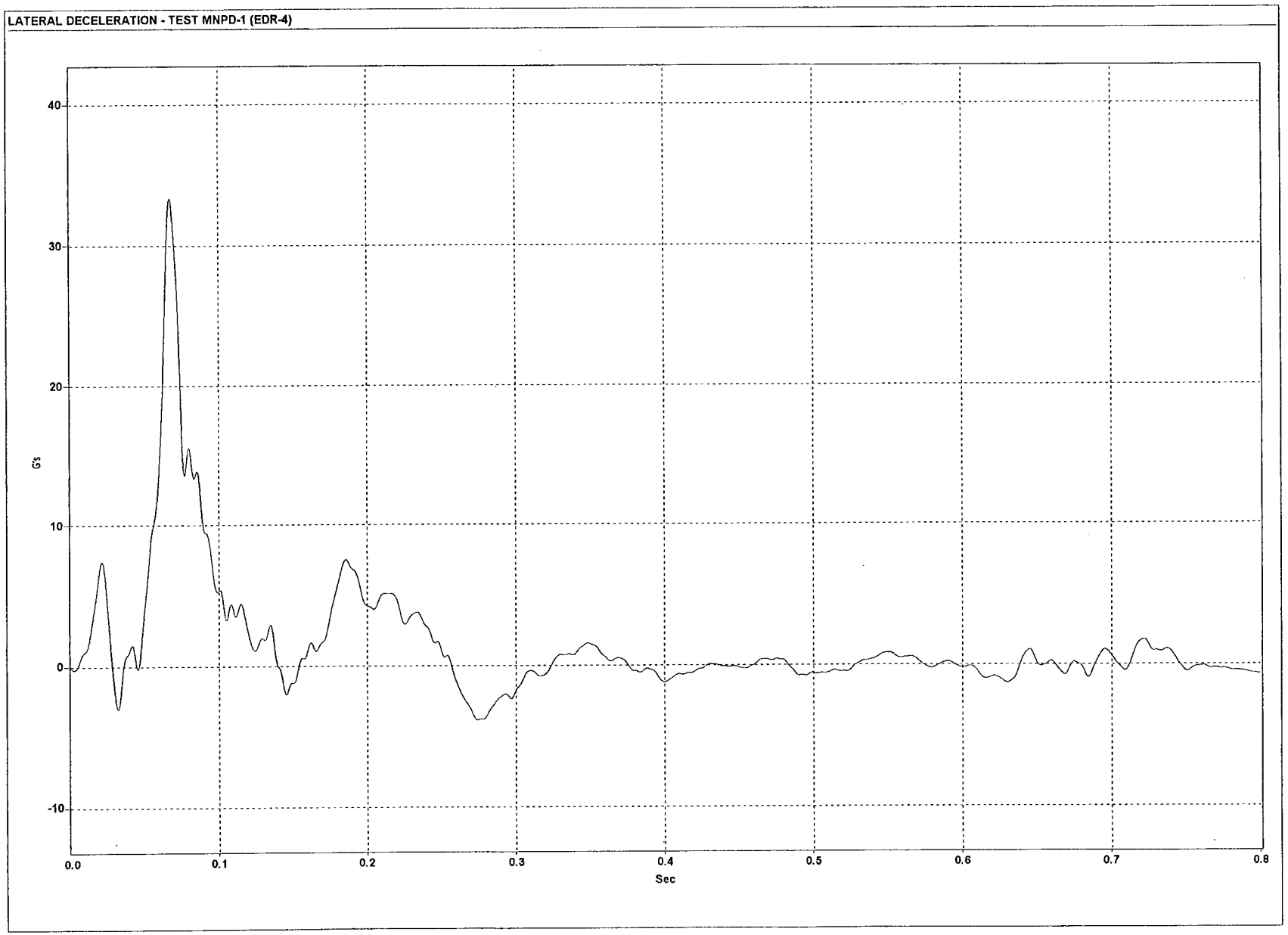

Figure A-4. Graph of Lateral Deceleration, Test MNPD-1

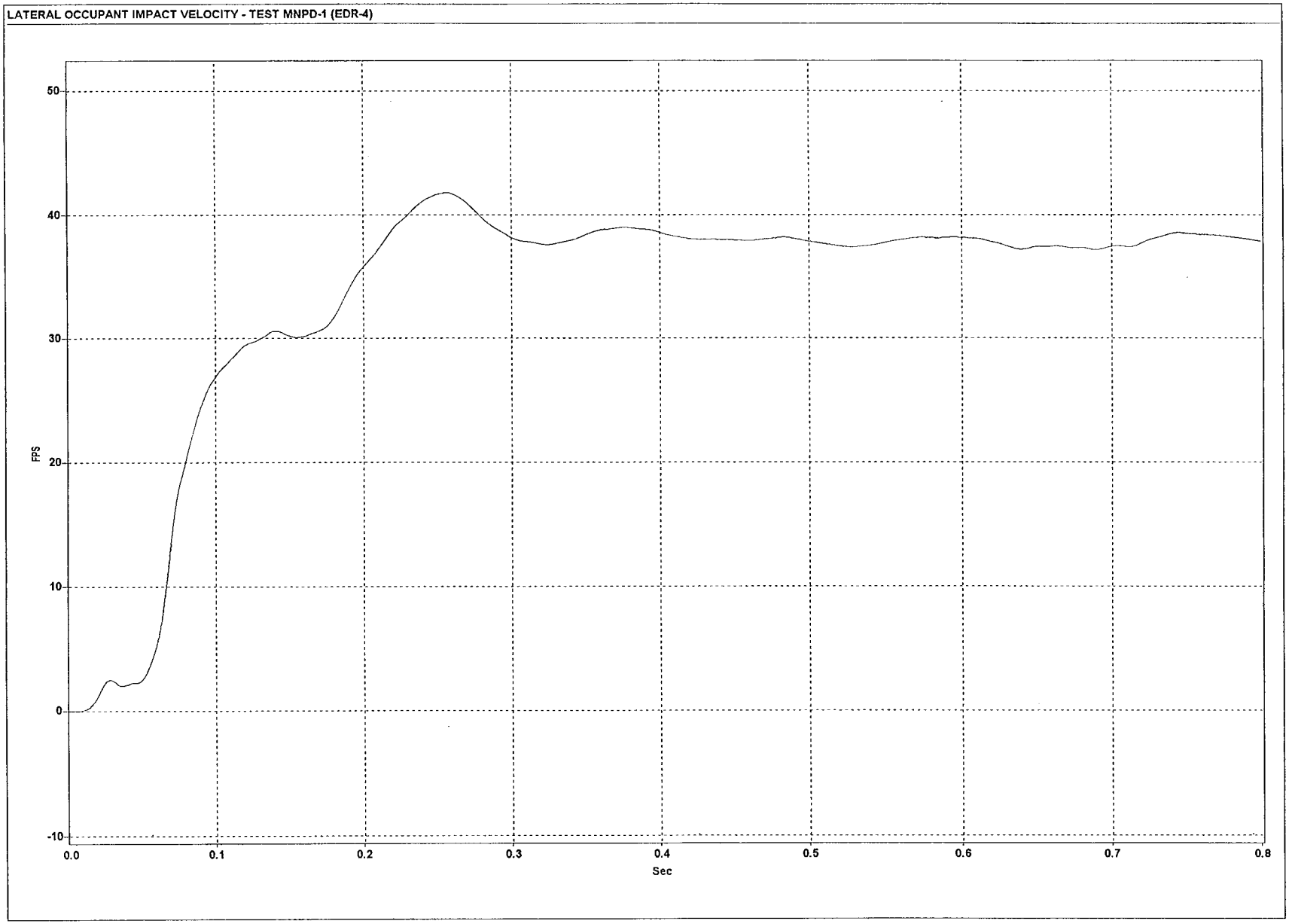

Figure A-5. Graph of Lateral Occupant Impact Velocity, Test MNPD-1

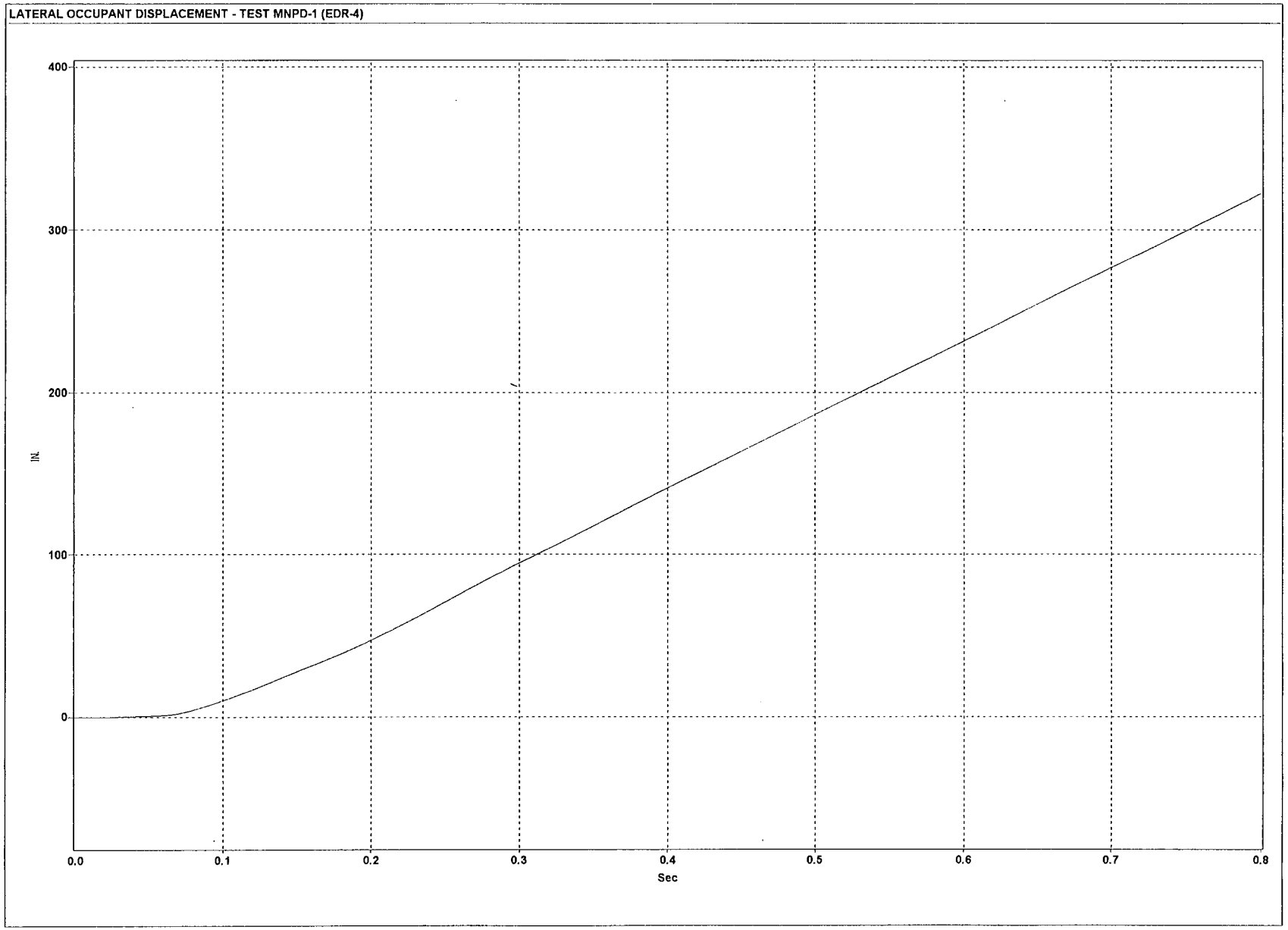

Figure A-6. Graph of Lateral Occupant Displacement, Test MNPD-1

APPENDIX B

Rate Transducer Data Analysis - Test MNPD-1

Figure B-1. Graph of Roll, Pitch, and Yaw Angular Displacements, Test MNPD-1

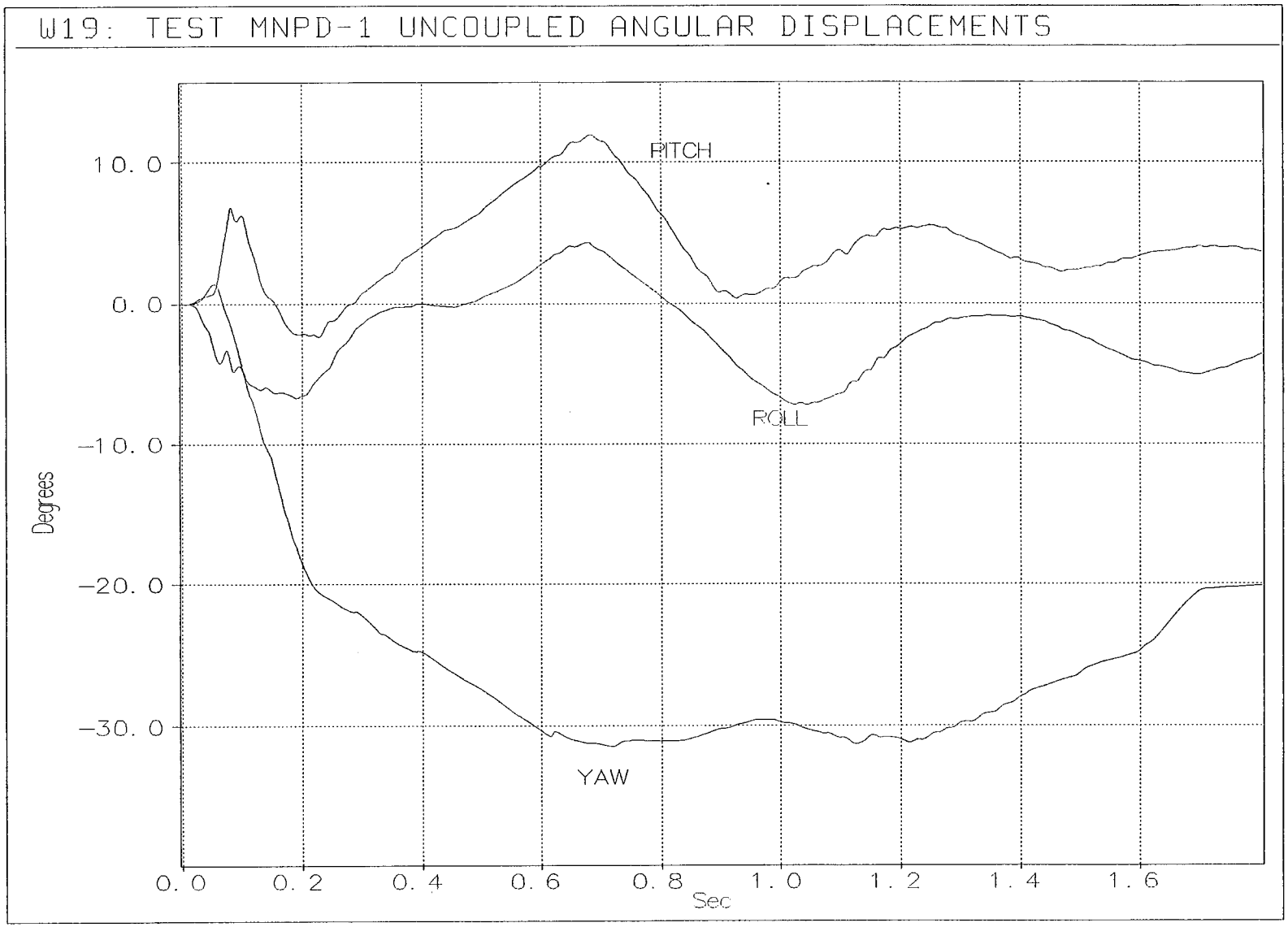

Figure B-1. Graph of Roll, Pitch, and Yaw Angular Displacements, Test MNPD-1

APPENDIX C

Strain Gauge Data Analysis - Test MNPD-1

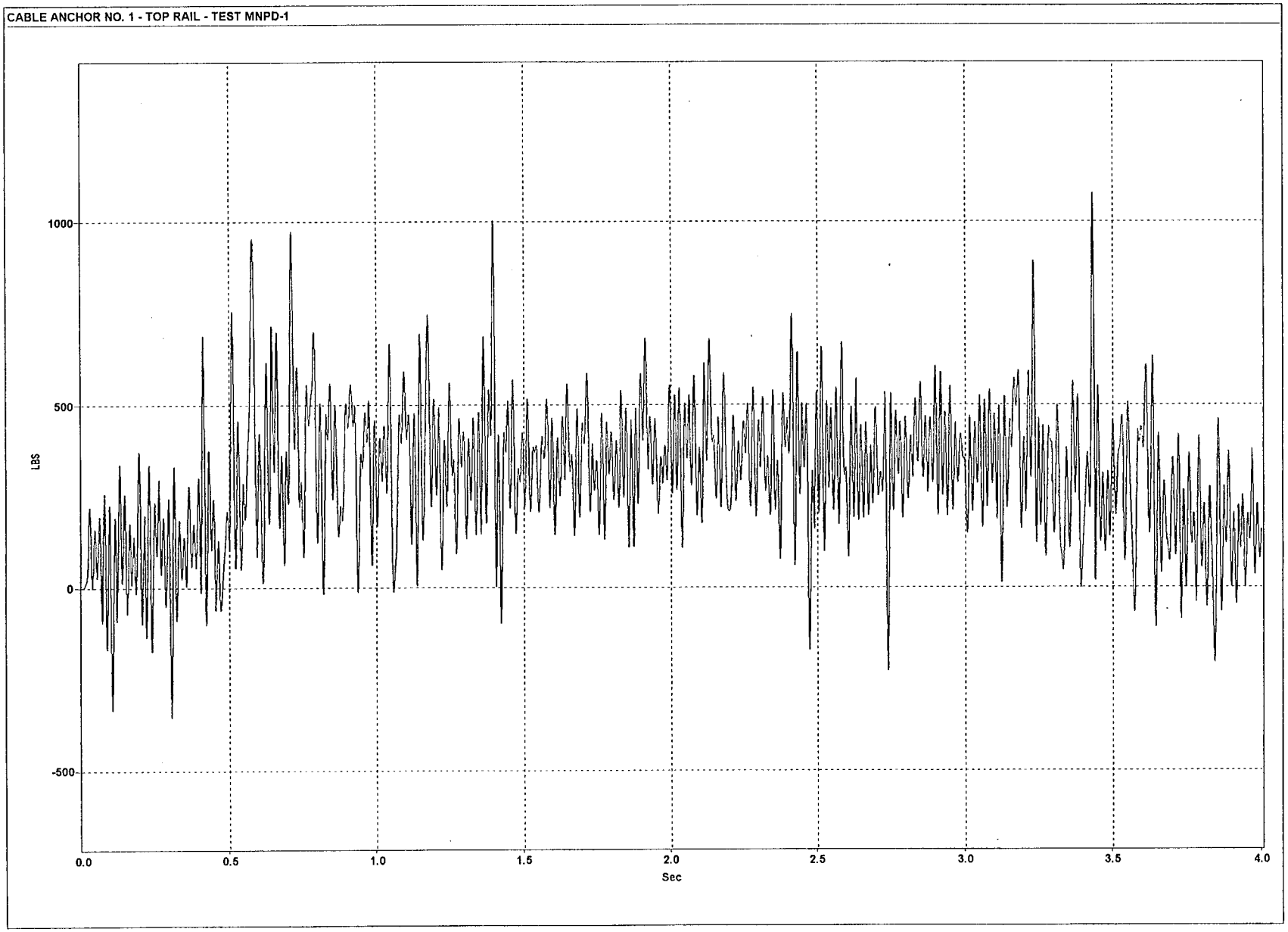

Figure C-1. Graph of Top Rail Cable Anchor Load, Test MNPD-1

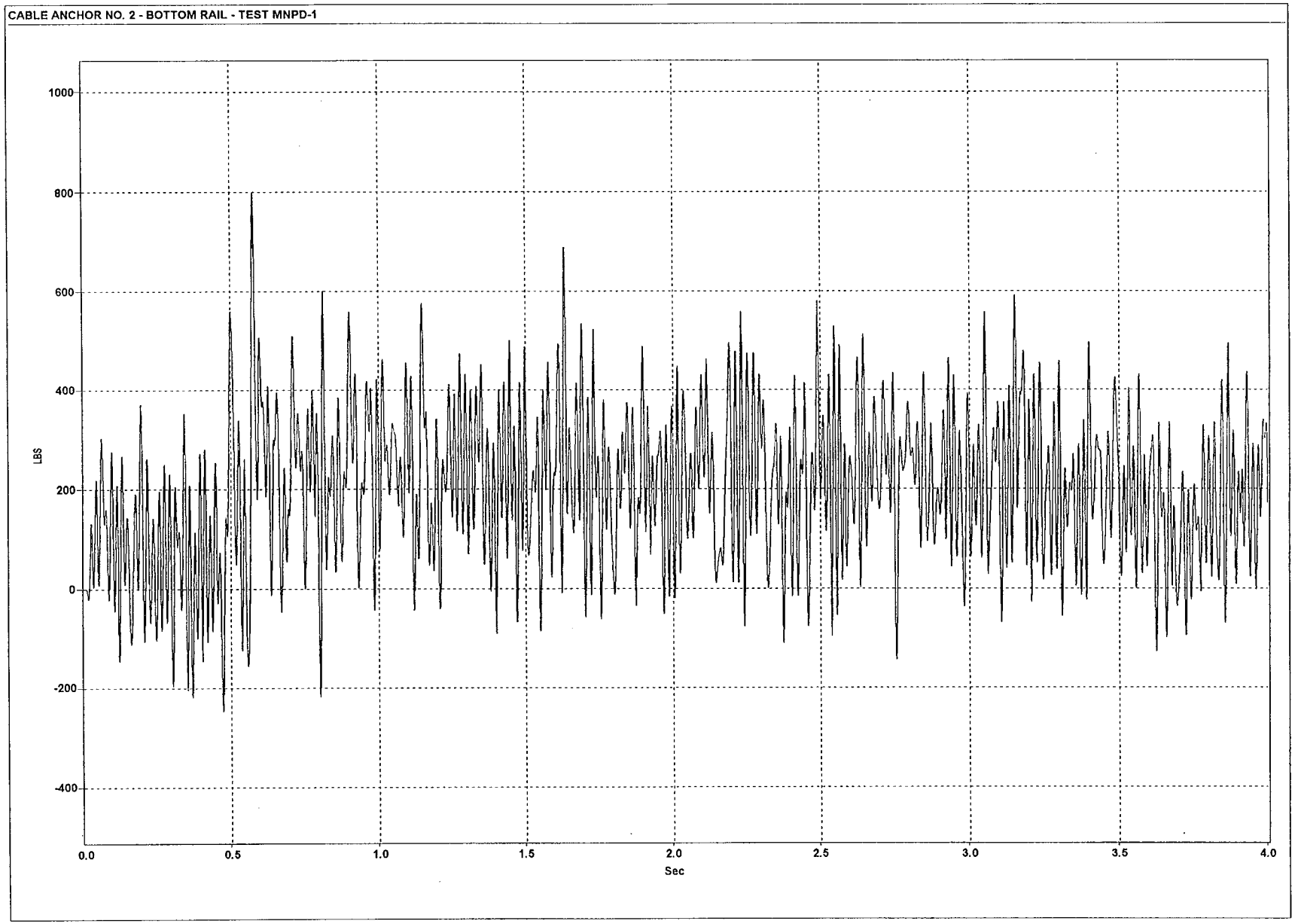

Figure C-2. Graph of Bottom Rail Cable Anchor Load, Test MNPD-1

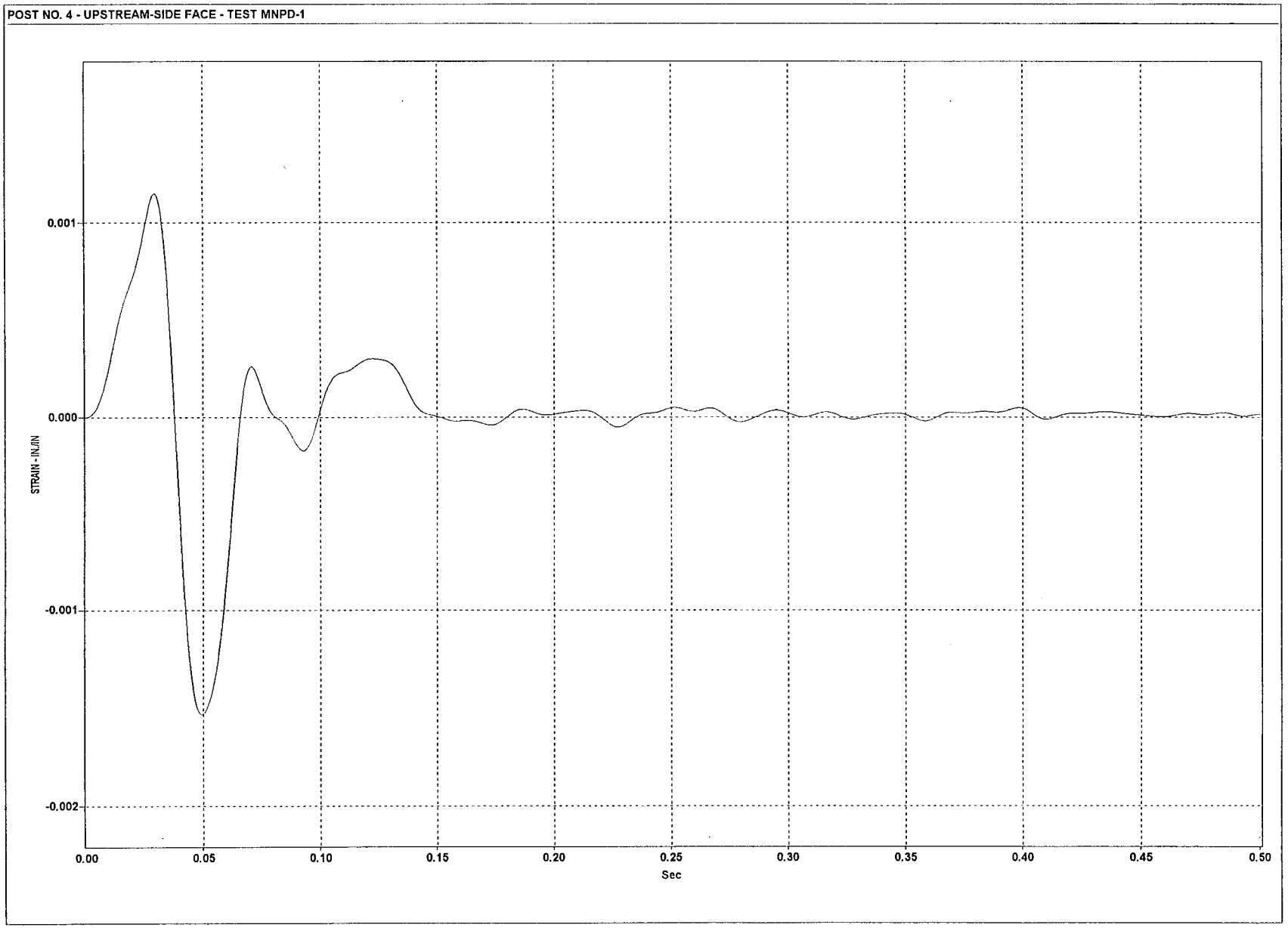

Figure C-3. Graph of Upstream-Side Post No. 4 Strain, Test MNPD-1

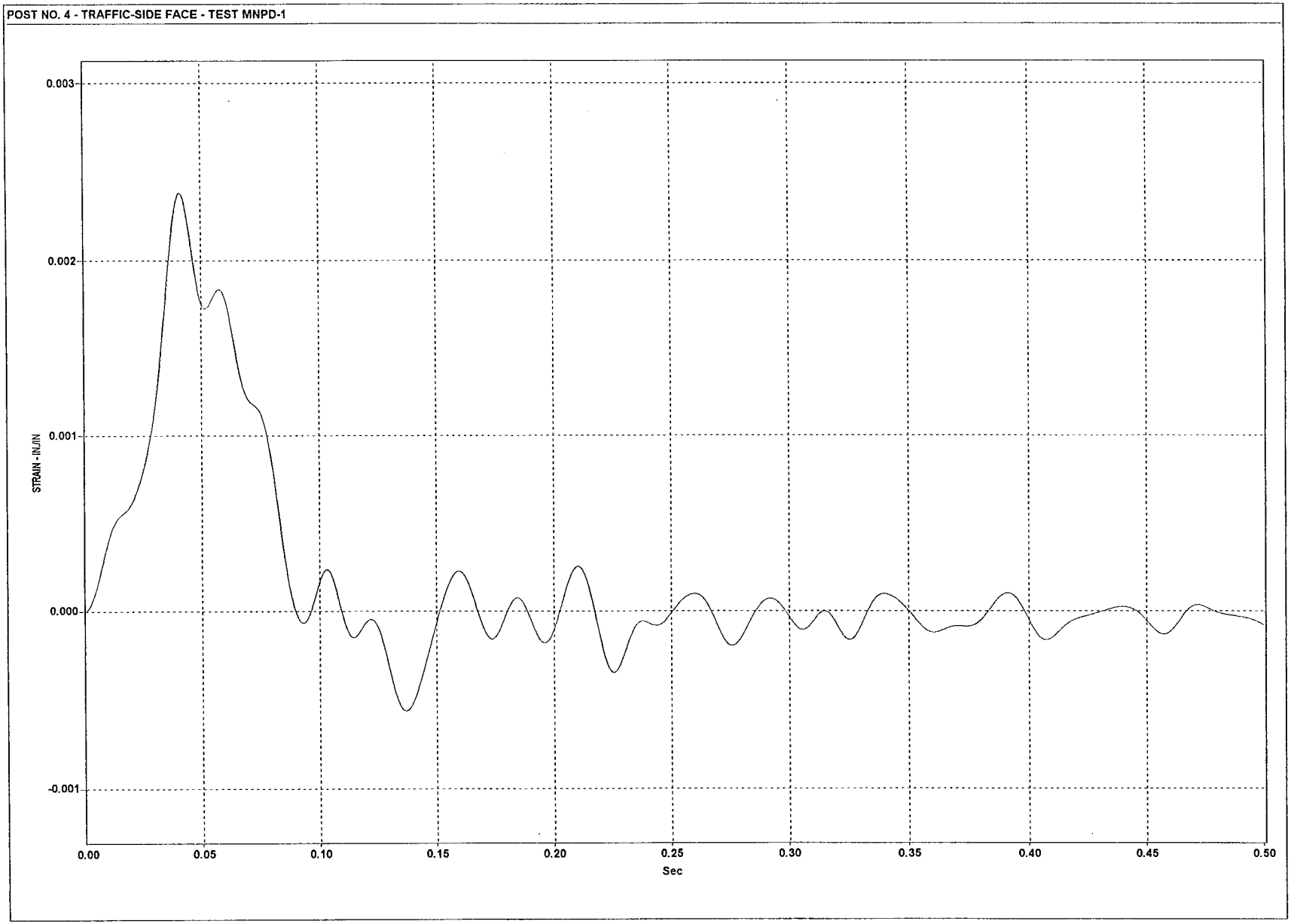

Figure C-4. Graph of Traffic-Side Post No. 4 Strain, Test MNPD-1

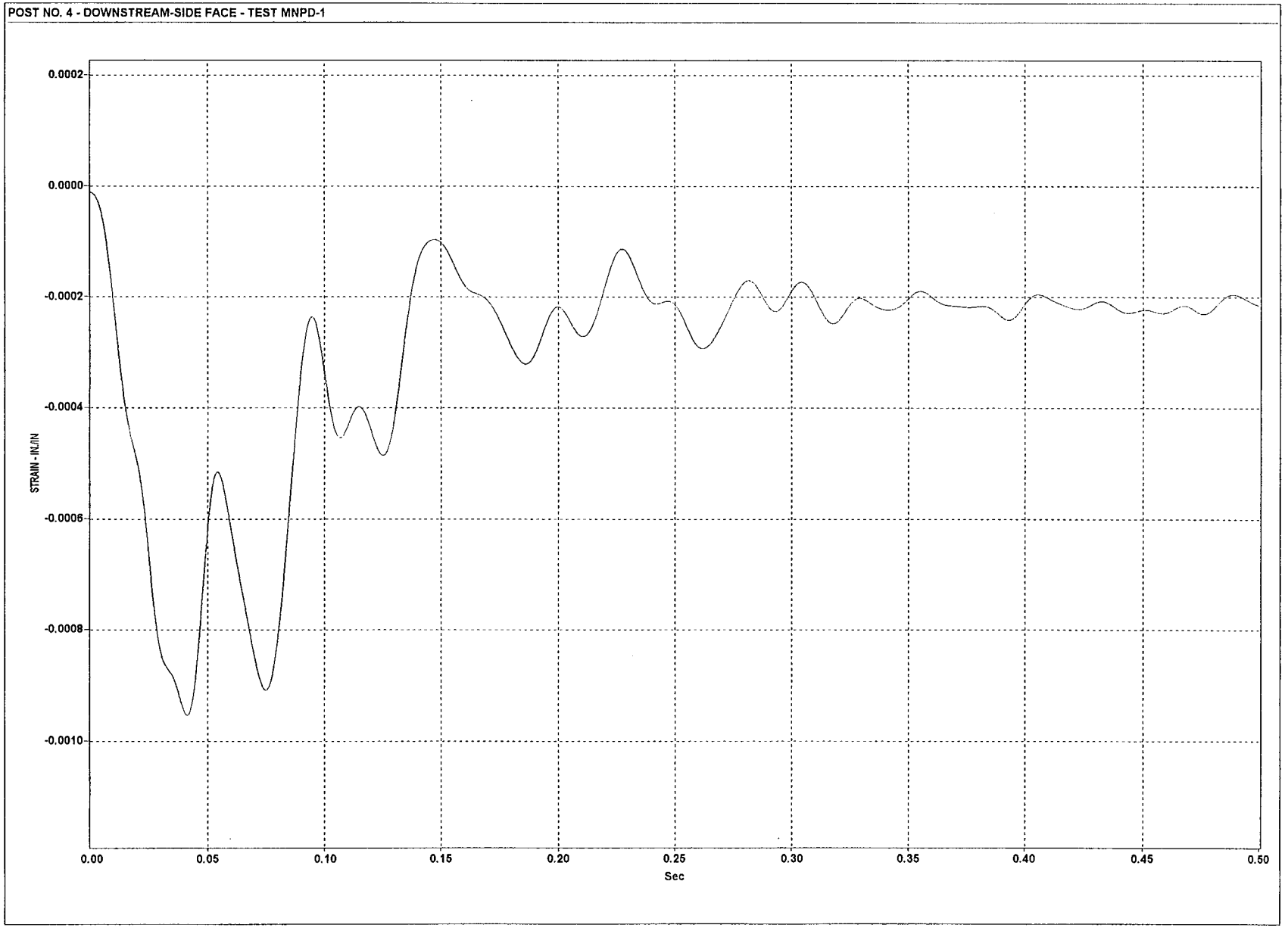

Figure C-5. Graph of Downstream-Side Post No. 4 Strain, Test MNPD-1

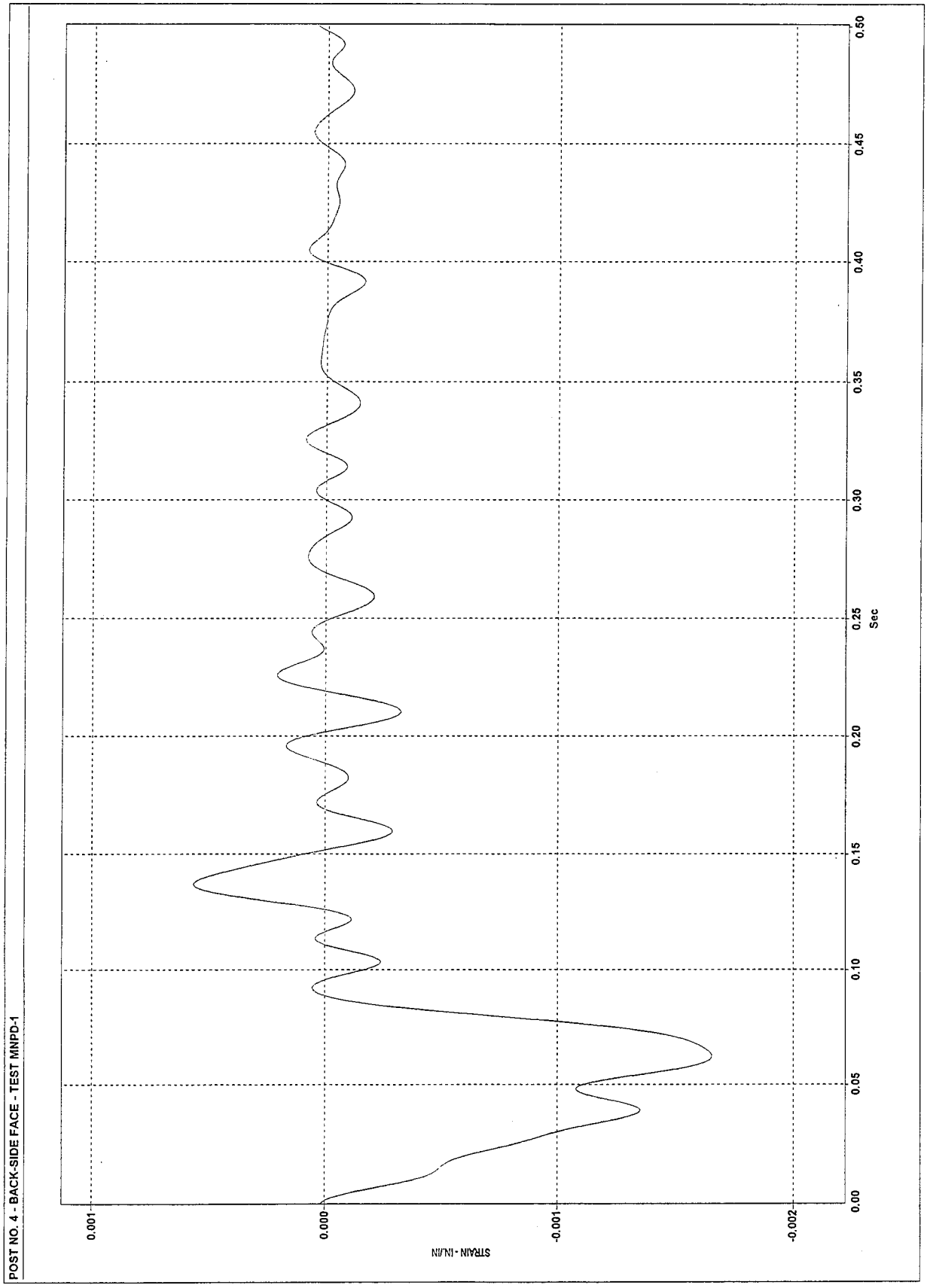

Figure C-6. Graph of Back-Side Post No. 4 Strain, Test MNPD-1

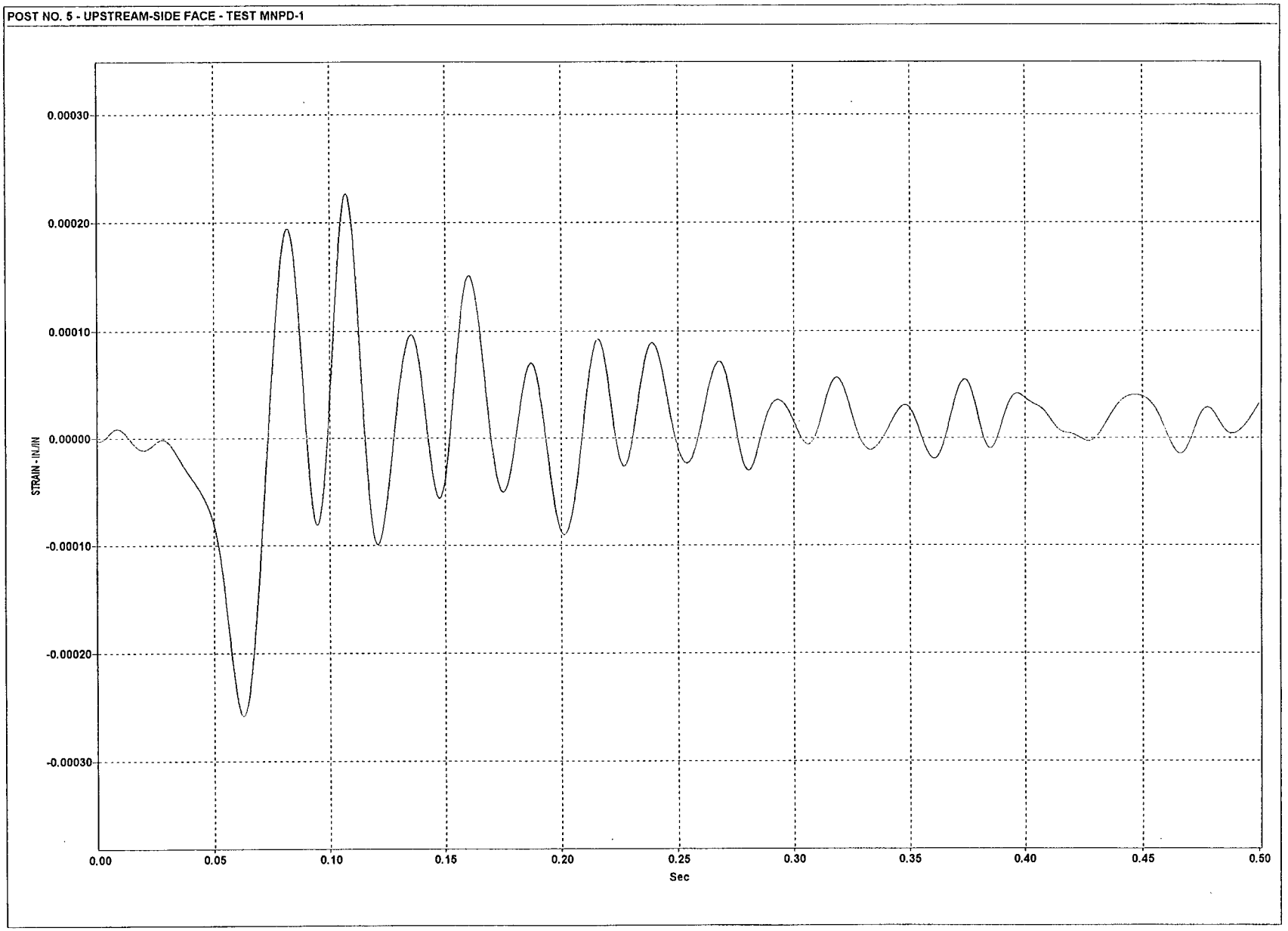

Figure C-7. Graph of Upstream-Side Post No. 5 Strain, Test MNPD-1

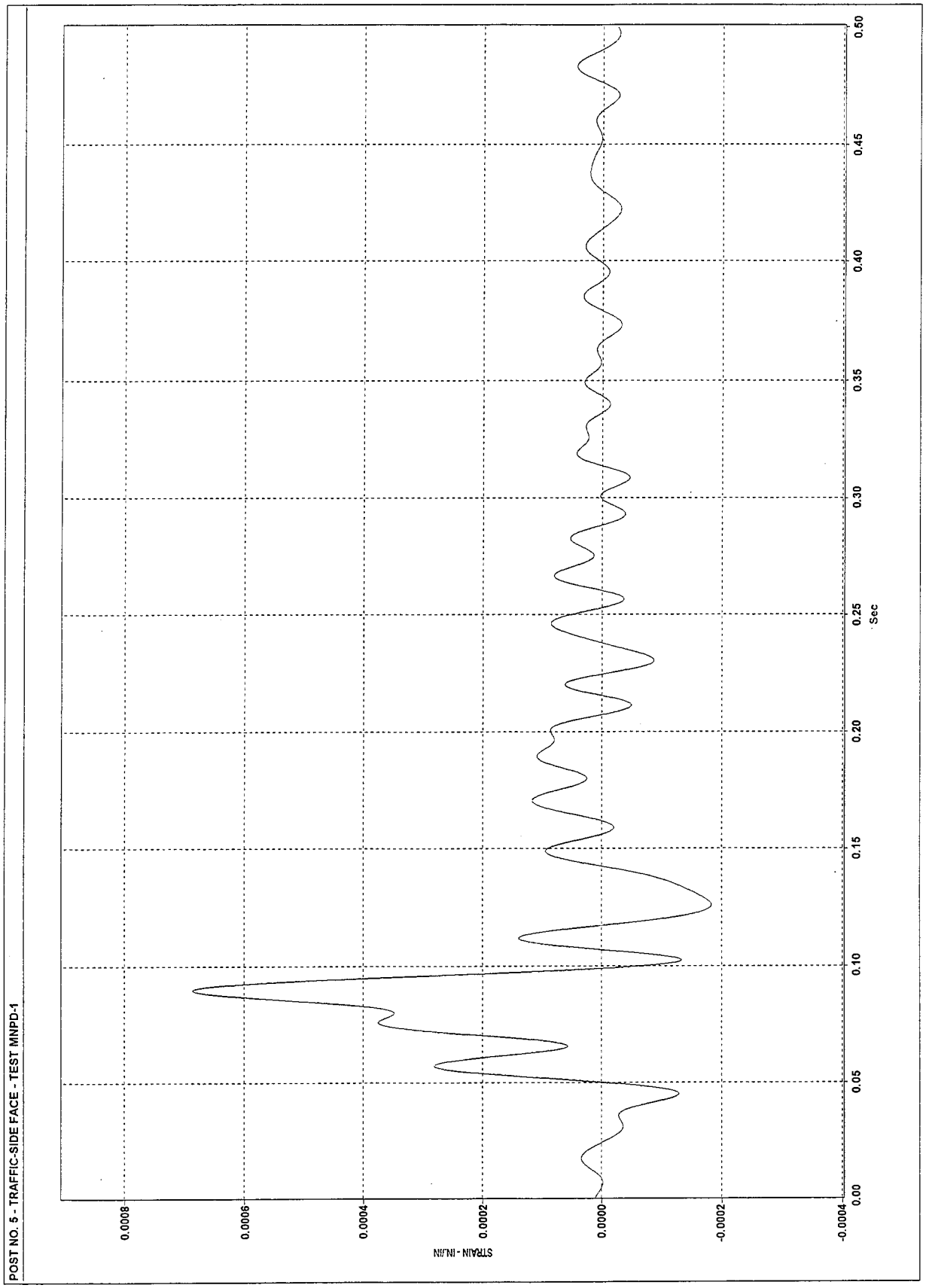

Figure C-8. Graph of Traffic-Side Post No. 5 Strain, Test MNPD-1

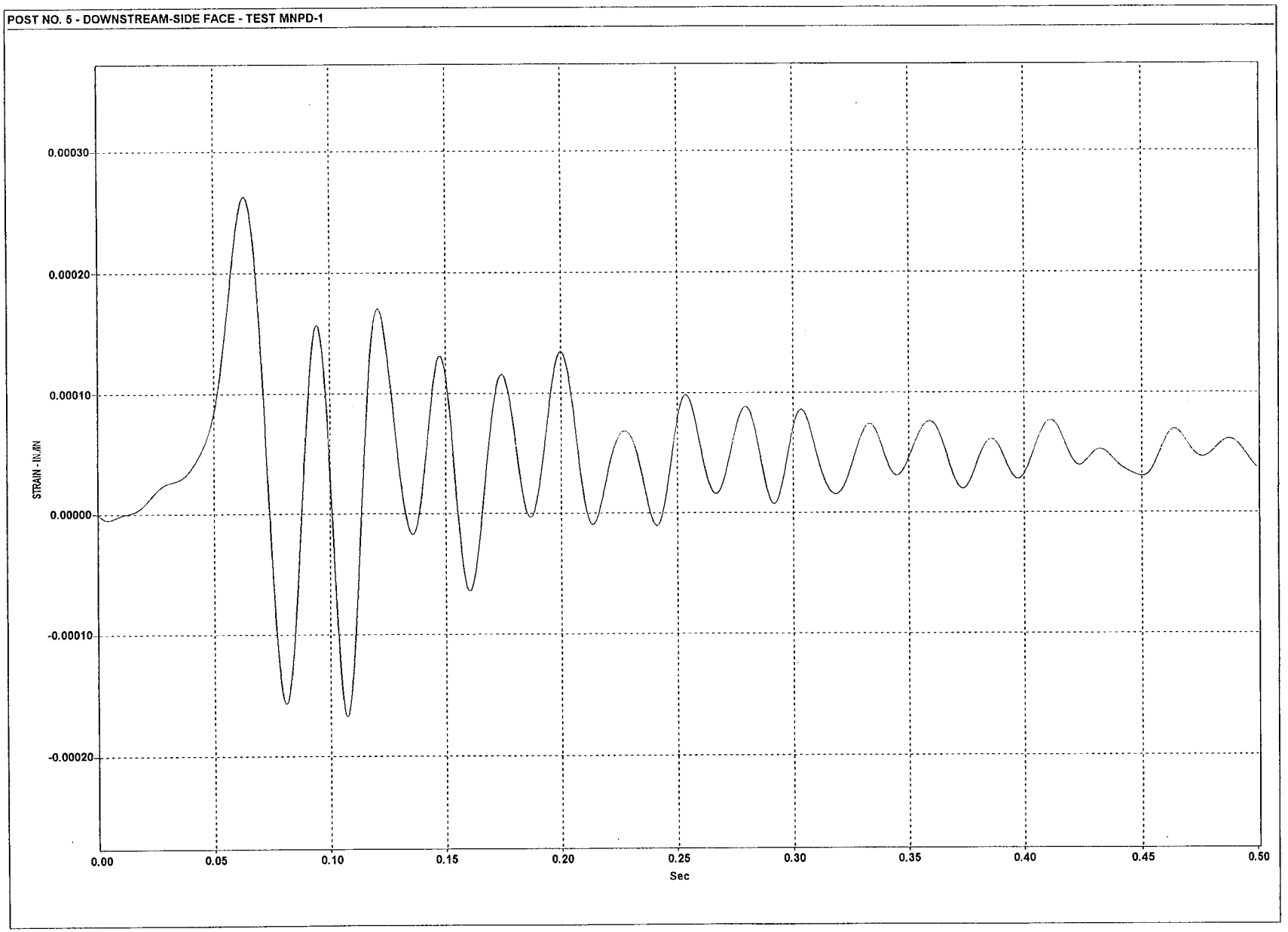

Figure C-9. Graph of Downstream-Side Post No. 5 Strain, Test MNPD-1

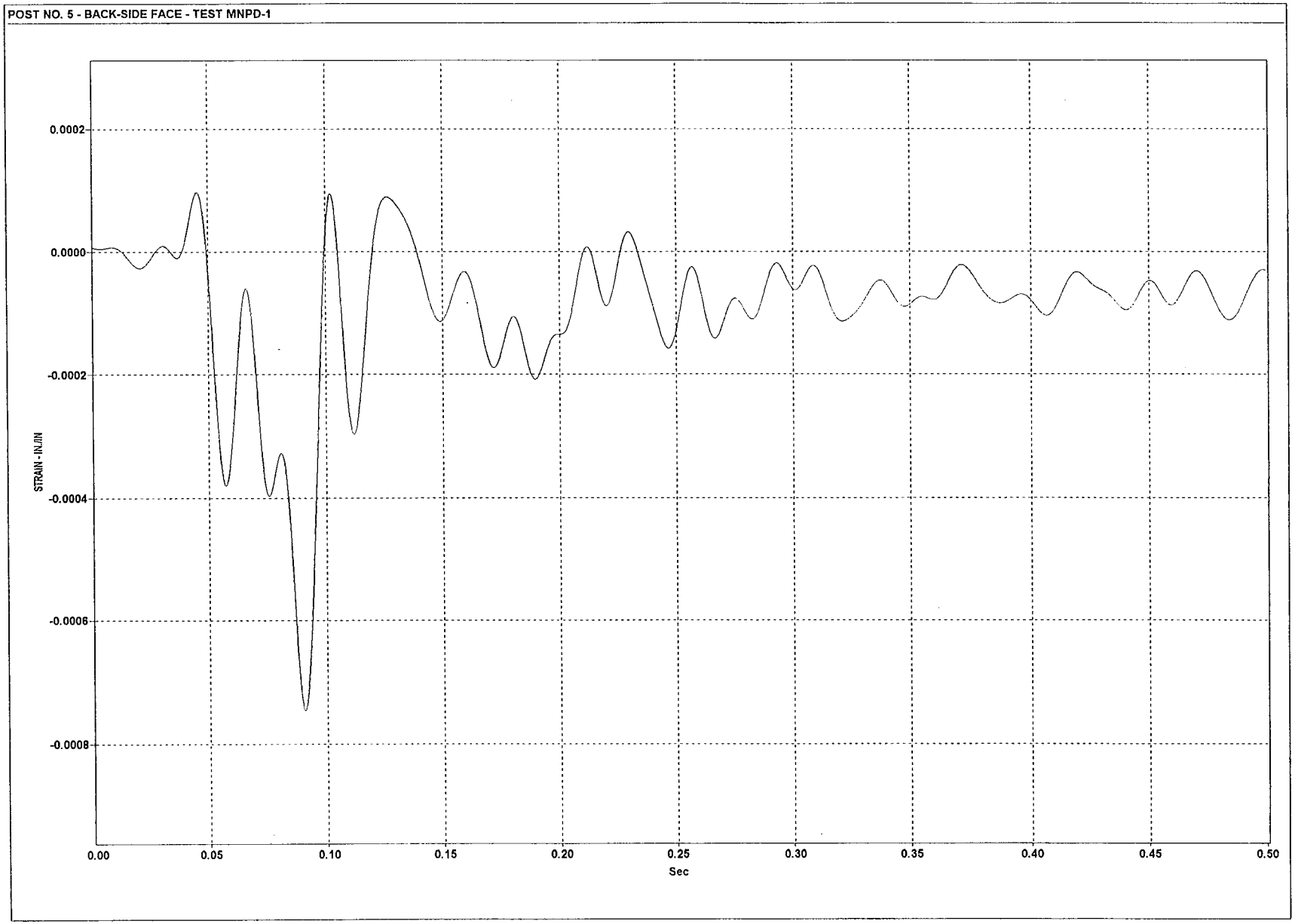

Figure C-10. Graph of Back-Side Post No. 5 Strain, Test MNPD-1

APPENDIX D

Accelerometer Data Analysis - Test MNPD-2

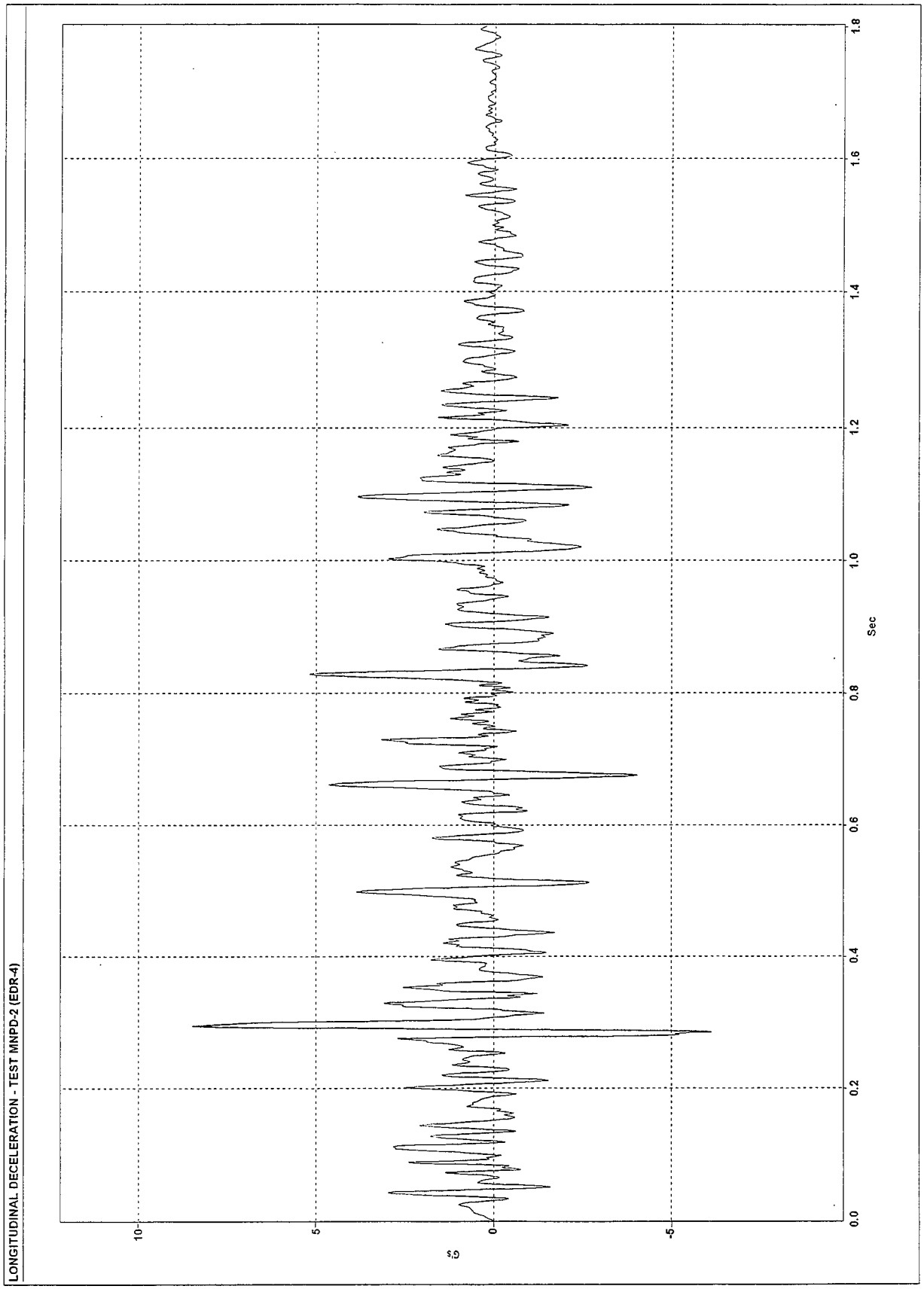

Figure D-1. Graph of Longitudinal Deceleration, Test MNPD-2

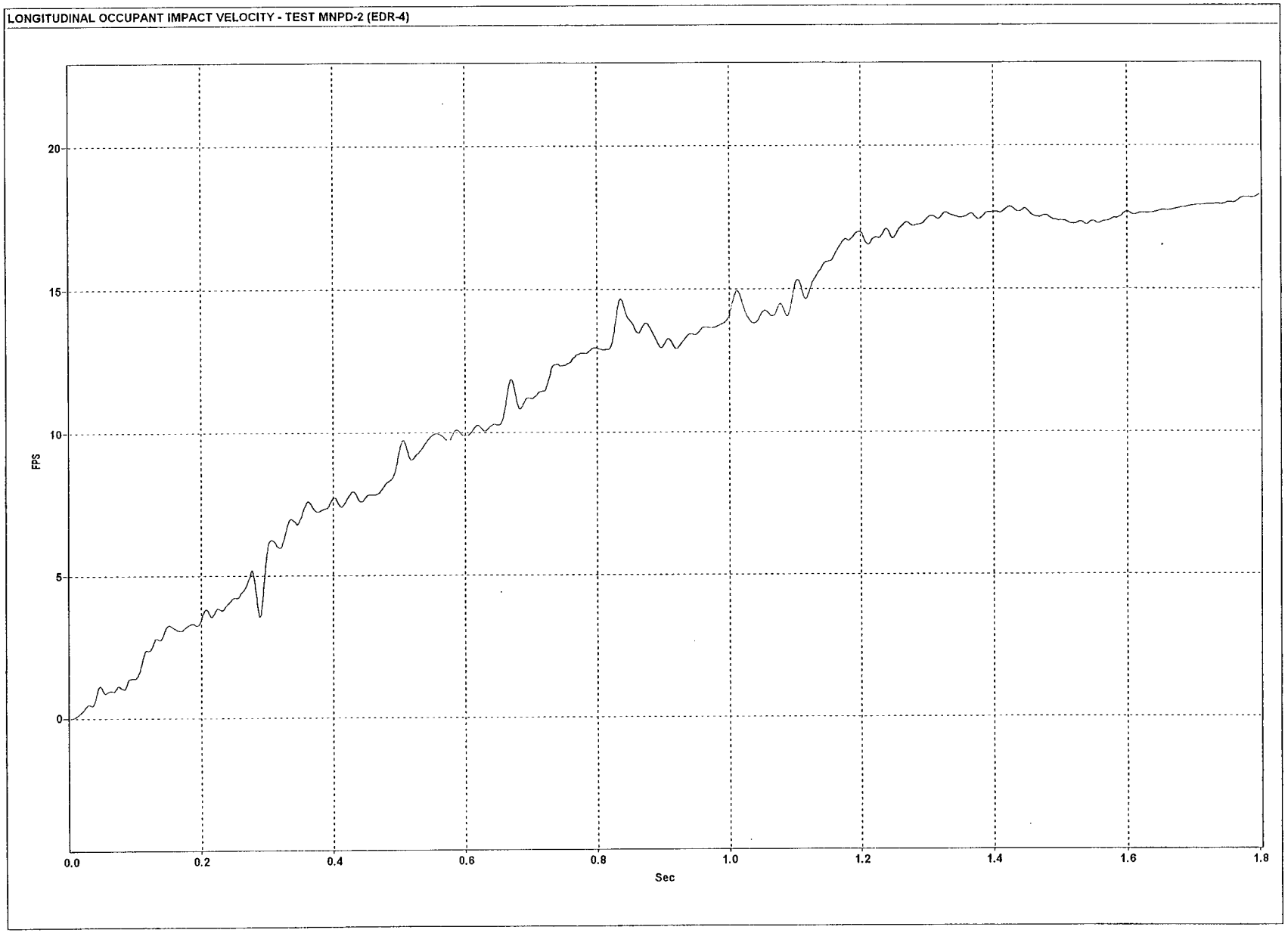

Figure D-2. Graph of Longitudinal Occupant Impact Velocity, Test MNPD-2

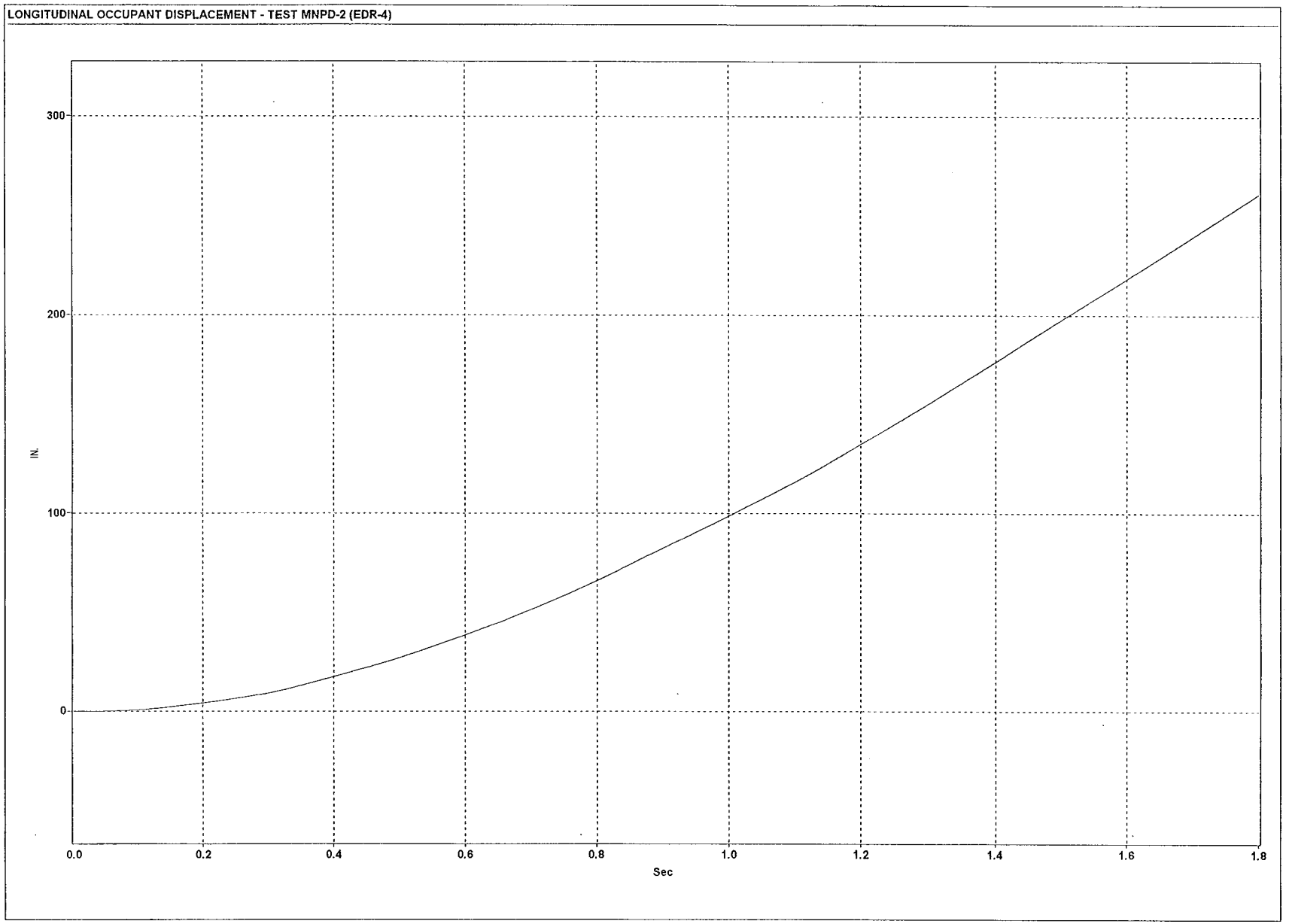

Figure D-3. Graph of Longitudinal Occupant Displacement, Test MNPD-2

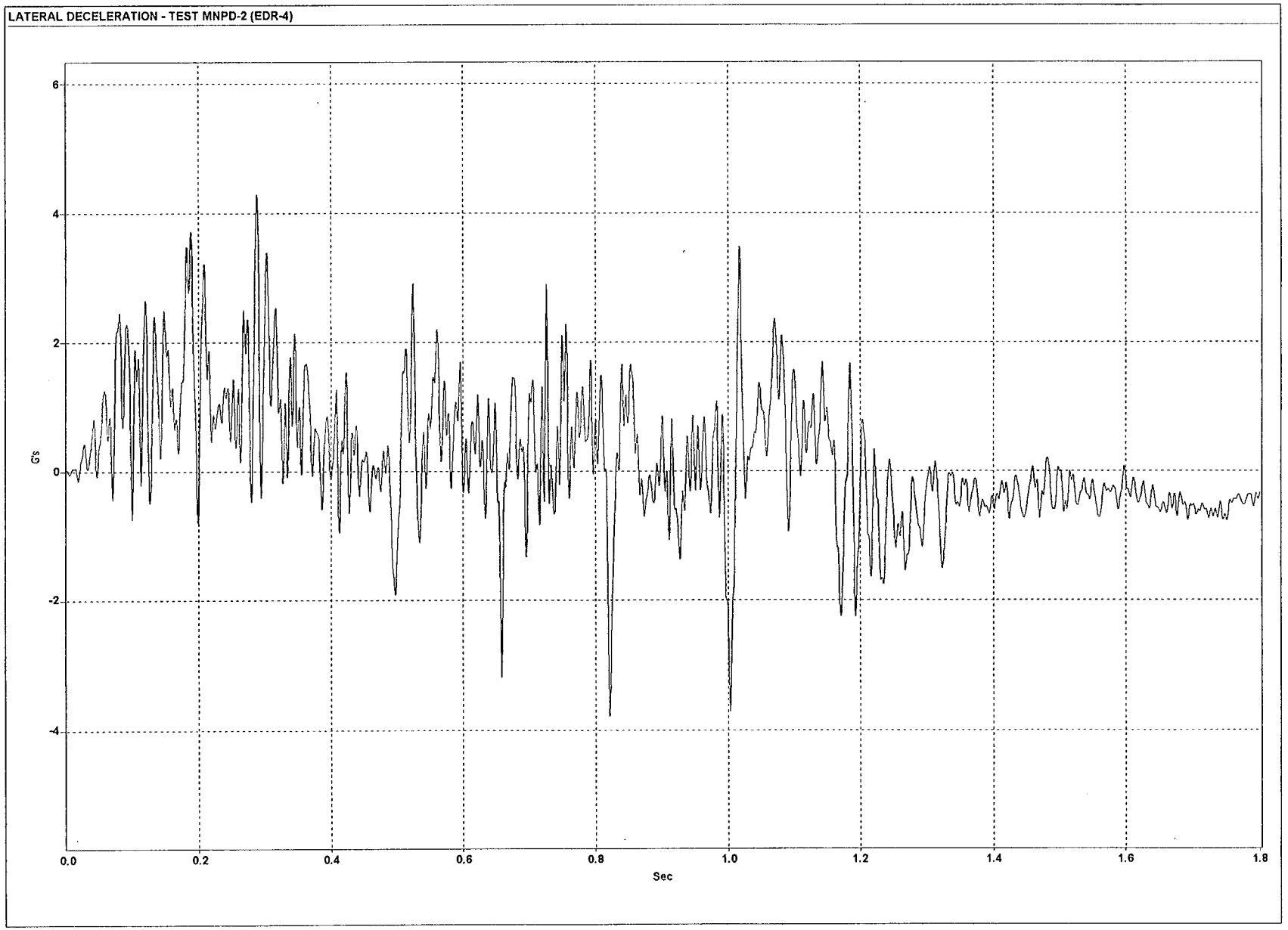

Figure D-4. Graph of Lateral Deceleration, Test MNPD-2

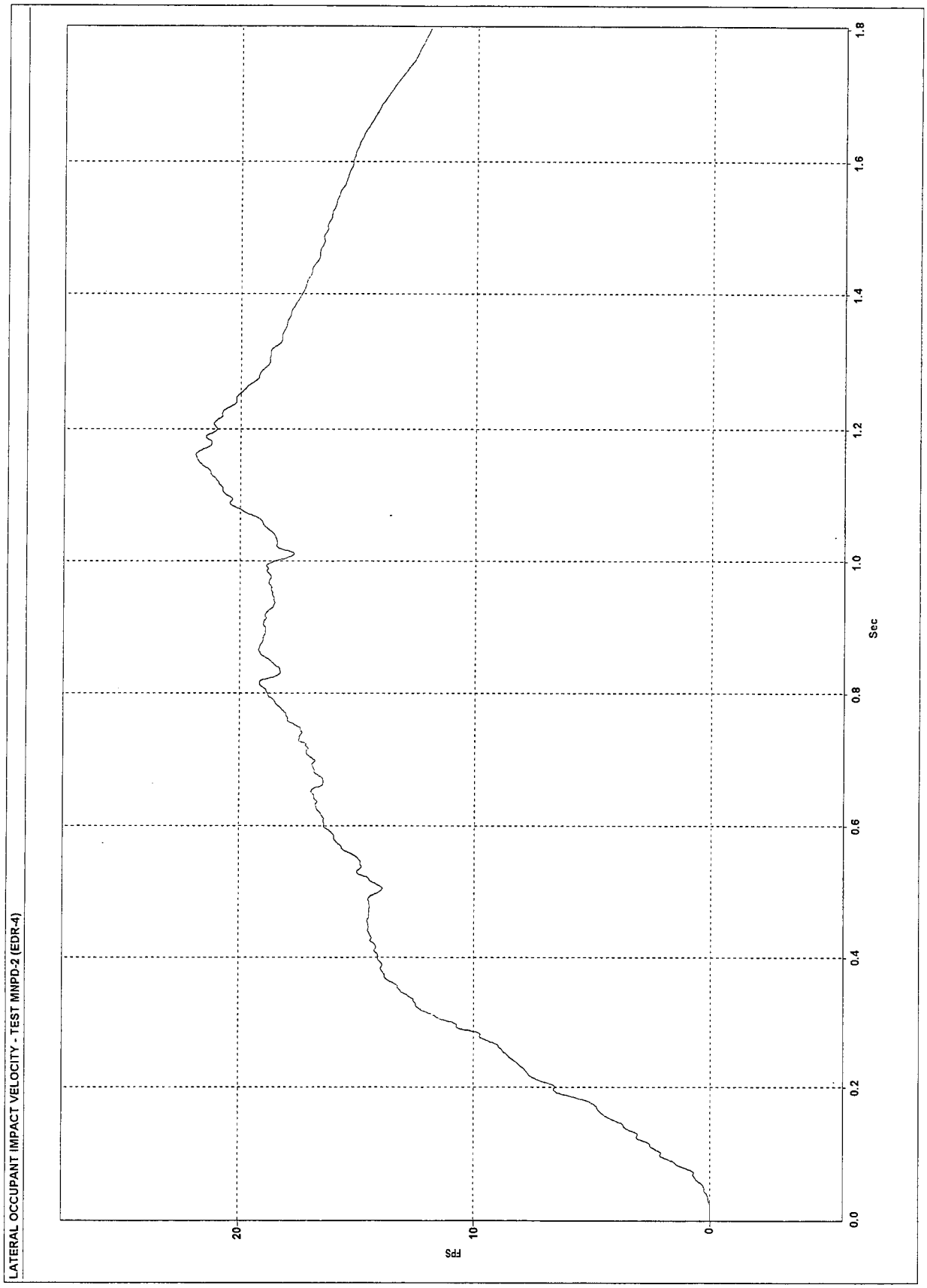

Figure D-5. Graph of Lateral Occupant Impact Velocity, Test MNPD-2

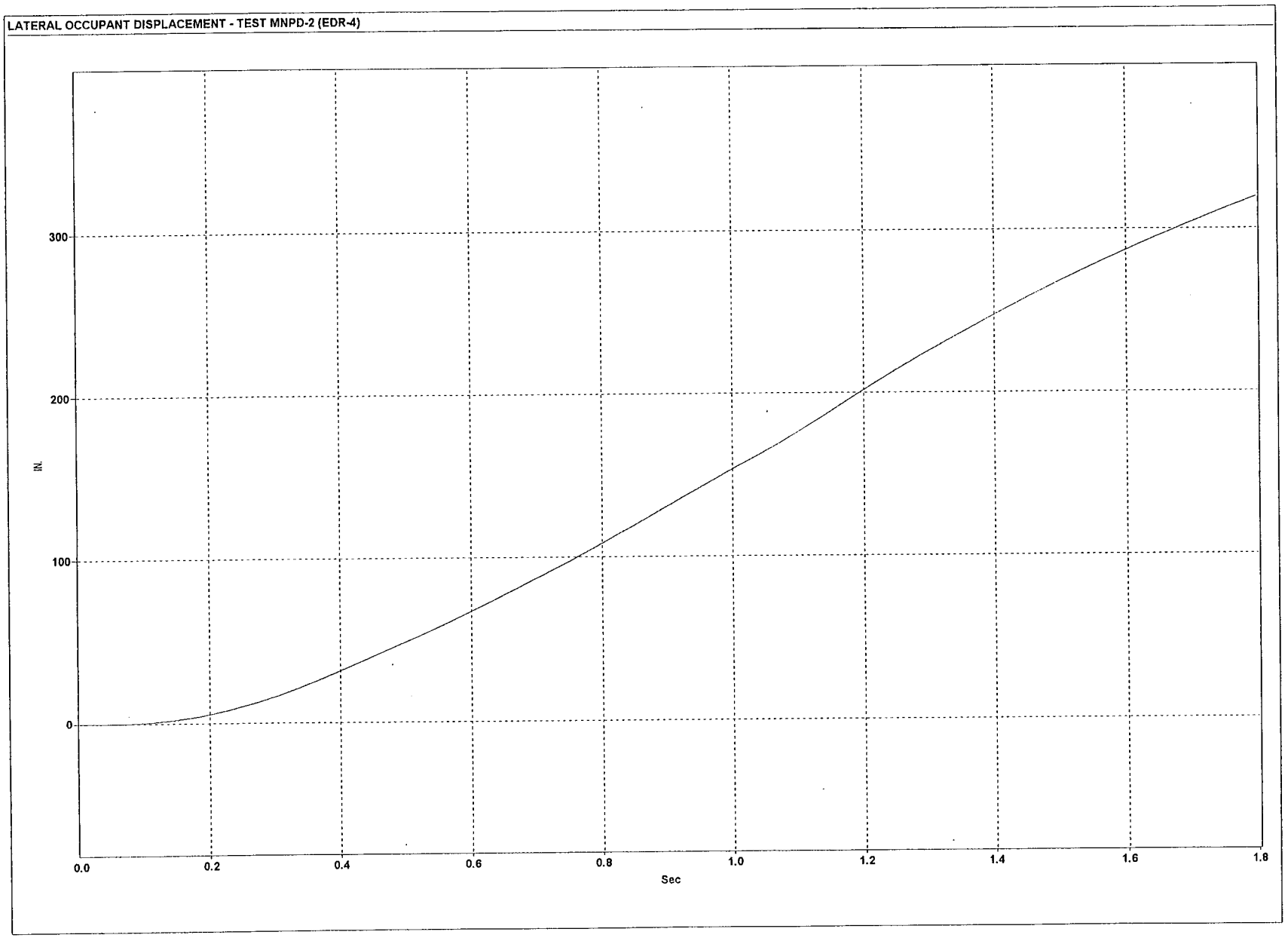

Figure D-6. Graph of Lateral Occupant Displacement, Test MNPD-2

APPENDIX E

Rate Transducer Data Analysis - Test MNPD-2

Figure E-1. Graph of Roll, Pitch, and Yaw Angular Displacements, Test MNPD-2

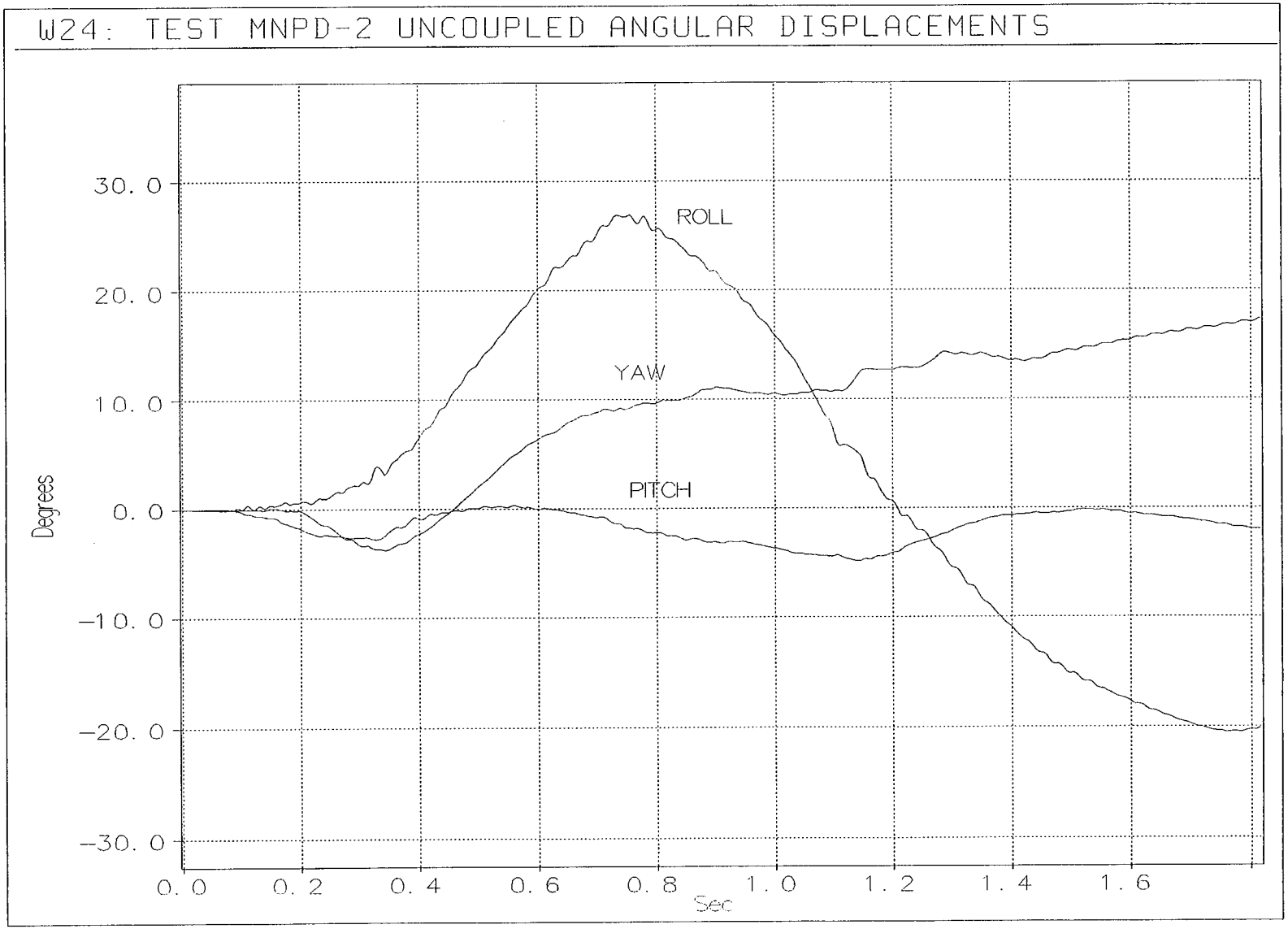

Figure E-1. Graph of Roll, Pitch, and Yaw Angular Displacements, Test MNPD-2

APPENDIX F

Strain Gauge Data Analysis - Test MNPD-2

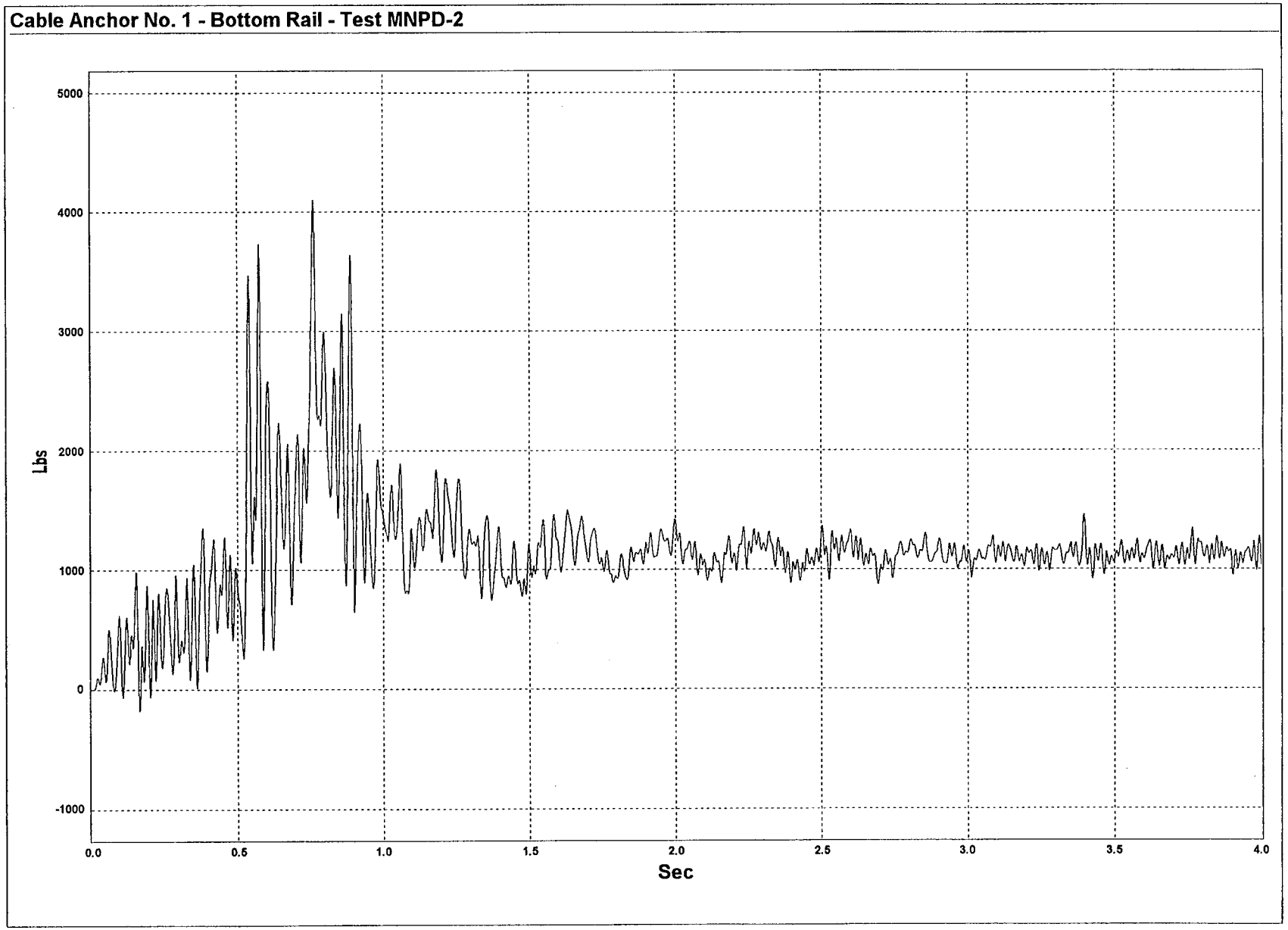

Figure F-1. Graph of Bottom Rail Cable Anchor Load, Test MNPD-2

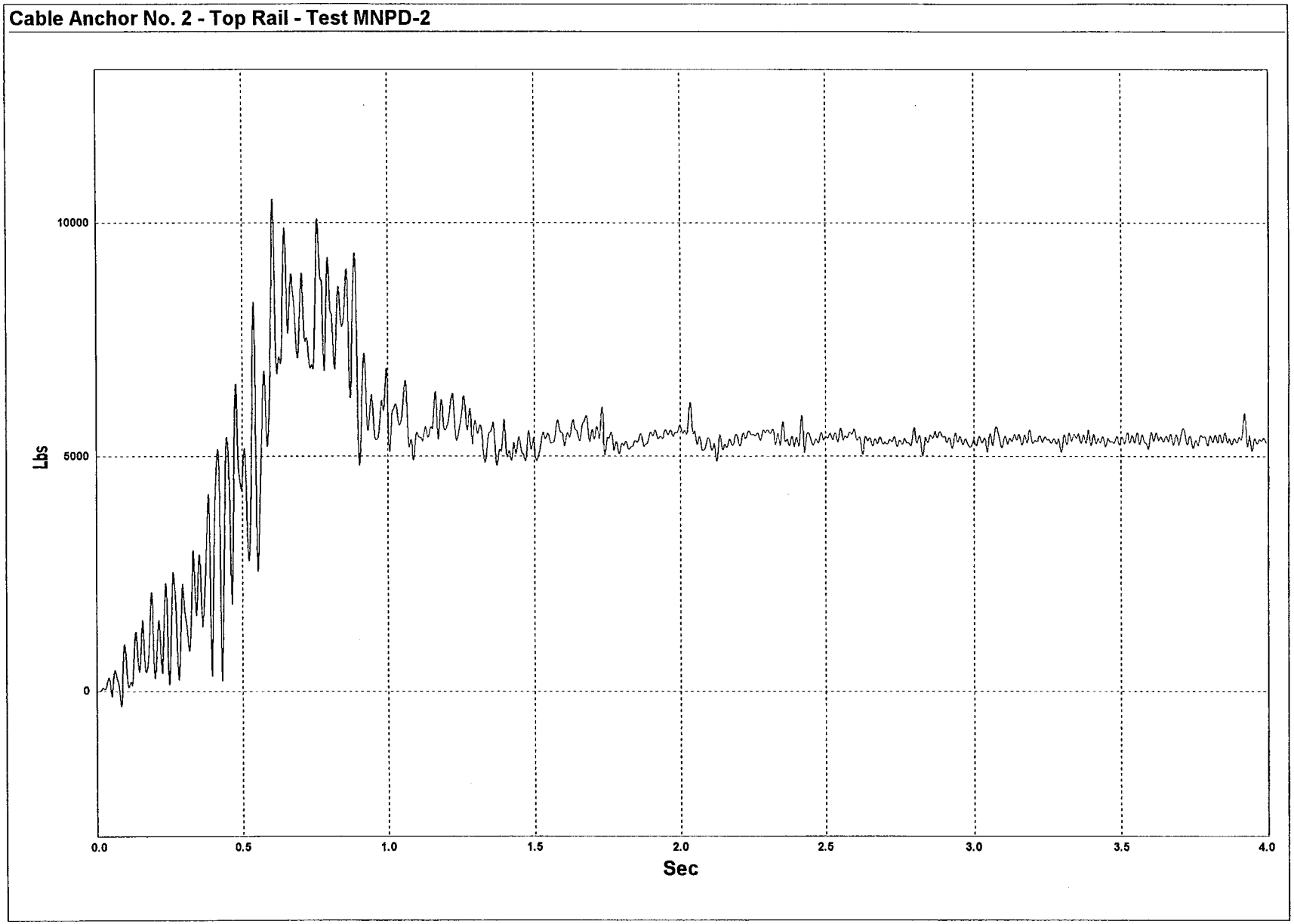

Figure F-2. Graph of Top Rail Cable Anchor Load, Test MNPD-2